



**DETECTING INDUSTRIAL CHEMICALS IN WATER WITH MICROBIAL
FUEL CELLS AND ARTIFICIAL NEURAL NETWORKS**

THESIS

Scott T. King, Major, USAF

AFIT-ENV-14-M-33

**DEPARTMENT OF THE AIR FORCE
AIR UNIVERSITY**

AIR FORCE INSTITUTE OF TECHNOLOGY

Wright-Patterson Air Force Base, Ohio

DISTRIBUTION STATEMENT A. APPROVED FOR PUBLIC RELEASE;
DISTRIBUTION UNLIMITED.

The views expressed in this thesis are those of the author and do not reflect the official policy or position of the United States Air Force, Department of Defense, or the United States Government. This material is declared a work of the U.S. Government and is not subject to copyright protection in the United States.

AFIT-ENV-14-M-33

DETECTING INDUSTRIAL CHEMICALS IN WATER WITH MICROBIAL FUEL
CELLS AND ARTIFICIAL NEURAL NETWORKS

THESIS

Presented to the Faculty

Department of Systems Engineering and Management

Graduate School of Engineering and Management

Air Force Institute of Technology

Air University

Air Education and Training Command

In Partial Fulfillment of the Requirements for the
Degree of Master of Science in Environmental Engineering

Scott T. King, BS, MS

Major, USAF

March 2014

DISTRIBUTION STATEMENT A. APPROVED FOR PUBLIC RELEASE;
DISTRIBUTION UNLIMITED.

DETECTING INDUSTRIAL CHEMICALS IN WATER WITH MICROBIAL FUEL
CELLS AND ARTIFICIAL NEURAL NETWORKS

Scott T. King, BS, MS

Major, USAF

Approved:

//signed//
Willie F. Harper, Jr., Ph.D., P.E. (Chairman)

Date

//signed//
LeeAnn Racz, Lt Col, USAF, Ph.D. (Member)

Date

//signed//
Jessica R. Williams, Ph.D. (Member)

Date

Abstract

Water quality monitoring is critically important in efforts to both limit human exposure to toxic chemicals and to protect ecosystems. Researchers have demonstrated potential in the use of microbial fuel cells (MFCs) for water quality monitoring. However, there is a need to demonstrate that MFCs can be used to identify specific industrial pollutants.

This study integrates artificial neural network (ANN) processing with MFC-based biosensing in the detection of three organic pollutants that have relevance to DoD operations: aldicarb, dimethyl-methylphosphonate (DMMP), and bisphenol-A (BPA). Overall, the use of the ANN proved to be more reliable than direct correlations with raw data in the prediction of both chemical concentration and type. The ANN made no errors in the identification and quantification of all chemicals in three concentration ranges and throughout a wide range of stepwise tests. Additionally, chemicals dissolved in the standard feed medium were accurately identified by the ANN even though the pollutant's effects on response charge were essentially masked. The ANN also accurately revealed the identity of chemical mixtures. Finally, the newly-tested response peak metrics of 10-hour Subsidence Rate (10SR) and First Moment (FrM) proved to be useful in ANN development.

This study is the first to incorporate ANN modeling with MFC-based biosensing for the detection and quantification of organic pollutants that are not readily biodegradable. It is also the first to investigate the characterization of response charges

by using the quantifiable properties of 10SR and FrM. Furthermore, this work provides insight into the flexibility of MFC-based biosensing as it pertains to limits of detection and its applicability to scenarios where mixtures of pollutants and unique solvents are involved. This research effort is expected to serve as a guide for future MFC-based biosensing efforts.

AFIT-ENV-14-M-33

To my Wife and Daughter

Acknowledgments

I would like to express my sincere appreciation to my research advisor, Dr. Willie Harper, Jr., for his guidance, support, and expertise throughout the course of this thesis effort. I would also like to thank my colleagues: Maj Marc Sylvander, for his assistance in the laboratory and Mekhakhem Kheperu, for her help with data organization. Notable contributions were also provided by the laboratory manager Dr. Daniel Felker, the hazardous materials manager John Hixenbaugh, and the employees at the Fairborn Water Reclamation Facility. Finally, I want to acknowledge the committee members: Lt Col LeeAnn Racz and Dr. Jesica Williams; for imparting their professional judgment and wisdom. The collective interest and devotion exhibited by these individuals toward research efforts helped to ensure the timely completion of this thesis.

Table of Contents

	Page
Abstract	iv
Acknowledgments.....	vii
Table of Contents	viii
List of Figures	xi
List of Tables	xiii
Glossary of Acronyms	xiv
I. Introduction	1
II. Literature Review	3
2.1 Microbial Fuel Cells (MFCs)	3
2.1.1 Bioelectricity Generation Using Microbial Fuel Cells	3
2.1.1.1 Electrode-reducing Microorganisms	5
2.1.1.2 Extracellular Electron Transfer (EET) Mechanisms	7
2.1.1.3 Competing Microorganisms and Metabolisms.....	9
2.1.1.4 Voltage and Power Generation.....	11
2.1.2 Other MFC Technologies	12
2.1.3 MFCs as Biosensors	13
2.2 Artificial Neural Networks (ANNs)	14
2.2.1 Overview and Theory	14
2.2.2 Development and Training	16
2.2.3 ANNs in Environmental Modeling	18
2.3 Organic Industrial Pollutants in the Environment.....	19

2.3.1 Aldicarb	20
2.3.2 Dimethyl Methylphosphonate (DMMP)	21
2.3.3 Bisphenol-A (BPA)	22
III. Research Objectives	24
IV. Materials and Methods	25
4.1 Microbial Fuel Cell Configuration and Operation	25
4.2 Synthetic Solutions	28
4.3 Enrichment	29
4.4 Analytical Methods	29
4.4.1 Quantification and Identification Testing.....	30
4.4.2 Solvent Effects Testing.....	30
4.4.3 Mixtures Testing.....	31
4.5 Artificial Neural Network Development	32
V. Results and Discussion.....	36
5.1 Quantification and Identification.....	36
5.1.1 Laboratory Tests	36
5.1.1.1 Quantifying Chemicals with Direct Correlations	36
5.1.1.2 Identifying Chemicals with Direct Correlations.....	49
5.1.2 Integration with ANNs	52
5.1.2.1 Quantifying Chemicals with ANNs.....	52
5.1.2.2 Identifying Chemicals with ANNs	56
5.2 Solvent Effects.....	58
5.2.1 The Effect of Solvents on Response Metrics	58

5.2.2 Using ANNs to Identify Chemicals Dissolved in Feed Medium	63
5.3 Mixtures.....	65
5.3.1 Laboratory Tests	65
5.3.2 Integration with ANNs	70
VI. Conclusion	72
VII. Future Work	74
Appendix A. Raw ANN Data for MFC #5	75
Appendix B. Raw ANN Data for MFC #10	76
Appendix C. Raw ANN Data for MFC #6	77
Appendix D. Raw ANN Data for MFC #7	78
Appendix E. Raw ANN Data for MFC #8.....	79
Appendix F. Raw ANN Data for MFC #9	80
Appendix G. Sample ANN Code using MATLAB	81
Appendix H. One-way Analysis Plots for MFC #5 and MFC #10.....	83
Appendix I. MFC #5 & MFC #10 Metric Correlations for Quantification Experiments ..	89
Appendix J. One-way Analysis Plots for MFC #8 and MFC #9	98
Appendix K. ANN Outputs for Solvent Effects Testing	104
Appendix L. Results for Tap Water Experiments.....	107
Appendix M. The Effect of Training Ratio on ANN Performance	110
Bibliography	111

List of Figures

Figure	Page
1. Typical Single-Chamber MFC Design	4
2. Electron Transfer Model to a MFC Anode (modeled after Lovley, 2008).....	6
3. Proposed Mechanisms for Electron Transfer to the Anode (modeled after Lovley, 2008)	8
4. McCulloch-Pitts Model of an Artificial Neuron (modeled after Krogh, 2008).....	15
5. Conceptual Illustration of a Hyperplane (modeled after Krogh, 2008).....	16
6. Feed-forward ANN	18
7. MFC Design and Configuration.....	27
8. Overview of System Set-up	28
9. Description of Metric Information for MFC Response Peaks	33
10. Corresponding Figure for Equation 1	34
11. Basic ANN Architecture	34
12. Operating History for MFC #5	38
13. Operating History for MFC #10	39
14. Typical Response Peaks for Aldicarb in MFC #10	42
15. Typical Response Peaks for DMMP in MFC #10	43
16. Typical Response Peaks for BPA in MFC #10.....	44
17. PH and PA Correlations with Aldicarb Concentration in MFC #5	47
18. PH and PA Correlations with Aldicarb Concentrations in MFC #10.....	48
19. One-way Analysis of AR(mA/hr) by Chemical Type in MFC #5.....	50
20. One-way Analysis of PH(mA) by Chemical Type in MFC #10.....	51

21. ANN Results for Aldicarb Quantification Tests.....	53
22. ANN Results for DMMP Quantification Tests.....	54
23. ANN Results for BPA Quantification Tests.....	55
24. ANN Results for Chemical Identification Tests.....	57
25. Operating History for MFC #6.....	60
26. Operating History for MFC #7.....	61
27. Representative peaks from MFC #7.....	62
28. ANN Results for Solvent Effects Testing Using [PH, PA, AR, FrM] as the Input Matrix for MFC #6.....	64
29. Operating History for MFC #8.....	67
30. Operating History for MFC #9.....	68
31. One-way Analysis of SR (mA/hr) By Chemical Type for MFC #8.....	69
32. ANN Results for Mixtures Testing.....	71

List of Tables

Table	Page
1. Chemical Structure of the Three Chemicals Under Study.....	20
2. Description of Metrics for MFC #5	45
3. Description of Metrics for MFC #10	45

Glossary of Acronyms

10-hr SR	10-hour Subsidence Rate
ANN	Artificial Neural Network
AR	Acceleration Rate
ATP	Adenosine Triphosphate
BES	Bromoethanesulfonate
BPA	Bisphenol-A
CE	Columbic Efficiency
CEM	Cation Exchange Membrane
COD	Chemical Oxygen Demand
DMMP	Dimethyl Methylphosphonate
DoD	Department of Defense
EET	Extracellular Electron Transfer
FM	First Moment
mA	milli-Ampere
MFC	Microbial Fuel Cell
NADH	Nicotinamide adenine dinucleotide
PA	Peak Area
PH	Peak Height
ppb	parts per billion
ppm	parts per million
RO	reverse osmosis
SR	Subsidence Rate

DETECTING INDUSTRIAL CHEMICALS IN WATER WITH MICROBIAL FUEL CELLS AND ARTIFICIAL NEURAL NETWORKS

I. Introduction

Fresh water is a finite resource and is vitally important to every aspect of human life. The availability of fresh water, or lack thereof, can impose socio-economic burdens on society and plays a major role in sustainable development. Pollutant discharges from industry, high nutrient levels leading to eutrophication, and the over-pumping of aquifers are all examples of prominent concerns regarding water quality degradation today. Water quality monitoring to detect contamination issues is therefore essential in protecting public health and the environment.

Biosensors can be used to monitor water quality. Biosensors combine a biological component and a physiochemical detector component to create a signal that can be processed in the detection of an analyte. MFCs, while best known for their potential to generate electricity, have also been used as biosensors for water quality monitoring (Feng et al., 2013a; Feng et al., 2013b; Tront et al., 2008; Kumlanghan et al., 2007). An MFC is a device that uses microorganisms to produce bioelectricity. The microorganisms survive in an anoxic environment near the anode and produce electrons from the oxidation of organic matter. These electrons are transported exogenously from the cell to the anode of the fuel cell. The electrons then travel from the anode to a cathode that is exposed to a terminal electron acceptor (e.g. oxygen). The amount and type of organic matter in the substrate has an effect on current generation in an MFC. Since this information can be measured and collected, the data can be correlated with

water quality data to determine the presence of certain organic compounds. Feng et al. (2013a, 2013b) successfully used MFC data to distinguish between four separate, readily biodegradable, simple organic substances and for different chemical oxygen demand (COD) concentrations.

This work further interprets the raw data generated by MFCs as biosensors with the establishment of never-before used metrics. Additionally, a proven nonlinear modeling technique is used to identify, characterize, and distinguish between 3 types of toxic organic pollutants that are relevant to Department of Defense (DoD) activities. This report is the first to utilize ANN processing to fully interpret the MFC electrical signals from organic pollutants in water for their identification and quantification.

II. Literature Review

2.1 Microbial Fuel Cells (MFCs)

2.1.1 Bioelectricity Generation Using Microbial Fuel Cells

A microbial fuel cell is a bioreactor that produces electrical energy from chemical energy in the bonds of organic substances. MFCs are similar to any other battery or fuel cell in that electrons are first generated, and then pass between two electrodes, an anode and a cathode, connected by a wire. The main difference, however, between MFCs and other fuel cells is that the electricity is generated through the work of electrode-reducing microorganisms.

A schematic of a typical MFC is shown in Figure 1. Electrode-reducing microorganisms in the anode chamber first transfer electrons to the anode. The anode chamber does not contain oxygen because it, being an excellent electron acceptor, would inhibit current generation by preventing electrons from reaching the anode. Electrons travel through a wire from the anode chamber to a cathode that is either air-exposed or in a separate chamber where there is available dissolved oxygen. The two chambers are sometimes separated by a membrane that allows for the transfer of protons. When the electrons reach the cathode, they combine with the protons to form water or another reduced compound. Finally, the current is determined with the use of a multimeter which measures a voltage drop across the resistor (Logan, 2008).

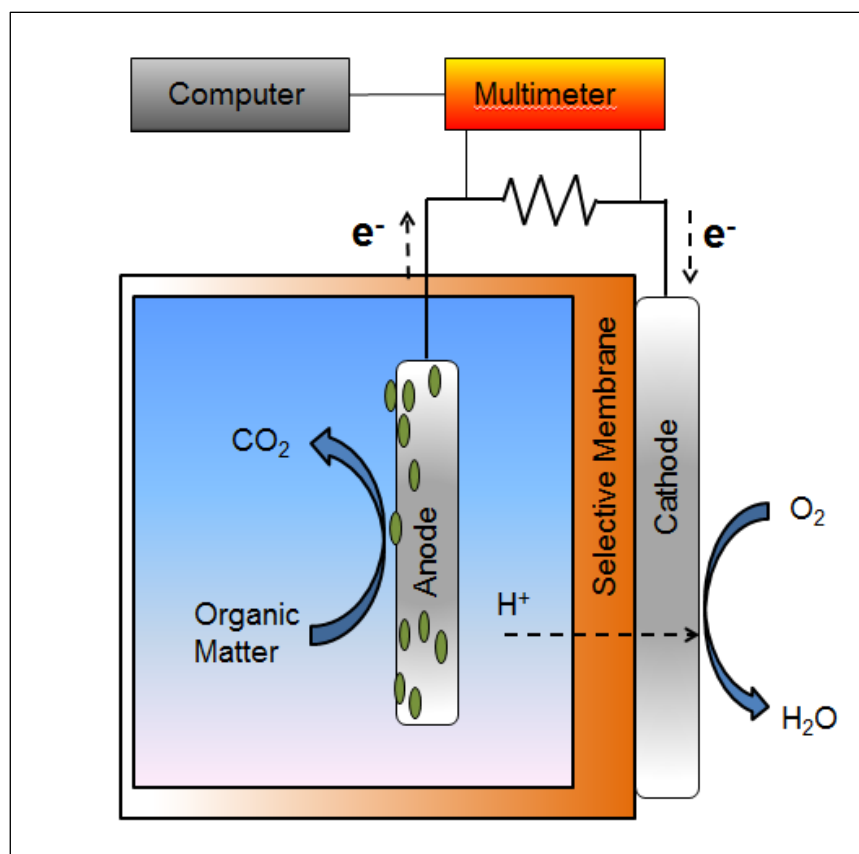


Figure 1. Typical Single-Chamber MFC Design

Evidence for the generation of electricity from microbial metabolism has existed for over 100 years. The first observations of this are credited to Potter in 1911 (Potter, 1911). MFC and bioelectricity research for the next 88 years, however, utilized chemical mediators that transferred electrons exogenously from the cell to an electrode. It wasn't until 1999 when Kim et al. revealed a breakthrough discovery that electrons could be efficiently transferred from microorganisms to an electrode via direct contact (Kim et al. 1999a; Kim et al. 1999b).

2.1.1.1 Electrode-reducing Microorganisms

Microorganisms that have the ability to interact with the anode and cathode of an MFC are known as electrode-reducing microorganisms (Lovley, 2008). To produce electricity, these electrode-reducing microorganisms first oxidize (degrade) organic matter in an MFC which produces electrons. The microorganisms then transfer electrons exogenously to an electrode; in this case the anode of the MFC (Logan, 2008). It should be noted that electrode-reducing microorganisms are distinctly different from most anaerobes that can only transfer electrons to soluble compounds that diffuse into the cell like nitrate or sulfate. The ability to transfer electrons outside of the cell (exogenously) to an anode is what allows an MFC to function. Microorganisms that can contribute electrons to fuel cell anodes are also known as: exoelectrogens, electrogenic microorganisms, electrochemically active bacteria, and anode-respiring bacteria (Lovley, 2008).

Energy conservation in the cell is maintained through respiration. This process involves the pumping of protons and the related transfer of electrons across the inner membrane. Nicotinamide adenine dinucleotide (NADH) derived from the oxidation of organic matter is taken up by protein complexes, which have the ability to force protons into the outer membrane. The energy for the movement of protons is generated by a number of electron transport complexes. After protons are moved into the outer membrane, another membrane complex called adenosine triphosphate (ATP) synthase uses the proton gradient that was created in the previous step to move the protons back toward the inner membrane. ATP synthase uses these protons in the regeneration of cellular energy in the form of ATP. Subsequent electron transfer steps (Figure 2) serve

mainly to dispose of electrons and are therefore not directly providing energy for the cell. However, it is these final electron transfer steps that allow the anode of the MFC to be reduced.

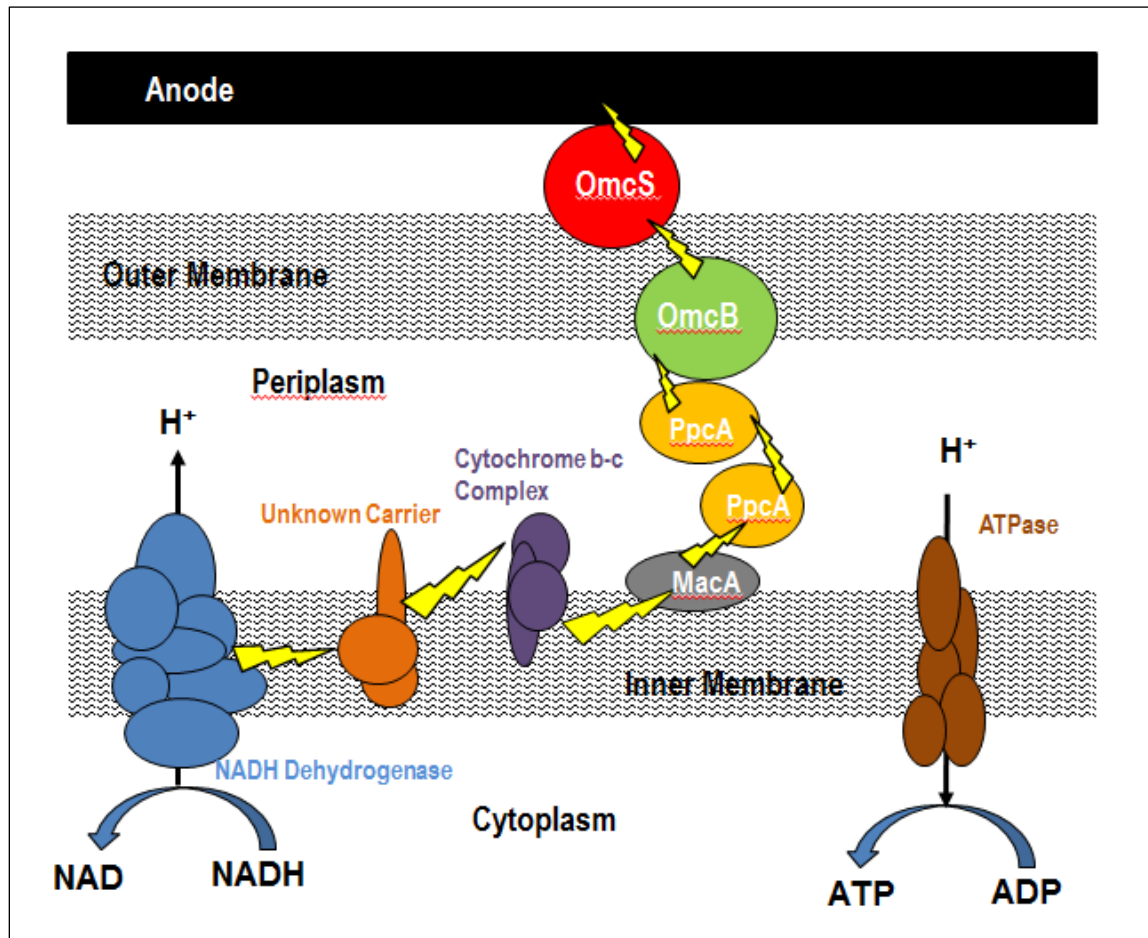


Figure 2. Electron Transfer Model to a MFC Anode (modeled after Lovley, 2008)

Many types of bacteria are capable of transferring electrons exogenously. However, two of the most prominent genera used in MFC research include *Shewanella* and *Geobacter* (Logan, 2008). Both of these groups have been used extensively in the inoculation of MFCs (Sun et al., 2010; Choi and Chae, 2013; Biffinger et al., 2008). *Geobacter* species are most commonly known to harvest electricity from organic

substrates and anaerobic aquatic sediments. They are known to produce the highest current densities amongst all organisms in MFCs (Lovley et al., 2011). *Shewanella* species are known to be more versatile having an ability to grow in both aerobic and anaerobic conditions. Additionally, *Shewanella* species can use a variety of electron acceptors and can secrete mediators that enhance electron transfer capabilities. For these reasons, it is often looked to for use in a variety of power applications (Biffinger et al., 2008).

2.1.1.2 Extracellular Electron Transfer (EET) Mechanisms

Research indicates that the mechanisms through which electrons are passed from the microorganisms to the anode can vary (Lovley, 2008). The four predominant theories (Figure 3) for microbe-electrode interaction pertaining to the transfer of electrons are: 1) transfer via conductive pili or nano-wires; 2) long-range transfer via soluble electron shuttles in the substrate; 3) transfer through a conductive biofilm and 4) direct contact with the anode surface (Lovley, 2008; Reguera et al., 2005; Holmes et al., 2006).

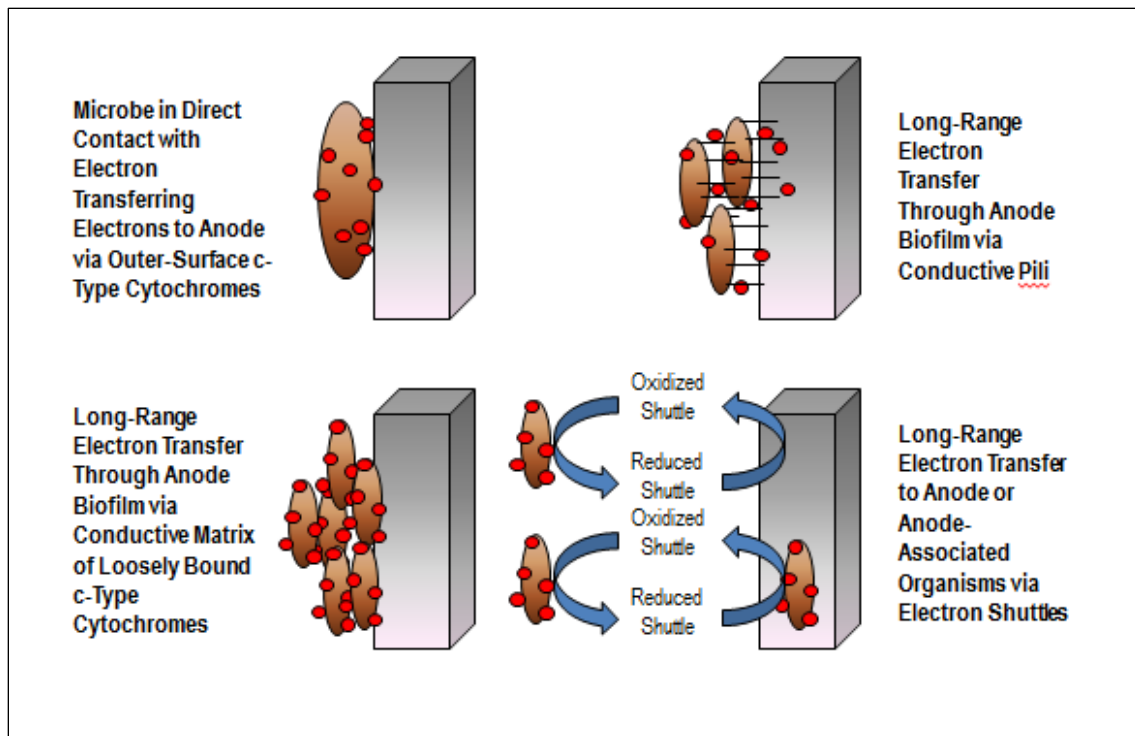


Figure 3. Proposed Mechanisms for Electron Transfer to the Anode (modeled after Lovley, 2008)

Gorby and Beveridge (2005) revealed that conductive “nanowires” or pili were present on both, *Geobacter* and *Shewanella* species of bacteria. They proved the electrical conductivity of these appendages by using scanning tunneling microscopy (STM) and concluded that these nanowires were capable of carrying electrons from the cell to the anode surface. Similarly, Reguera et al. (2005) observed that *G. sulfurreducens* possesses conductive pili or nanowires. In addition, they noted that there is a difference between the structure of the nanowires produced by *G. sulfurreducens* and that of *S. oneidensis*. The appendages of *G. sulfurreducens* are thin and appear to be composed of single strands while the appendages of *S. oneidensis* appear to be thicker “cables” that are made up of smaller conductive nanowires. Reguera et al. (2005)

concluded that the pili of *S. oneidensis* were not conductive, demonstrating that other electron transfer mechanisms can play a role even if cells possess nanowires.

It is also well documented that soluble electron shuttles or chemical mediators can be added to a fuel cell in order to facilitate electron transfer from inside the cell to the outside (Logan, 2004; Bond et al., 2002; Rabaey and Verstraete, 2005). Chemical mediators used in the past include neutral red (Park et al. 1999), thionin potassium ferricyanide (Bond et al. 2002), methyl viologen (MV) (Aulenta et al., 2007; Steinbusch et al., 2010) and anthraquinone-2, 6-disulfonate (AQDS) (Hatch and Finneran, 2008). However, it is now known that mediators do not have to be added to cultures since they are often self-produced. For instance, pyocyanin is an endogenous chemical mediator produced by *Pseudomonas aeruginosa* that can shuttle electrons to the electrode of an MFC (Rabaey et al. 2004). Marsili et al. (2008) showed that riboflavin is another endogenous mediator that is produced by *S. oneidensis* that is capable of shuttling electrons.

Finally, it has been shown that both conductive biofilms and direct contact with the anode may also be viable mechanisms for electron transfer. Reguera et al. (2006) has shown that *G. sulfurreducens* can form a thick, conductive biofilm and that the biofilm is essential for the transfer of electrons in fuel cells that use this culture. Furthermore, *G. sulfurreducens* has been shown to transfer electrons to the anode through c-type cytochromes on the cell surface (Holmes et al., 2008; Kim et al., 2008).

2.1.1.3 Competing Microorganisms and Metabolisms

The efficient conversion of organic material to electricity depends on the microorganism's ability to completely oxidize their organic fuels to carbon dioxide.

However, some microbial populations are simply not capable of achieving complete oxidation (Lovely, 2008). Additionally, some microbial populations are inherently diverse and therefore possess metabolic pathways that are concurrent to oxidation. It is theorized that the anode serves as a convenient surface for attachment and that many microorganisms are carrying out a wide variety of metabolic processes besides electrogenesis. These competing side reactions can divert electrons away from current production (Rismani-Yazdi et al., 2013; Lovely, 2008). An example of a competing reaction process in MFCs is methanogenesis.

The presence of methanogens can be particularly problematic in MFCs because their growth conditions are similar to that of electrode-reducing microorganisms. Additionally, methanogens are prevalent in anaerobic digester sludge, a common inoculum for MFCs (Chae et al., 2010). Since they compete with electrode-reducing bacteria for their substrate at the anode, methanogens inhibit the performance of MFCs. Much research has accomplished to find ways of inhibiting methanogens including air and heat exposure, acid/base treatment, and chemical inhibitors (Kim et al., 2004; Li and Fang, 2007). Primary methanogens for anodic methanogenesis include *Methanosarcinaceae*, *Methanosaetaceae*, *Methanosaeta*, and *Methanobacteriales* (Chae et al., 2010).

Chae et al. (2010) found that lowering resistance and the injection of 2-Bromoethanesulfonate (BES) were effective at inhibiting methanogens. By lowering the resistance from 600 to 50 Ohms, electron loss was reduced by 24%. The addition of BES increased coulombic efficiency (CE) from 35% to 70%. They also concluded that oxygen

stress was effective, but had a detrimental effect on electrode-reducing bacteria. Jung et al. (2005) also performed experiments with BES that yielded a 70% increase in CE.

2.1.1.4 Voltage and Power Generation

The working voltage of MFCs commonly range from 0.3-0.7 V (Logan, 2008). For the purpose of comparison, typical voltages for flashlight batteries is in the range of 1.5 V, car batteries have a voltage of 12 V, and power companies in the United States typically supply 110 V to consumers. The voltage of an MFC, however, is difficult to predict since it is dependent upon the various electron-generating metabolisms of microorganisms. It takes time for bacteria to colonize, competing metabolisms exist, and different bacteria possess different levels of ability in transferring electrons outside of the cell (Logan, 2008).

Many types of MFC designs have been developed. Two-chamber (Oh and Logan, 2006), single-chamber (Liu et al., 2005) flat (Min and Logan, 2004), and tubular (Zuo et al., 2011) designs have all be used in research. Single-chamber air cathode MFCs, however, are known as the easiest ones to scale up because of their high power output, simple design, and lower cost (Cheng and Logan, 2011). MFCs with oxygen have been optimized to reach power densities of 6.9 W/m^2 (normalized to the anode area) (Fan et al., 2008) and 1.55 kW/m^3 (normalized to reactor volume) (Fan et al., 2007). Furthermore, high power densities have only been achieved in laboratory settings with volumes of less than 30 mL (Zhang et al., 2010a; Zhang et al., 2010b; Zhang et al., 2010c). Testing with MFCs of larger volumes has generally resulted in lower power densities of less than 35 W/m^3 (Dekker et al., 2009; Liu et al., 2008). This is an indication of a scale-up issue in the development of MFCs as a source of power

generation. Many variables, including surface area of the electrode (Cheng and Logan, 2007), electrode surface treatments (Feng et al., 2010), solution composition (Liu et al., 2008), and pH (Clauwaert et al., 2009), have been tested in order to better understand scaling factors that contribute to electricity generation.

2.1.2 Other MFC Technologies

MFCs are most notably thought of as either a solution for renewable energy production in the form of electricity or hydrogen gas, wastewater treatment, or a combination of both. Liu et al (2004) furnished the first study that revealed that MFCs could be used to treat wastewater to practical levels while still producing electricity. This demonstration as well as the similar contribution of others (Kim et al. 1999c; Reimers and Tender, 2001; Rabaey et al. 2003) initiated a race to create practical applications and scalable technologies for MFCs in the areas of wastewater treatment and energy production. It is now known that the potential energy benefit from domestic wastewater is large enough to power a treatment plant at 100% energy recovery (Logan, 2008). MFC technologies have energy efficiency values from 2% to 50% (Liu and Logan 2004; Rabaey et al. 2003).

Other well-known MFC technologies include applications as sediment MFCs and as a tool for bioremediation. Reimers and Tender (2001) were the first to publish a paper about sediment MFC technology. With sediment MFCs, the anode is placed into the sediment of the ocean floor where there is a naturally-occurring anaerobic environment and naturally-occurring anode reducing bacteria. The cathode is placed in the seawater above that contains dissolved oxygen. The salinity of the water allows for good ion conduction to connect the anode and cathode. Sediment MFC technologies could be used

as a remote power device to harvest energy from the seafloor or to power data-collecting devices in the ocean.

Bioremediation with MFC technologies is possible as has been shown through the works of Gregory et al. (2004) in nitrate reduction and Gregory and Lovley (2005) to reduce uranium (VI) (2005). With this technology, the anode receives electrons from the degradation of a long-lasting substrate like chitin. At the cathode, also known as a biocathode, electrons are used by bacteria to reduce the contaminants (Logan, 2008). Gregory et al. (2004) used biocathode technology to reduce nitrate to nitrate using river sediments. However, complete denitrification to nitrogen gas was not achieved. Gregory and Lovley (2005) used biocathode technology to reduce soluble uranium (VI) to insoluble uranium (IV). Uranium (IV) was readily removed from solution by the electrodes, and 87% was recovered from the electrode surface.

2.1.3 MFCs as Biosensors

MFC-based biosensing has already been proven to be relevant in the field of water quality monitoring. For example, Di Lorenzo et al. (2009) used single-chamber MFCs with an air cathode for the determination of biochemical oxygen demand (BOD) in wastewater. They found that the MFC outputs correlated linearly with BOD concentrations of up to 350 mg BOD/cm³. Kumlanghan et al. (2007) also used single-chamber MFCs as biosensors in the detection of glucose in solution, further proving the usefulness of MFCs as detectors for organic matter. In this study they correlated the MFC outputs linearly with glucose concentrations in the range of 0.025 to 25 g/L. Additionally, Stein et al. (2012) used MFCs and Butler-Volmer-Monod modeling of the current outputs to evaluate nickel toxicity in water.

A particularly sophisticated approach to modeling the signals produced by an MFC-based biosensor was used by Feng et al. (2013a, 2013b) while using artificial neural networks (ANNs). Their research resulted in the successful prediction of COD concentrations and the identification of four different readily-degradable substrates: acetate, butyrate, glucose, and corn starch. They accomplished this by creating quantifiable metrics that described the MFC signals and inputted them into the ANN. The fully-developed and trained ANNs made no errors in any of the chemical identification or COD concentration tests. This research effort was the first of its kind.

2.2 Artificial Neural Networks (ANNs)

Advances in the development of intelligent systems have led to the design of artificial neural networks (ANNs) to solve many types of problems. ANNs are inspired by human biological neural networks and are differentiated from other computer models for their ability to “learn” like the human brain. These models have become powerful tools in areas such as prediction, forecasting, and recognition in a variety of applications and in various fields including environmental engineering.

2.2.1 Overview and Theory

The human biological neural network functions via an interconnected network of axons, synapses, and dendrites. A neuron receives signals of information through its dendrites and transmits signals back out through its axon. The neural contacts between the nerve cells are called synapses. These synapses are influenced by weighed inputs which can essentially either enhance or inhibit the emission of electrical impulses. The synapse also has a dependence on history which allows it to become more efficient.

When a person experiences something new, changes occur at the synapses and dendrites and new connections are made. The reinforcement of those connections, such as when something is experienced repeatedly, is what forms the building blocks for human learning and memory.

An ANN is a network of computational models that resemble natural neurons. Within this framework an artificial neuron accepts information (inputs) and applies weights to the information. Then, a summation of the weighted inputs is formulated and a computational model within the neuron known as the activation function then determines whether or not the neuron will be activated. In a simple model such as the McCulloch-Pitts model (McColloch and Pitts, 1990), activation depends on a threshold value. A value of either 0 or 1 is assigned as the output depending on whether or not the weighted sum meets the threshold and the information propagates forward. Figure 4 illustrates the concept of an artificial neuron.

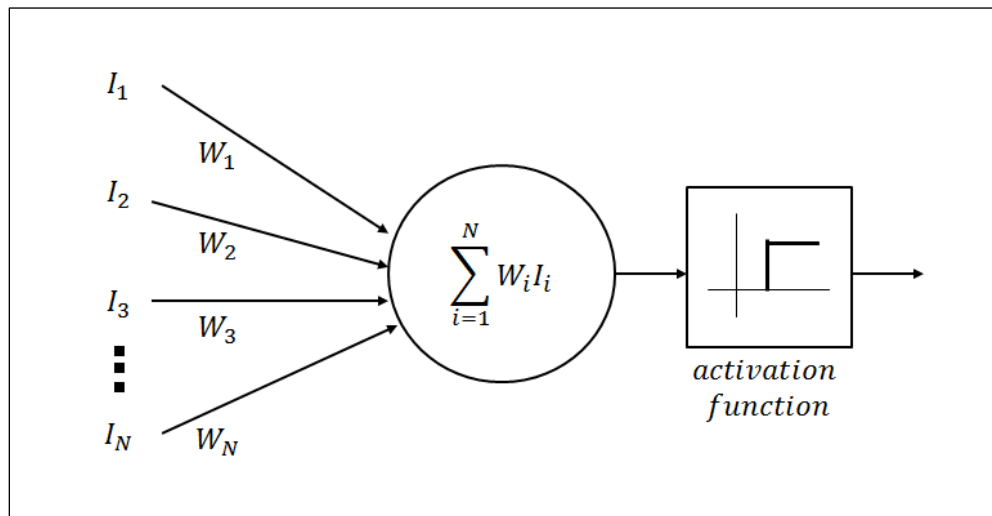


Figure 4. McCulloch-Pitts Model of an Artificial Neuron (modeled after Krogh, 2008)

In a simple classification problem, a hyperplane exists to help differentiate the inputs that result in a 0 and inputs that result in a 1. A hyperplane, as shown in Figure 5, can be thought of as a regular plane in space. For a two dimensional problem, the hyperplane is simply a straight line. This hyperplane represents the threshold value. The ANN takes on the task of determining where the hyperplane is for every neuron in the network so that it can correctly solve the problem.

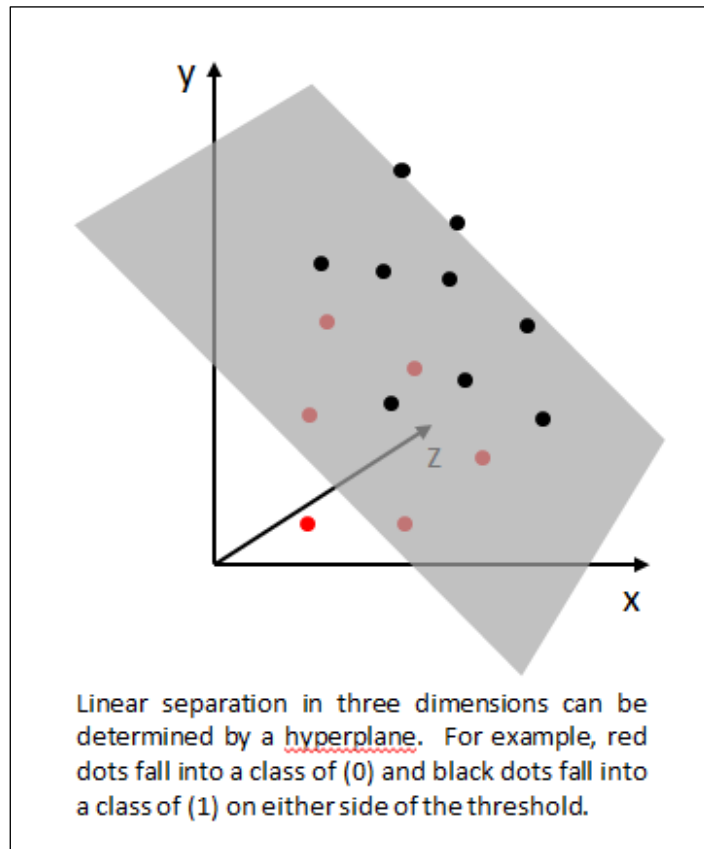


Figure 5. Conceptual Illustration of a Hyperplane (modeled after Krogh, 2008)

2.2.2 Development and Training

The process of setting weights to the inputs and the determination of a threshold value is how the ANN is trained. Each time the ANN receives new information,

algorithms allow it to make small changes to the weights and thresholds. The result is that the hyperplane shifts slightly. This happens incrementally until the error in the model is minimized to the fullest extent possible.

Feed-forward ANNs function through the implementation of a back-propagation algorithm. Initially, the inputs are assigned random weights and an output is generated. Then the system-generated output is compared to the desired output and the amount of error is calculated. Errors are propagated backwards through the model, the weights are adjusted, and more outputs are generated until the error is minimized. This pattern of events occurs every time something new is experienced by the model and is often repeated hundreds of times until the either the error is minimized or there is no error in the model. Corrections like this can be accomplished analytically in linear regression. However, there is no analytical solution in ANNs that possess multiple layers of hidden neurons as is shown in Figure 6.

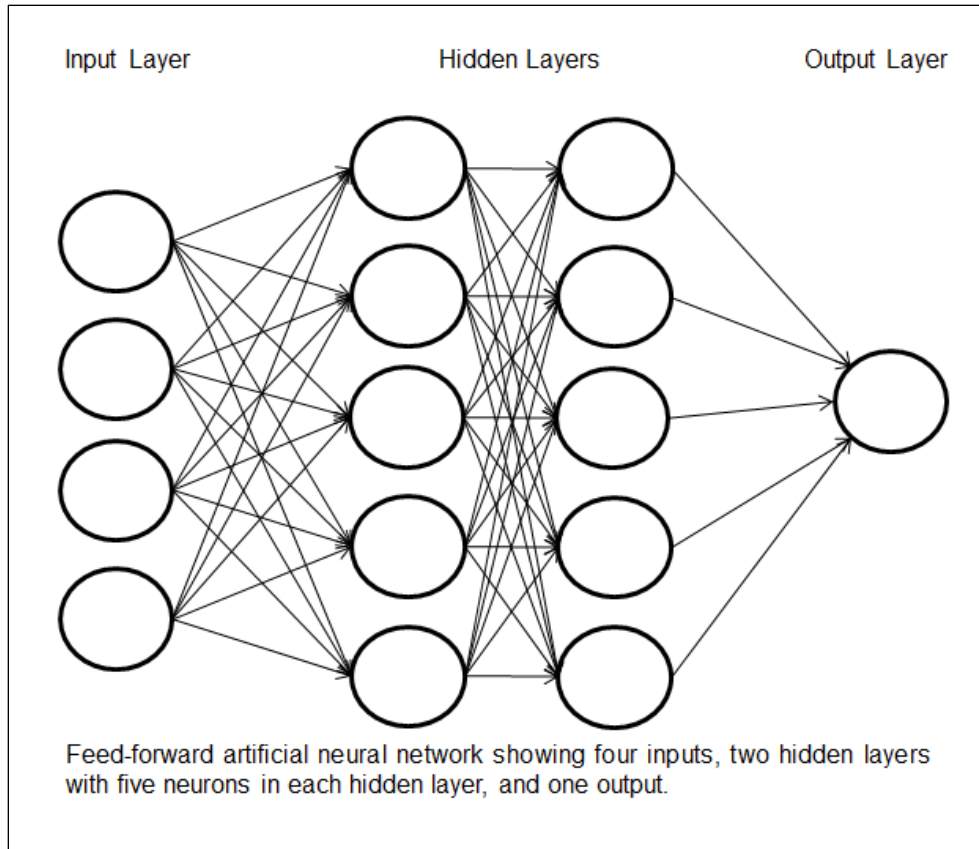


Figure 6. Feed-forward ANN

2.2.3 ANNs in Environmental Modeling

Aside from the aforementioned works of Feng et al. (2013a, 2013b), ANNs have been used for multiple applications in environmental modeling efforts. For example, Maier et al. (2004) used ANN modeling in order to predict optimal alum doses and other water quality parameters. They used raw data from Australian surface waters to train and develop an ANN that successfully predicted turbidity, color, and ultraviolet absorbance with coefficient of correlation (R^2) values ranging from 0.90 to 0.98 in a comparison of the predicted values to actual values. They also formulated an ANN model that accepted those water quality parameters as inputs and generated residual alum concentrations and

pH as outputs. The R^2 values for these outputs were 0.96 for alum concentrations and 0.85 for pH. This ANN model was developed into a simulation tool for water treatment operators to use, saving time over traditional jar tests.

In another water quality application, Gazzaz et al. (2012) designed a three-layer ANN for the calculation and forecasting of water quality index for the Kinta River in Malaysia. They used multiple water quality parameters as inputs in a feed-forward ANN with water quality index as the output. The predicted values had strong correlations ($R^2 = 0.977$) to the actual values. The intent of the study was to provide analysts with an alternative to time-consuming water quality index calculations.

ANNs have also been applied to air quality matters. Perez (2012) used local air quality data in Santiago, Chile to develop an ANN that could be used in air quality forecasting. The ANN was combined with a nearest neighbor method to predict particulate matter (PM-10) conditions with accuracy levels of the order of 90%. This model was actually used by environmental authorities for air quality management in Santiago from 2009 to 2011 substantiating its use as a tool for air pollution control elsewhere.

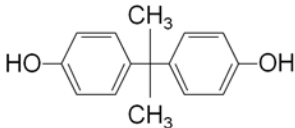
2.3 Organic Industrial Pollutants in the Environment

Three organic chemicals have been chosen for analysis in this study for their potential relevance to Department of Defense (DoD) applications. Aldicarb, dimethyl methylphosphonate (DMMP), and bisphenol-A (BPA) all represent classes of chemicals known to pose priority industrial chemical hazards and risks to deployed troops and military operations (Hauschild and Bratt, 2005). These chemicals are not readily

biodegradable and have never before been used in the testing of MFC-based biosensing.

The structures of the studied chemicals are shown in Table 1.

Table 1. Chemical Structure of the Three Chemicals Under Study

Organic Industrial Pollutant	IUPAC Chemical Name	Structure
<u>Aldicarb</u>	2-Methyl-2-(methylthio)propanal O-(N-methylcarbamoyl)oxime	$ \begin{array}{c} \text{CH}_3 \qquad \qquad \text{O} \\ \qquad \qquad \qquad \\ \text{CH}_3-\text{C}-\text{HC}=\text{N}-\text{O}-\text{C}-\text{NH}-\text{CH}_3 \\ \\ \text{S}-\text{CH}_3 \end{array} $
<u>Dimethyl methylphosphonate</u>	(methoxy-methylphosphoryl)oxymethane	$ \begin{array}{c} \text{O} \\ \\ \text{H}_3\text{C}-\text{P}-\text{OCH}_3 \\ \\ \text{OCH}_3 \end{array} $
<u>Bisphenol-A</u>	4,4'-(propane-2,2-diyl)diphenol	

2.3.1 Aldicarb

Aldicarb ($\text{C}_7\text{H}_{14}\text{N}_2\text{O}_2\text{S}$) is a carbamate pesticide and nematicide and is produced in the United States by Bayer CropScience under trade name Temik. It is a systemic insecticide that is taken up by the roots of plants, protecting them from pests such as aphids, mites, flies, beetles, and maggots. As of 2007, the pesticide was used on a wide variety of crops such as peanuts, potatoes, sorghum, soybeans, sweet potatoes, citrus fruits, and many others (USEPA, 2007). However, in 2010 the EPA announced its intentions to terminate all uses of the chemical because of its potential to cause neurotoxic effects in humans. A risk assessment was conducted by the EPA resulting in the agency's determination that the chemical no longer met food safety standards and that

it might pose unacceptable dietary risks to infants and children. As a result, the primary producer of the chemical, Bayer CropScience, agreed to voluntarily phase out production of the chemical by 2015 and end all remaining uses in 2018. Aldicarb is not available to the public for residential applications (USEPA, 2010). The toxic effects of aldicarb have led to bans or restrictions in other countries (e.g. Europe). However, aldicarb is still used for agricultural applications in some countries around the world (Maran et al. 2009).

Both the production of aldicarb and the use of the chemical as a pesticide can lead to direct releases to the environment. Aldicarb is highly soluble in water (4930 ppm) and degrades slowly with half-lives of approximately 62 days (anaerobic conditions) and 34-94 days (aerobic conditions) (H.S.D.B., 2013a). K k et al. (1999) has shown that aldicarb can be moderately biodegradable, observing complete degradation in 4 days using cultures of *Methylosinus*. Hydrolysis half-lives for aldicarb in water have been reported in ranges from 6 days (pH 9.85; 20 C) to 559 days (pH 6.02; 20 C) (Given and Dierberg, 1985). Aldicarb is not known to readily adsorb to suspended solids or sediment and volatilization from water surfaces is not expected to be an important environmental fate process. The persistence of aldicarb in soil can range from 1-15 days (H.S.D.B., 2013a).

2.3.2 Dimethyl Methylphosphonate (DMMP)

Dimethyl methylphosphonate (C₃H₉O₃P) is a colorless liquid that has an industrial application as a flame retardant, a preignition additive for gasoline, an antifoam agent, a plasticizer and stabilizer, a textile conditioner and antistatic agent, and an additive for solvents and low-temperature hydraulic fluids. DMMP also belongs to a group of chemicals known as organo-phosphorous compounds and shares similarities to nerve

agents. In 1976, the U.S. Army selected the chemical for toxicological and carcinogenic research because it was being considered for use as an anticholinesterase agent simulant (D.H.H.S., 1987). The military has used the chemical as a Sarin simulant in the testing of personal protective equipment such as gas masks and filters (Mahle et al., 2003). It is a weak cholinesterase inhibitor and is an irritant of the skin, eyes, mucous membranes and upper respiratory tract (N.O.A.A., 2013). There is some evidence of carcinogenic activity for DMMP in animal studies, though it is not currently listed as a human carcinogen (H.S.D.B., 2013c).

If DMMP is released into the environment, it has a high mobility in soil and possesses a moderate volatility from water surfaces. Volatilization half-lives have been modeled to be 22 days for rivers and 240 days in lakes (H.S.D.B., 2013c). Additionally, DMMP is fully miscible in water (Bennett and Philip, 1928). The chemical has an estimated bioconcentration factor of three, which means that it has a low potential for bioconcentration in aquatic organisms. DMMP can be persistent in the water with a hydrolysis half-life of 124 days at pH 7. Finally, biodegradation in water is not considered a prominent environmental fate process (H.S.D.B., 2013c).

2.3.3 Bisphenol-A (BPA)

BPA ($C_{15}H_{16}O_2$) is widely used in the production of certain polyester resins, flame retardants, epoxy, and polycarbonate. These products are used in food and drink packaging, dental fillings, and many other products. As a result, it is common to detect BPA in industrial and municipal wastewater (Stasinakis et al., 2010). BPA is a known endocrine disrupting compound, is weakly estrogenic, and has been shown to cause reproductive and developmental effects in animal studies (USEPA, 2013).

The production of BPA and use in industrial applications can lead to releases to the environment. It is estimated that over one million pounds of BPA is released into the environment per year in the U.S. (USEPA, 2013). BPA has a low volatility, low solubility (300 ppm), and it is not readily degradable in water (H.S.D.B., 2013b). However, there is evidence to suggest that BPA is moderately biodegradable (Robinson and Hellou, 2009) in natural environments such as seawater. It should also be noted that studies have shown no evidence of biodegradation in seawater (Kang and Kondo, 2005) and groundwater aquifers (Ying et al., 2003) indicating that some microbial communities may be more suitable than others in the biodegradation of BPA.

III. Research Objectives

The overall goal of this study is to evaluate the potential of MFC-based biosensing for the purpose of monitoring water quality for industrial chemicals that are relevant to DoD activities. The specific objectives are as follows:

- (1) The first objective is to determine if an analysis of the raw metrics can produce correlations that can be used in the identification of chemical type or chemical concentration.
- (2) The second objective is to integrate ANNs into MFC-based biosensing for the identification and quantification of specific organic pollutants.
- (3) The third objective is to determine the effect of using the feed medium as a solvent on the identification of organic pollutants via the ANN.
- (4) The fourth objective is to determine the effect of chemical mixtures on the identification of organic pollutants via the ANN.

This study is expected to be the first to provide insight into the usefulness of MFC-based biosensing to detect and quantify organic pollutants that are toxic and not readily biodegradable. All of the efforts described within this work aim to expand upon the existing knowledge base of MFCs as biosensors and to demonstrate the usefulness of MFCs as a water quality monitoring device.

IV. Materials and Methods

The overall strategy involved the injections of aqueous solutions of dissolved chemicals into the MFCs in order to generate a response in the form of electric current. Each injection of chemical resulted in a single electric current profile that was evaluated on the basis of six separate metrics. Those metrics were: Peak Height (PH), Peak Area (PA), Acceleration Rate (AR, i.e. rate of increasing charge), Subsidence Rate (SR, i.e. rate of decreasing charge), 10-hour Subsidence Rate (10SR, i.e. rate of decreasing charge over a 10 hour period), and First Moment (FrM). For each set of experiments, manual correlations were attempted first in order to determine whether further processing of the data was required. For example, each metric was plotted against chemical concentration to evaluate basic correlations within the data. Then, ANNs were trained and tested with the same data sets to see if the required correlations could be made and to determine if useful outputs could be generated to support the use of ANNs with biosensors in the detection of organic pollutants in water. Systematic testing was accomplished for the purpose of quantification of chemical concentration and identity of the chemical. In addition, testing included the determination of chemical type when the feed medium was used as a solvent. Lastly, experiments were performed to determine whether or not the discrimination of mixtures was possible.

4.1 Microbial Fuel Cell Configuration and Operation

Six single-chamber MFCs were utilized and operated as batch reactors in this study. Two MFCs were used for each of the three sets of stepwise tests. MFC #5 and MFC #10 were used for quantification and identification experiments. MFC #6 and MFC

#7 were used in the evaluation of solvent effects. Finally, MFC #8 and MFC #9 were used in the tests incorporating mixtures of chemicals.

Two different single-chamber MFC designs were used. The only difference between the designs was a slight variation in the construction of the anode. In one design, an acrylic tube (2.25" OD; 2" ID) served as the anode chamber and was clamped between two acrylic plates (3" x 3" x 0.38"). In the other MFC design, the only notable difference was that it had been constructed by using three acrylic plates instead of two. In this design, the housing for the anode chamber was created by hollowing out the middle plate instead of using an acrylic tube. All MFCs in both designs had an anode chamber volume of approximately 40 mL. Carbon fiber was used as the anode and inlet and outlet valves were inserted into the anode chamber for draining and feeding. A cation exchange membrane (CEM) and an air-exposed cathode was also used. The air-exposed cathode was coated with powdered activated carbon and 5% platinum, then further enhanced with a separate piece of carbon fiber to increase contact area with the alligator clips. Both electrodes were connected via alligator clips and an external resistor. Both 47 Ω (MFC #5, #6, #7 and #8) and 470 Ω (MFC #9 and #10) resistors were used. Electrodes were connected via copper wire to a Keithley meter (Model 2750) to monitor voltage outputs from the MFCs. The Keithley meter served as a volt meter to measure the voltage drop across the resistors. Data collected by the Keithley meter was converted into electronic database format via the ExceLINX program (Keithley Co.) for analysis. The operating temperature in the laboratory was approximately 21 °C . These MFCs were originally built and inoculated for research performed by Feng et al (2013a, 2013b).

Figure 7 and Figure 8 show details pertaining to MFC design and the overall system set-up used in this study.

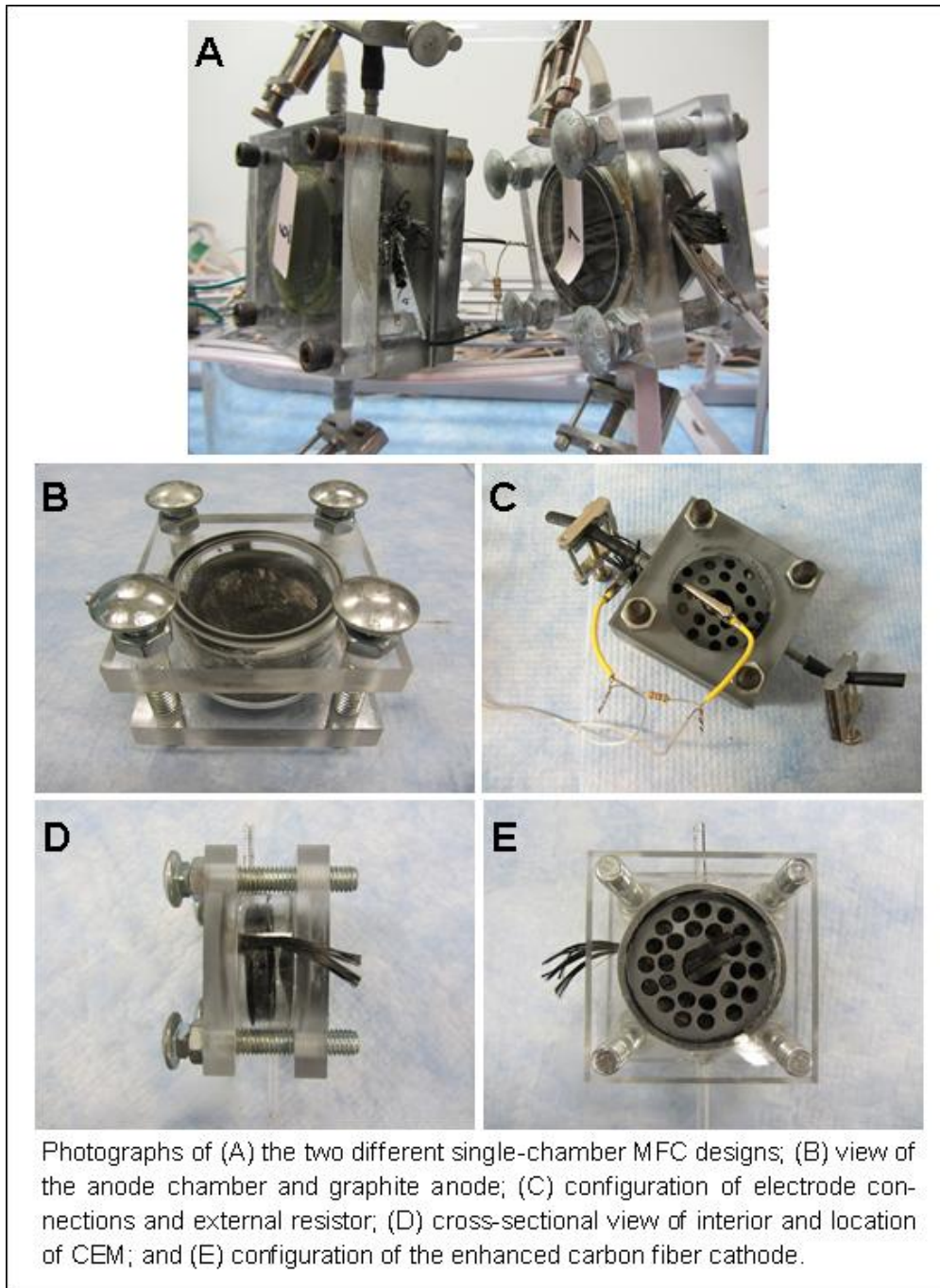


Figure 7. MFC Design and Configuration

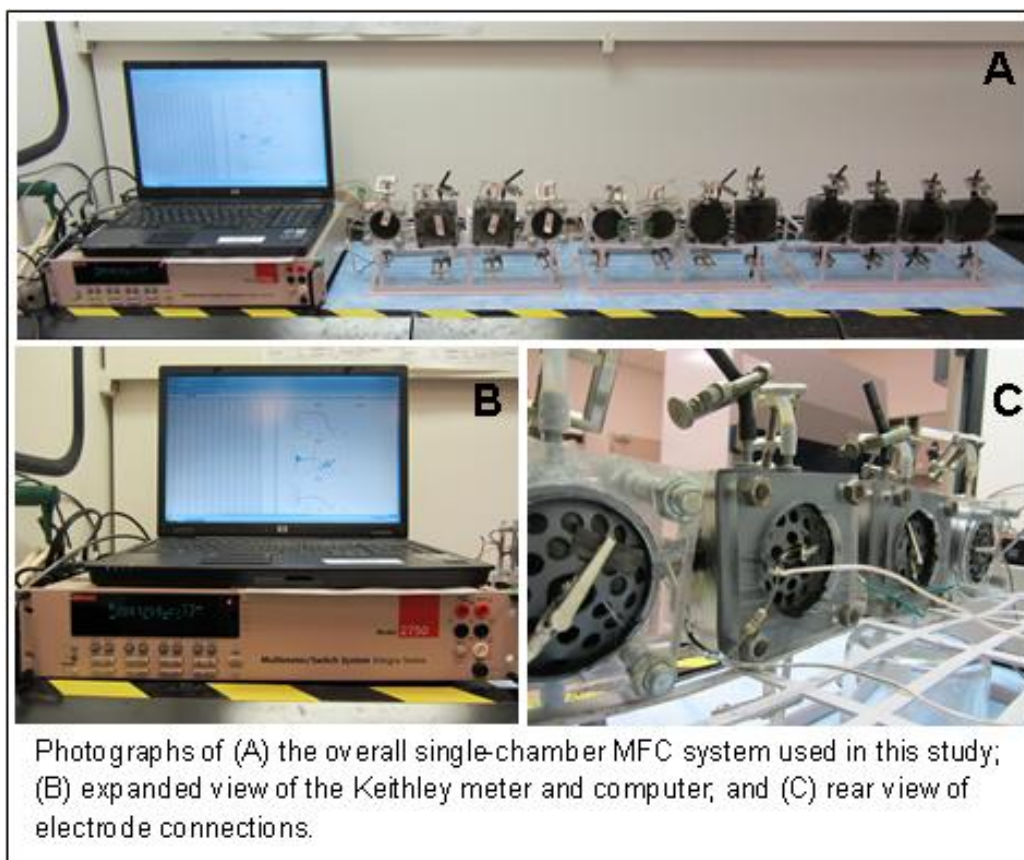


Figure 8. Overview of System Set-up

4.2 Synthetic Solutions

Four types of synthetic solutions were used for the duration of the experiment. A standard feed medium, adopted from Feng et al. (2013a, 2013b), was used as a proven source of reliable charge. The feed medium was an acetate-based aqueous solution composed of the following substrates: $C_2H_3NaO_2$, 430 ppm; NH_4Cl , 20 ppm; KH_2PO_4 , 1360 ppm; K_2HPO_4 , 200 ppm; $MgCl_2$, 250 ppm; $CoCl_2$, 20 ppm; $ZnCl_2$, 10 ppm; $CuCl_2$, 10 ppm; $CaCl_2$, 4 ppm; and $MnCl_2$, 10 ppm. Additionally, aqueous solutions for each of the three chemicals used in the experiment were created at different concentration levels. The three chemicals tested included aldicarb, DMMP, and BPA. Aldicarb was purchased

from Ultra Scientific in a solvent matrix form at a concentration of 100 $\mu\text{g/mL}$ in acetonitrile. DMMP was purchased from Sigma Aldrich in a purum ($\geq 97\%$) liquid form. BPA was purchased from Sigma Aldrich in a crystalline solid (97% purity) form. Since BPA has a low solubility in water, 8E-3 g of the chemical was first dissolved into 2 mL of Methanol, then dissolved into 1.0 L of water. Finally, this 8 ppm stock solution of BPA was diluted to the concentrations outlined in this study. All water used in the composition of solutions was purified through reverse osmosis (RO).

4.3 Enrichment

All MFCs were inoculated with activated sludge as a source of bacteria. Previous studies have also utilized activated sludge as an inoculation medium for MFCs (Park and Zeicus, 2003; Kim et al., 2004b; Fan et al., 2007). All activated sludge was obtained from the Fairborn Water Reclamation Facility in Fairborn, Ohio. Raw activated sludge was mixed with the feed medium in a 1:3 ratio and injected into the MFCs until the response peaks stabilized for a minimum of three consecutive feedings. Stabilization was measured by a $\pm 5\%$ change in maximum charge. After stabilization was achieved, the MFCs were deemed ready for the stepwise testing experiments. Feeding intervals for inoculation was spaced at a time period of approximately 48 hours and injections were accomplished by using a 60 mL disposable syringe.

4.4 Analytical Methods

Testing schedules and procedures were similar for each of the three main experiments in this study. For this stage of testing the overall methodology involved the injection of the chemical solution for eight consecutive injections, an intermittent

injection of standard feed medium, followed by eight consecutive injections of chemical solution for the next stage of testing. The intermittent injection of feed medium was introduced in order to revive the microbial community within the MFC since it was not known whether the chemicals would have a detrimental effect on the microbial population. The amount of consecutive injections was set at eight because it was deemed a conservative amount to enable the collection of enough data for ANN processing. This pattern proceeded until the experiment was complete. Stability of the peaks was not sought after since the testing was intended to simulate real-time monitoring. Intervals between injections remained constant at roughly 48 hours.

4.4.1 Quantification and Identification Testing

Stepwise testing for each chemical was accomplished for the quantification and identification testing. Each chemical was introduced at three concentration levels during the stepwise tests and in the pattern described above. Both aldicarb and BPA were introduced at the concentrations of 800 ppb, 400 ppb, and 200 ppb, and in that order. DMMP was injected at concentrations of 916 ppm, 458 ppm, and 229 ppm so that (1) charge outputs from a wider range of chemical concentrations could be observed and (2) the higher concentrations might better simulate a chemical spill event where MFC-based biosensing could be used as a decision support tool.

4.4.2 Solvent Effects Testing

The goal of the solvent effects experiments was to determine whether or not the presence of the feed medium as a solvent, as opposed to RO water as a solvent, would have an effect on the ability to detect the chemical type. Since the feed medium promotes microbial activity and the exogenous transfer of electrons, increased microbial

activity could either enhance the responses making them more easily discernible or serve to mask any inhibiting effect that the chemical had on the electrode-reducing microorganisms.

During these tests only one concentration per chemical was used. For consistency, the maximum concentrations used in the quantification and identification tests were selected for use. For instance, a concentration of 800 ppb was used for both aldicarb and BPA and a concentration of 916 ppm was used for DMMP. During these tests an aqueous solution of a chemical was injected for eight consecutive feedings, followed by an injection of feed medium, followed by eight consecutive feedings of the same chemical dissolved in feed medium. This pattern of feedings continued until all chemicals were tested in both their aqueous and feed medium form and the experiment was complete.

4.4.3 Mixtures Testing

Testing with mixtures was intended to determine if the ANN could be used to distinguish mixtures of chemicals from individual chemicals. During this set of experiments the concentrations of each chemical remained constant for both reasons of simplicity and consistency with the other experiments. For aldicarb and BPA an aqueous concentration of 800 ppb was used. For DMMP an aqueous concentration of 916 ppm was used. For mixtures such as a mixture of BPA and DMMP, the solution contained 800 ppb of BPA and 916 ppm of DMMP. The testing procedure involved eight consecutive injections of each mixture (aldicarb/BPA, aldicarb/DMMP, and DMMP/BPA) with an intermittent injection of the feed medium. Then, each chemical

was individually injected at its own respective concentration for eight consecutive injections with an intermittent injection of the feed medium.

4.5 Artificial Neural Network Development

ANNs have a proven ability to solve complex problems via algorithms that mimic the learning processes of the human brain. In this study a customized, feed-forward network was developed and tested with matrices of four simultaneous inputs, up to five hidden layers, and one output.

The quantitative metrics obtained from charge profiles and used as ANN inputs included Peak Height (PH), Peak Area (PA), Acceleration Rate (AR), Subsidence Rate (SR), 10-hr Subsidence Rate (10SR), and First Moment (FrM). PH, PA, AR, and SR were selected because of their proven usefulness in the ANN as discovered by Feng et. al (2013a, 2013b). Additionally, two new metrics that have never been used before (10SR and FrM) were created to determine their utility as inputs. A visual description of these metrics can be seen in Figure 9. Response peaks that were caused by defective electrode connections or other errors were omitted from all analysis.

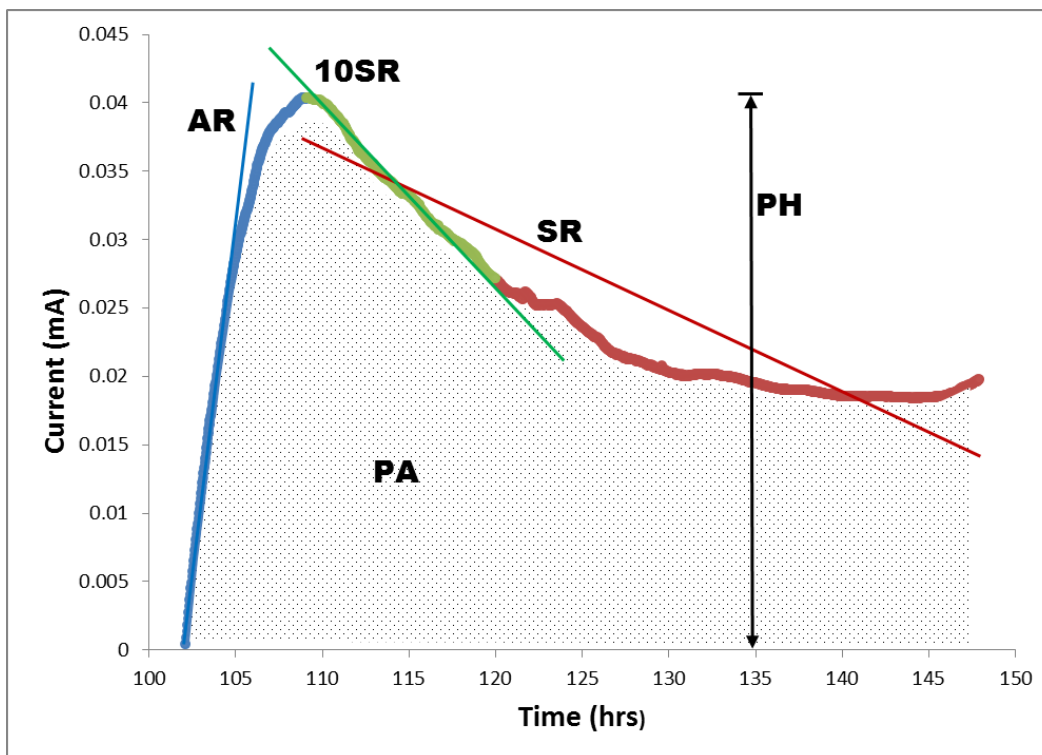


Figure 9. Description of Metric Information for MFC Response Peaks

Excluded from Figure 9 is a description of FrM. FrM is typically used in the finding of centroids and centers of mass. However, in this study it was selected as a way to characterize the wide variety of response curve shapes that were produced by the introduction of different chemicals. FrM, often referred to as the first of area about the y-axis, is calculated by Equation 1 and Figure 10 below.

$$Q_y \approx \sum_a^b x \delta A = \sum_a^b x f(x) \delta x \rightarrow \int_a^b x f(x) dx \quad (1)$$

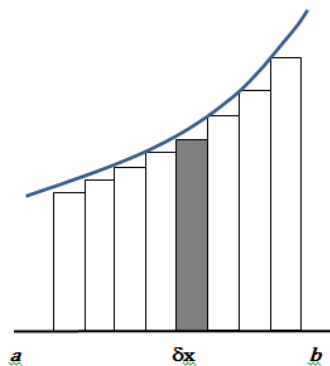


Figure 10. Corresponding Figure for Equation 1

The ANN code used during this study accepted a matrix of four metrics in the input layer. The first set used was [PH, PA, AR, SR] which mirrored the proven input set used by Feng et al (2013a, 2013b). Additionally, to incorporate the new un-tested metrics the input sets of [PH, PA, AR, 10SR] and [PH, PA, AR, FrM] were used. All three sets of inputs were used for each set of experiments in this study. Figure 11 describes the basic architecture of the feed-forward ANN.

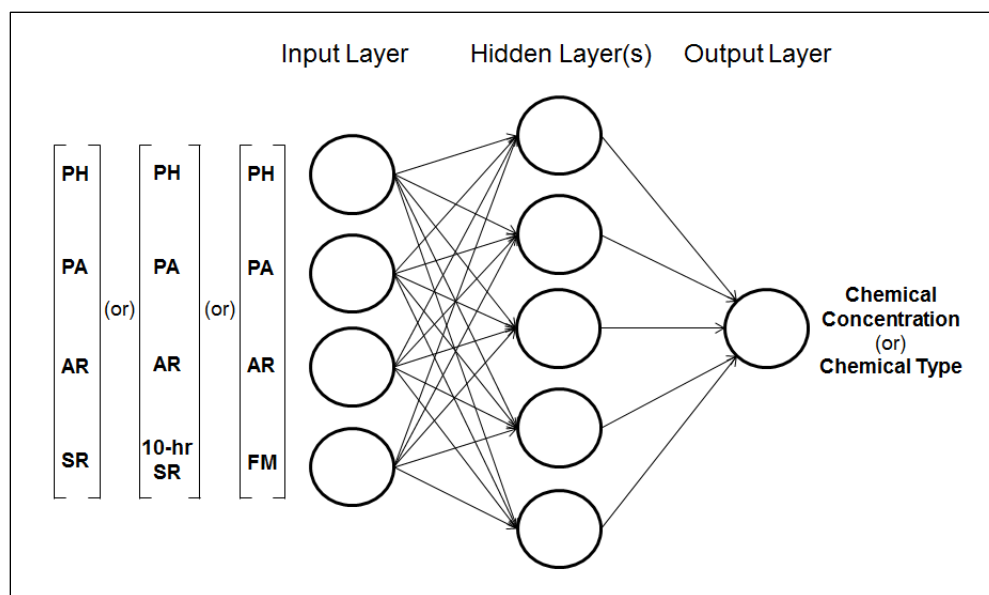


Figure 11. Basic ANN Architecture

The ANN functions through a three-step process of training, validation, and testing. First, the ANN interprets each response curve via a matrix of four input values that are associated with it. The model randomly selects and uses 80% of the data set to train and develop its own correlations, weights, and network parameters within the data. This parameter (80%) was selected to optimize the performance of the ANN (Appendix M). Second, the ANN uses 10% of the data for validation. In this step, the performance of the network is estimated and stopping points for training are established. Third, another randomly selected 10% of the data is used to test the ANN. During testing, the effectiveness of the stopping points and the overall performance of the model are evaluated. Five tests are accomplished during every ANN run to evaluate the use of 1 to 5 hidden layers of artificial neurons. During testing, the model generates a value for a specified output parameter (i.e. concentration or chemical type) based on its own correlations, then matches that predicted value against the actual value to determine accuracy. The ability to evaluate the MFC responses via multiple metrics simultaneously is what gives the ANN so much more utility over basic manually-derived correlations.

V. Results and Discussion

5.1 Quantification and Identification

5.1.1 Laboratory Tests

5.1.1.1 Quantifying Chemicals with Direct Correlations

Figure 12 and Figure 13 display the operating history for MFC #5 and MFC #10, respectively. The figures display all response data from the beginning of the stepwise testing stages to the end of the experiment. Intermediate feedings with the standard feed medium are annotated in red. Intermediate use of the feed medium between the DMMP concentrations of 916 and 458 ppm were not recorded due to a loss of communication between the Keithley Meter and the computer. Several electrical signals with PH greater than 0.45 mA were observed MFCs 5 and 10. Although the reason for these peaks is not clear, they are unlikely to be related to the biological activity in the MFCs and are not included in the correlations presented in this thesis. Most of the electrical signals begin with a region showing negative current; this is likely due to faulty electrical connections and corrosion occurring on the alligator clips. Both of these MFCs were operated under the same conditions. Qualitatively, all response peaks generally display an expected rise in current followed by a slower, more gradual, subsidence rate. Figure 12 shows that when 800 ppb of aldicarb was injected into MFC #5, the PH was initially around 0.05 mA and it gradually increased to approximately 0.20 mA. When the aldicarb concentration was 400 ppb PH decreased from approximately 0.15 mA to 0.05 mA, and when the aldicarb concentration was 200 ppb, the PH values were between 0.15 and 0.20 mA. These data, as well as the data shown in Figure 13 show that the PH of the signals

was highly dynamic. The DMMP signals were qualitatively different from aldicarb signals and smaller, with PH values less than 0.019 mA. Furthermore, the BPA signals were qualitatively different from the other two chemicals with PH values less than 0.009 mA.

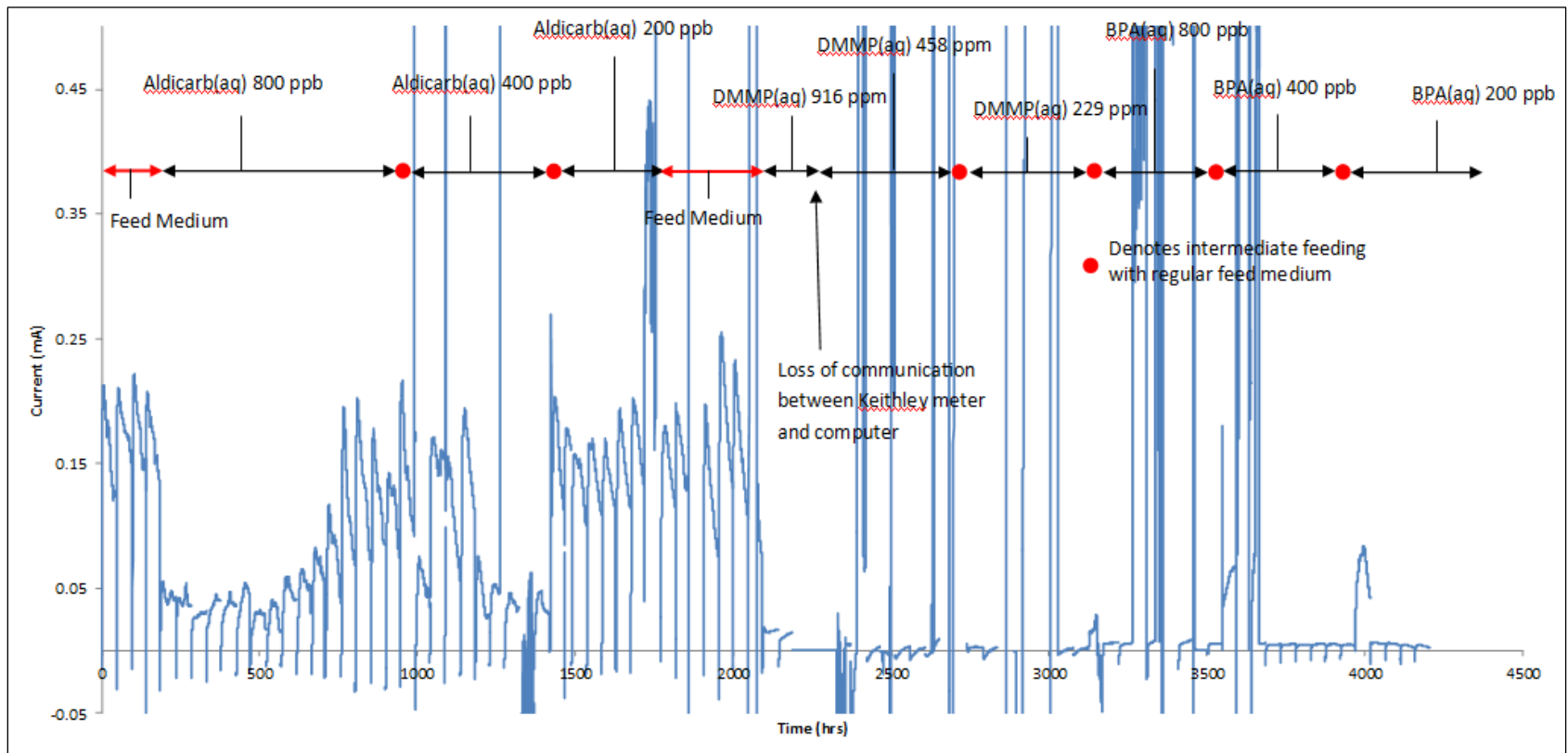


Figure 12. Operating History for MFC #5

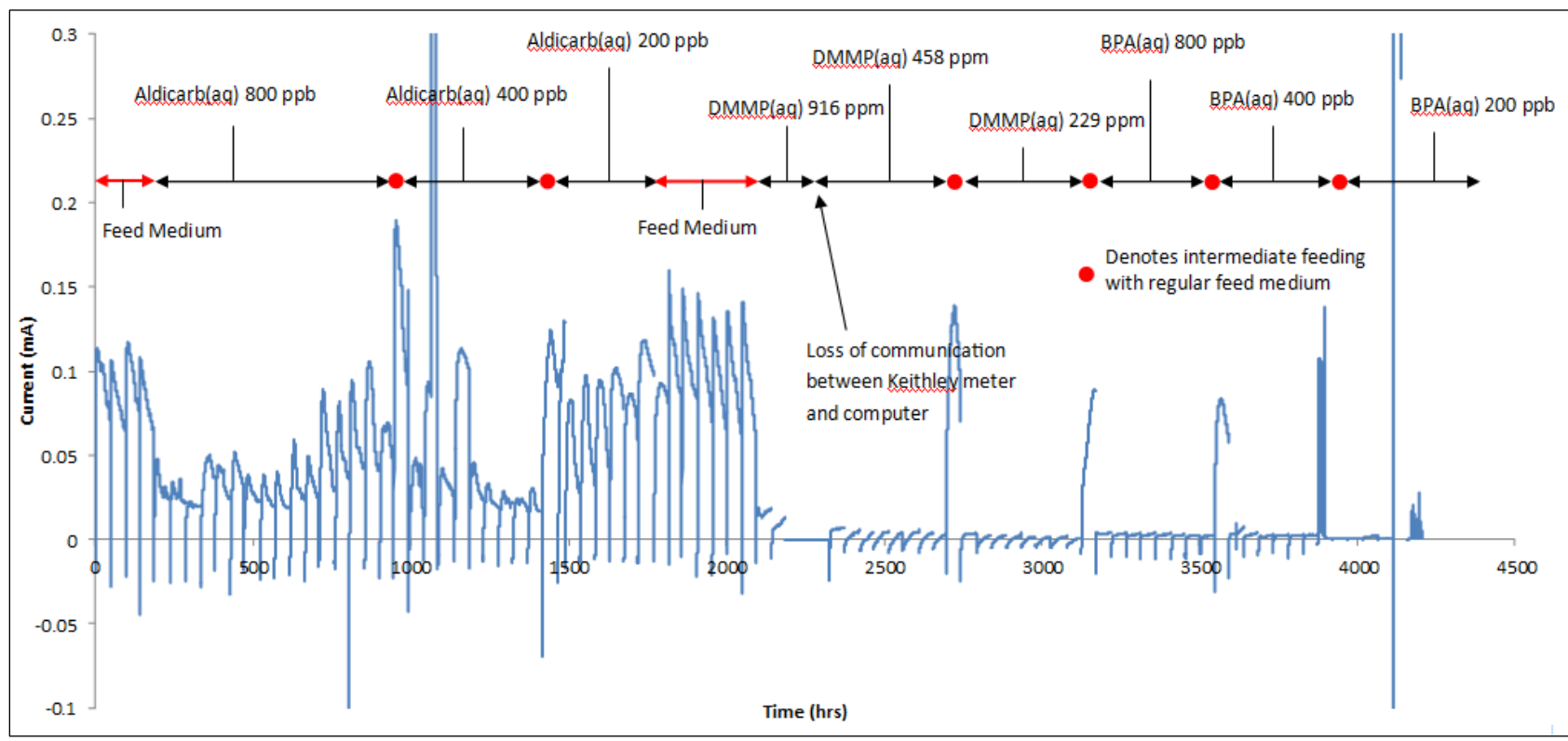


Figure 13. Operating History for MFC #10

Table 2 and Table 3 show the minimum and maximum quantitative properties for all categories of response peak metrics. A comparison of the two tables reveals the quantitative similarities between the two MFCs. Even the relative scale and shape of the response peaks of MFC #5 and MFC #10 are similar, which can be seen in Figure 12 and Figure 13. This is surprising considering the differences between resistor values (47 Ω :MFC #5: and 470 Ω :MFC #10), MFC design, and the complexities and variables associated with the two microbial populations.

Figure 14, Figure 15, and Figure 16 show typical peaks generated by all three chemicals and at each concentration in MFC #10. Figure 14 shows that, in the case of aldicarb, the 800 ppb signals had smaller PH and PA values than the 200 ppb signals, while the smallest PA and PH values were associated with 400 ppb signals. These findings are consistent with the idea that aldicarb is unlikely to serve as a substrate for electrode-reducing microorganisms, because the largest signals are associated with the smallest aldicarb concentration (i.e., 200 ppb). However, it is likely affecting the electrode-reducing microorganisms in a number of ways, including direct inhibition or by inhibiting competing populations (e.g. methanogens). The DMMP signals did not have normally distributed current values, and they tended to plateau after approximately 24 hours making them qualitatively distinguishable from aldicarb signals (Figure 15). The largest PA and PH values were associated with the 916 ppm signals, while the 458 and 229 ppm signals had similar PH and PA values. The BPA signals showed a quick rise in electrical current, followed by a relatively stable current. The BPA signals reached a plateau after approximately 10 hours. The size of the signals increased as the BPA

concentration increased. Figure 14 through Figure 16 are also representative of the type of data obtained for MFC #5.

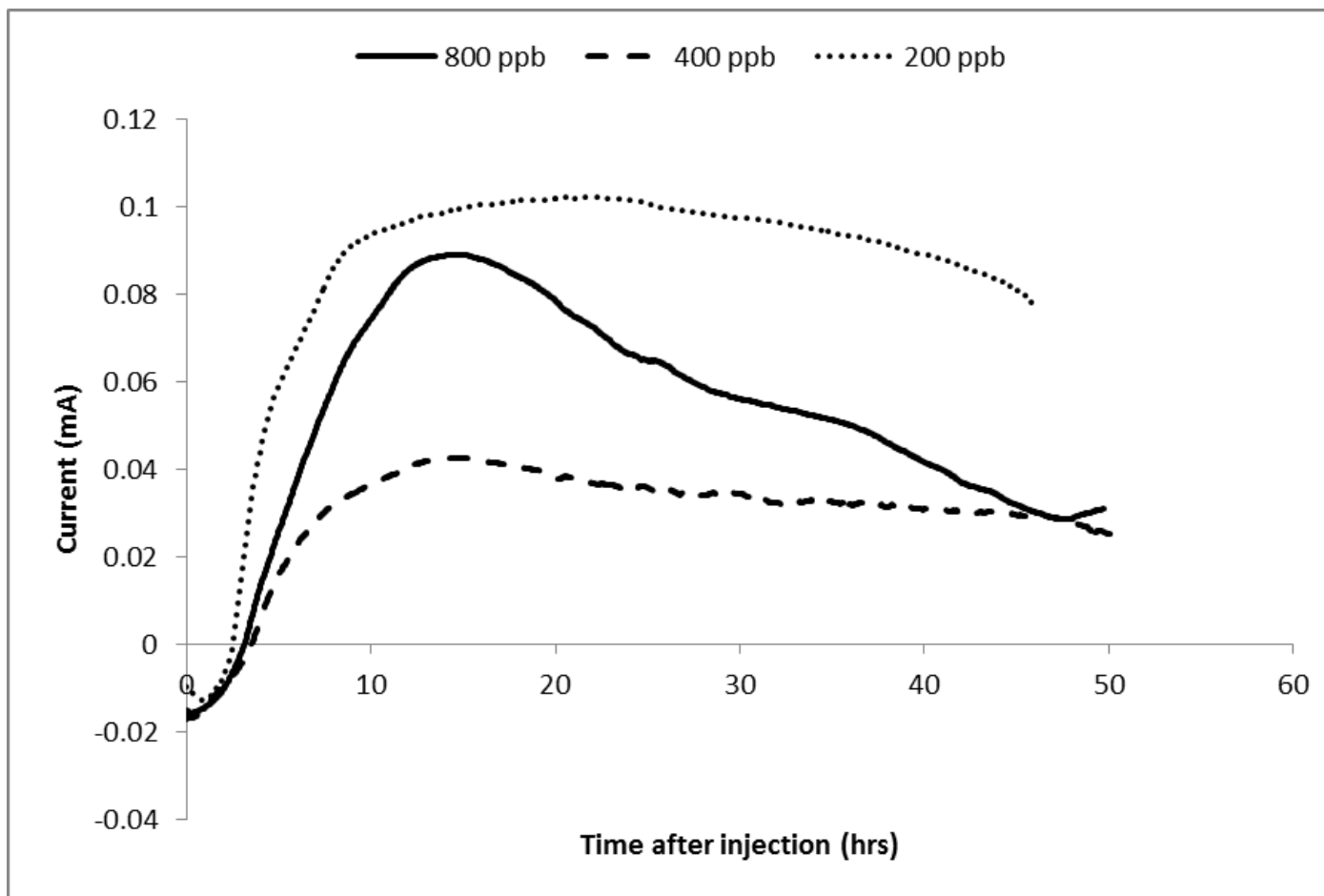


Figure 14. Typical Response Peaks for Aldicarb in MFC #10

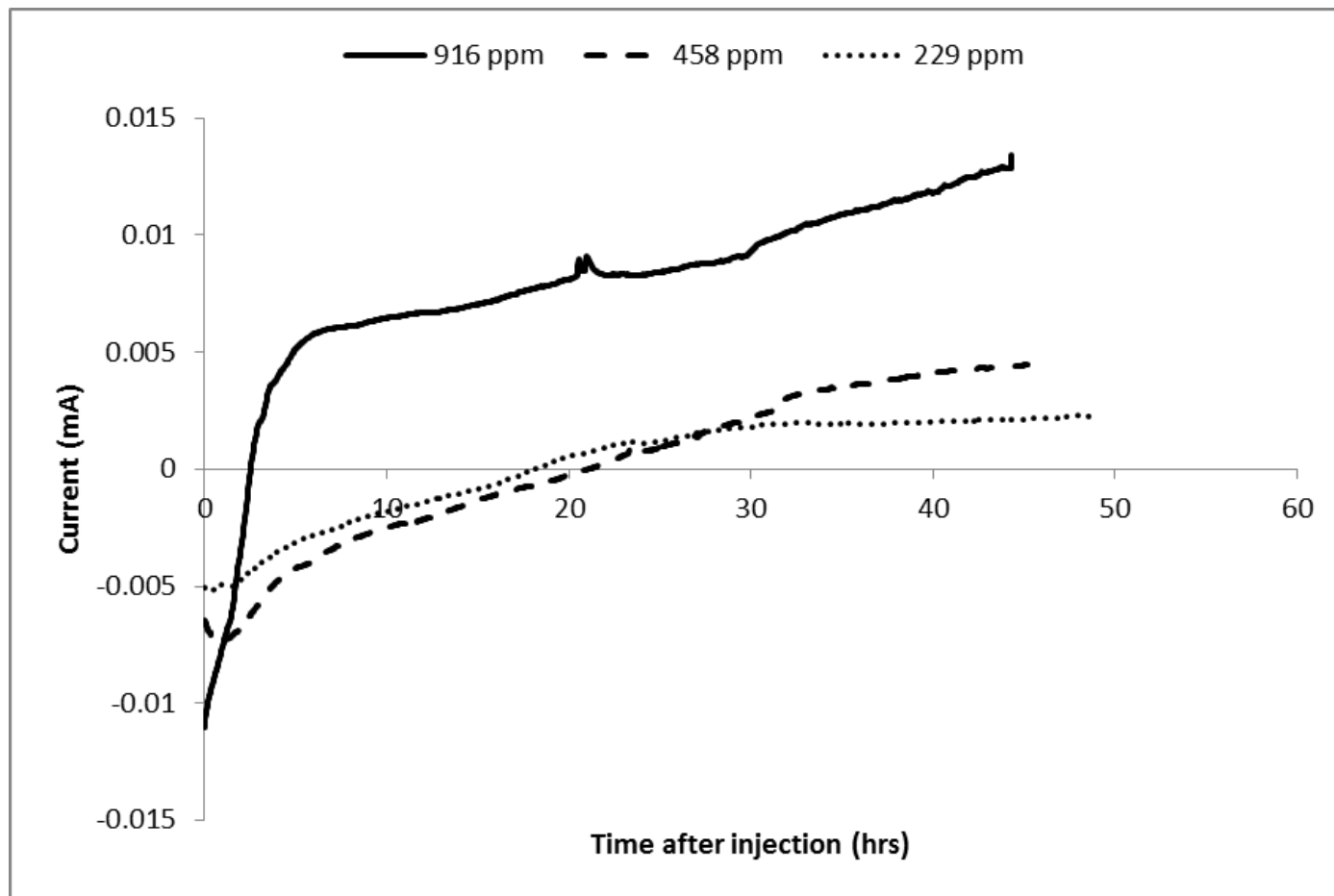


Figure 15. Typical Response Peaks for DMMP in MFC #10

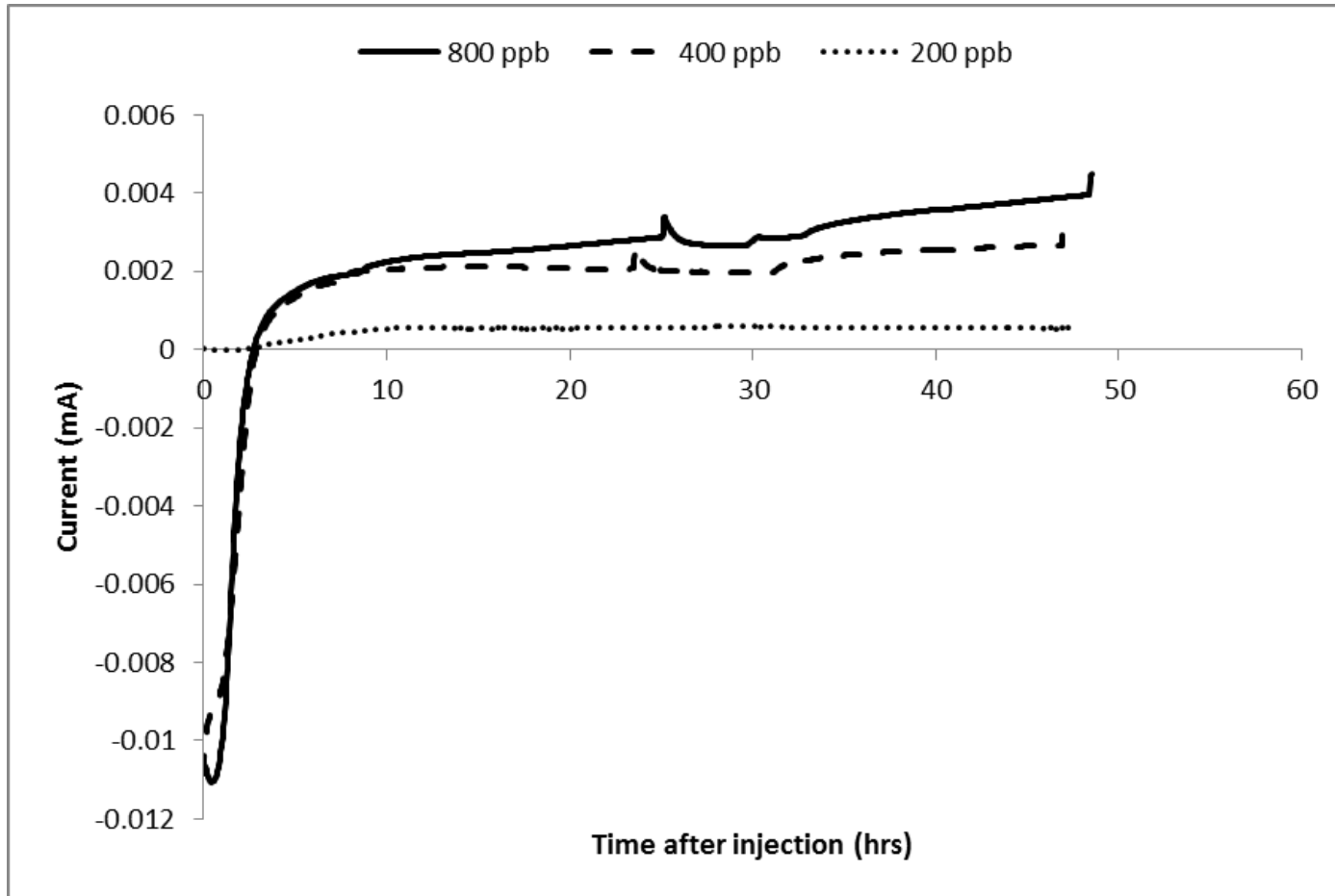


Figure 16. Typical Response Peaks for BPA in MFC #10

Table 2. Description of Metrics for MFC #5

		Aldicarb		DMMP		BPA	
		Min	Max	Min	Max	Min	Max
MFC #5	PH	4.50E-02	2.02E-01	2.00E-03	1.90E-02	4.00E-03	9.00E-03
	Area	1.94E-01	6.97E+00	-4.60E-02	7.11E-01	1.19E-01	2.81E-01
	AR	4.58E-03	9.06E-02	1.80E-04	7.56E-03	3.25E-03	1.24E-02
	10-hr SR	-6.92E-03	2.07E-03	-3.90E-04	0.00E+00	-1.40E-04	0.00E+00
	SR	-3.49E-03	-9.00E-05	0.00E+00	3.00E-05	-1.10E-04	0.00E+00
	FM	3.35E+01	4.67E+03	4.36E-01	1.77E+01	2.31E+00	7.35E+00

Table 3. Description of Metrics for MFC #10

		Aldicarb		DMMP		BPA	
		Min	Max	Min	Max	Min	Max
MFC #10	PH	3.00E-02	1.18E-01	1.00E-03	1.90E-02	1.00E-03	4.00E-03
	Area	9.13E-01	5.28E+00	-4.60E-02	7.43E-01	8.00E-03	1.72E-01
	AR	3.57E-03	9.87E-02	3.90E-04	8.42E-03	6.00E-05	1.32E-02
	10-hr SR	-4.06E-03	-1.80E-04	-5.40E-04	0.00E+00	-1.00E-05	0.00E+00
	SR	-9.50E-03	-4.00E-04	0.00E+00	6.00E-05	-1.00E-05	0.00E+00
	FM	2.01E+01	1.33E+02	1.10E-01	1.86E+01	5.70E-01	4.50E+00

All recovered metrics in each category (PH, PA, SR, 10SR, AR, and FrM) were plotted against the measured concentrations of each respective chemical. This was accomplished to determine whether or not correlations existed in the raw data. If high coefficients of determination (e.g. $R^2 > 0.95$) were observed, then further data processing with the ANN might not be necessary. Additionally, correlations like this would point toward metrics that may be better than others in the determination of concentration information. A similar approach was used by Feng et al. (2013b), who plotted metrics in the categories of PH, PA, AR, and SR against COD concentration data. Their work revealed that one metric, PA, produced strong correlations with influent COD

concentrations. The research described in this work is notable because this type of analysis has never been accomplished with organic pollutants in water, nor has it been attempted with the metrics of 10SR and FrM.

An example of the correlations between metrics and chemical concentration can be seen in Figure 17. Overall, all combinations of metrics and concentrations resulted in non-linear correlations with weak coefficients of determination (R^2). All plots of correlations between raw metric data and chemical concentration can be found at Appendix I. Examples of these correlations can be observed in Figure 17 and Figure 18 which display the results for Aldicarb only. It appears that stronger non-linear correlations were obtained when the data set was smaller. For instance, the highest R^2 values were observed only in plots involving DMMP, where the data sets were either very small or contained only one data point for a given concentration. For the DMMP plots, R^2 values as high as 1.0 were observed. However, these results may not be as reliable since the small data sets make them statistically prone to error as compared to the larger data sets associated with the other chemicals. The next highest correlation was observed in the relationship between AR and BPA concentration in MFC #10 ($R^2=0.64$), which was derived from a more meaningful data set. Most coefficients of determination ranged from 0.02 to 0.64 for both MFCs. Based on the results, non-linear correlations within the raw metric data did not prove to be useful in the determination of chemical concentration.

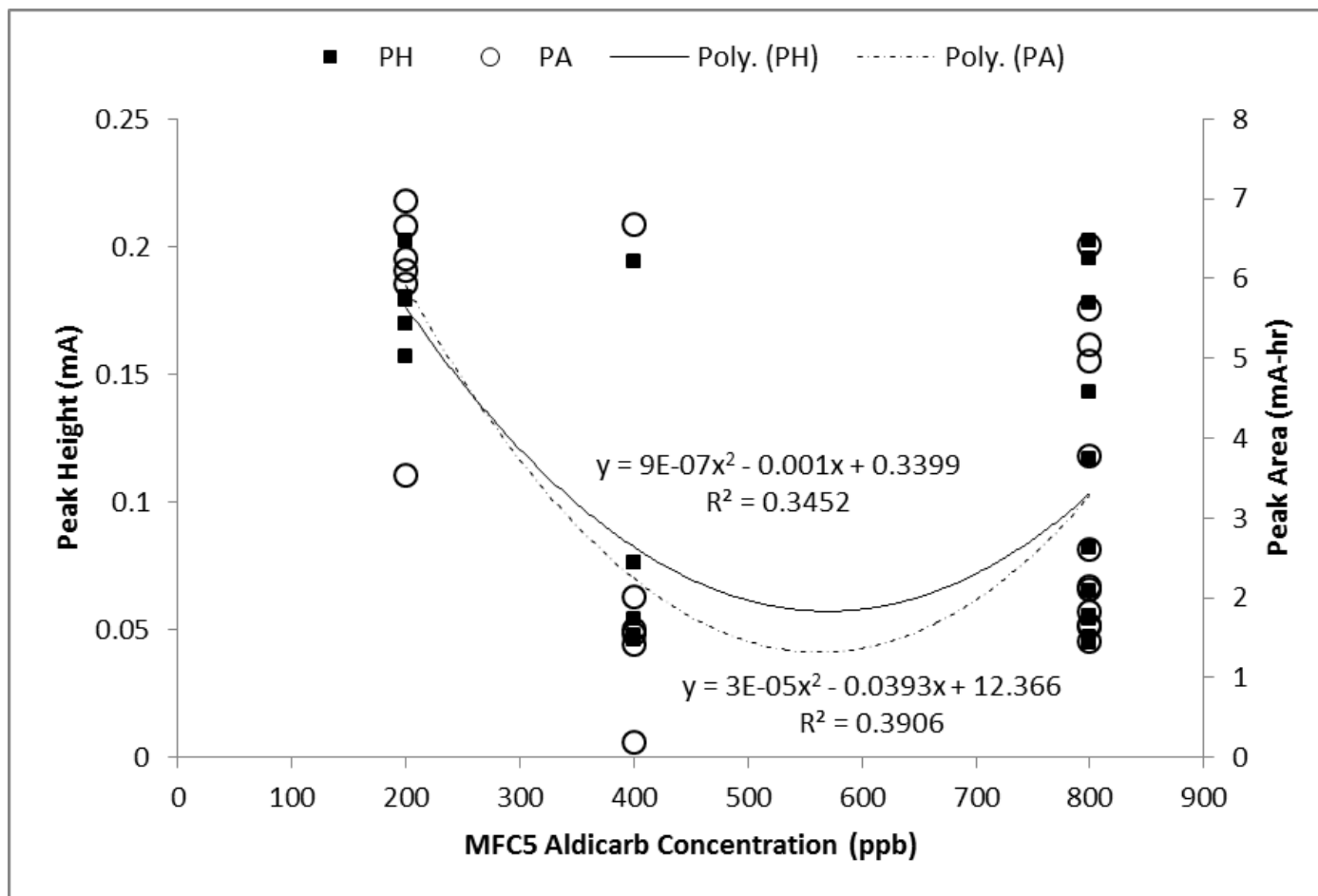


Figure 17. PH and PA Correlations with Aldicarb Concentration in MFC #5

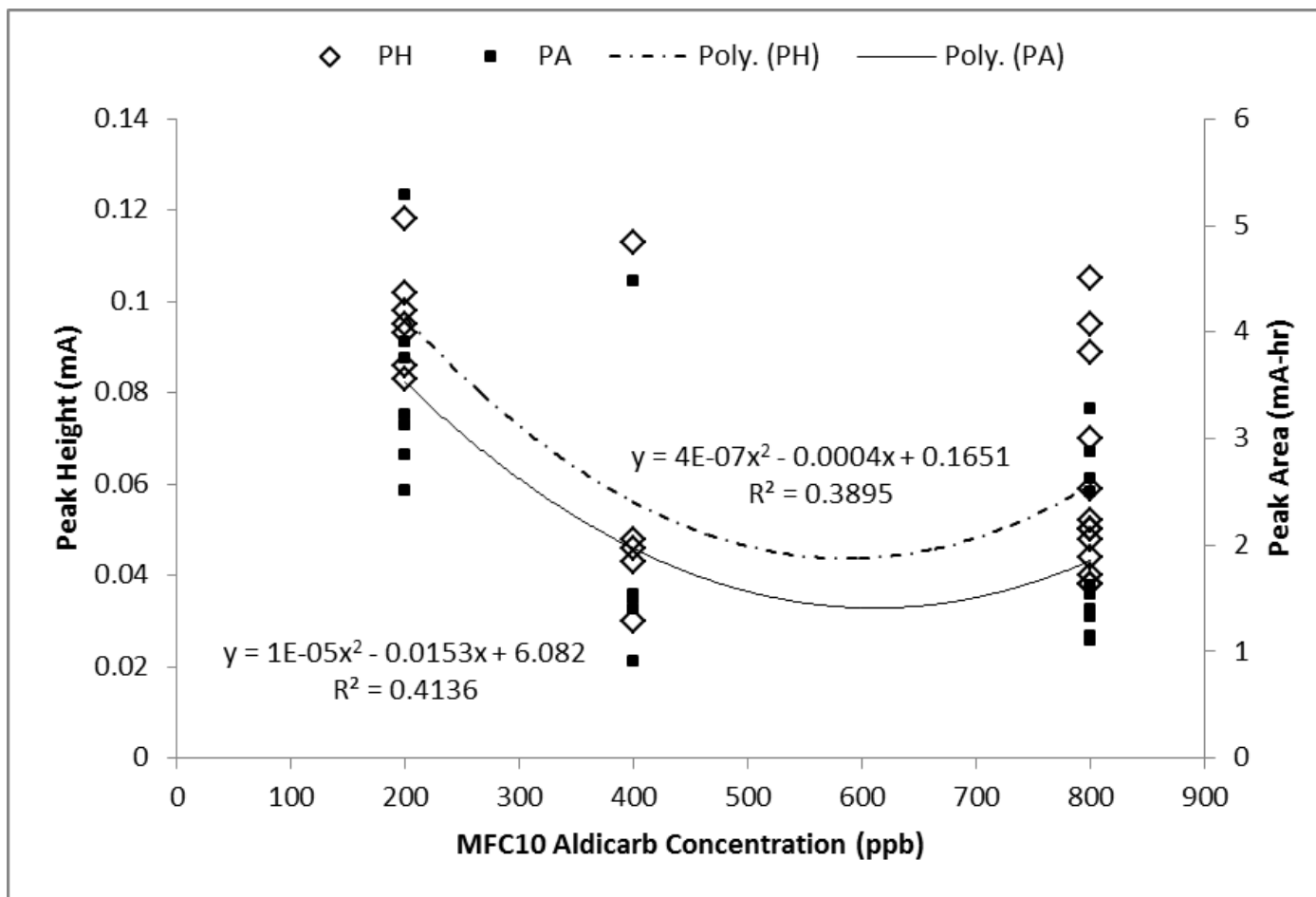


Figure 18. PH and PA Correlations with Aldicarb Concentrations in MFC #10

5.1.1.2 Identifying Chemicals with Direct Correlations

The same data set used in the quantification of chemical concentration was also used for the purpose of identification. An evaluation of each individual metric was accomplished to determine whether or not the raw data was suitable for the identification of chemicals. Figure 19 presents an example of this analysis for MFC #5, which shows outlier box plots to help describe AR data for all three chemicals that were tested. As can be seen in the figure, it would be hard to distinguish between chemical types if one were examining a single data point. For example, an AR value of 0.007 mA/hr is not unique to a particular chemical in Figure 19. Figure 20 shows the ranges of PH values observed across all concentrations levels and shows that aldicarb PH values were discernible from DMMP and BPA, but the latter two chemicals had PH ranges that overlapped. No single metric took on unique values that allowed for the identification of all three chemicals at the same time (i.e., showing dependence only on the chemical type). This was true for both MFC #5 and MFC #10. All one-way analysis plots for metrics are provided at Appendix H. The results show that there are limitations to the use of the raw data to identify chemicals.

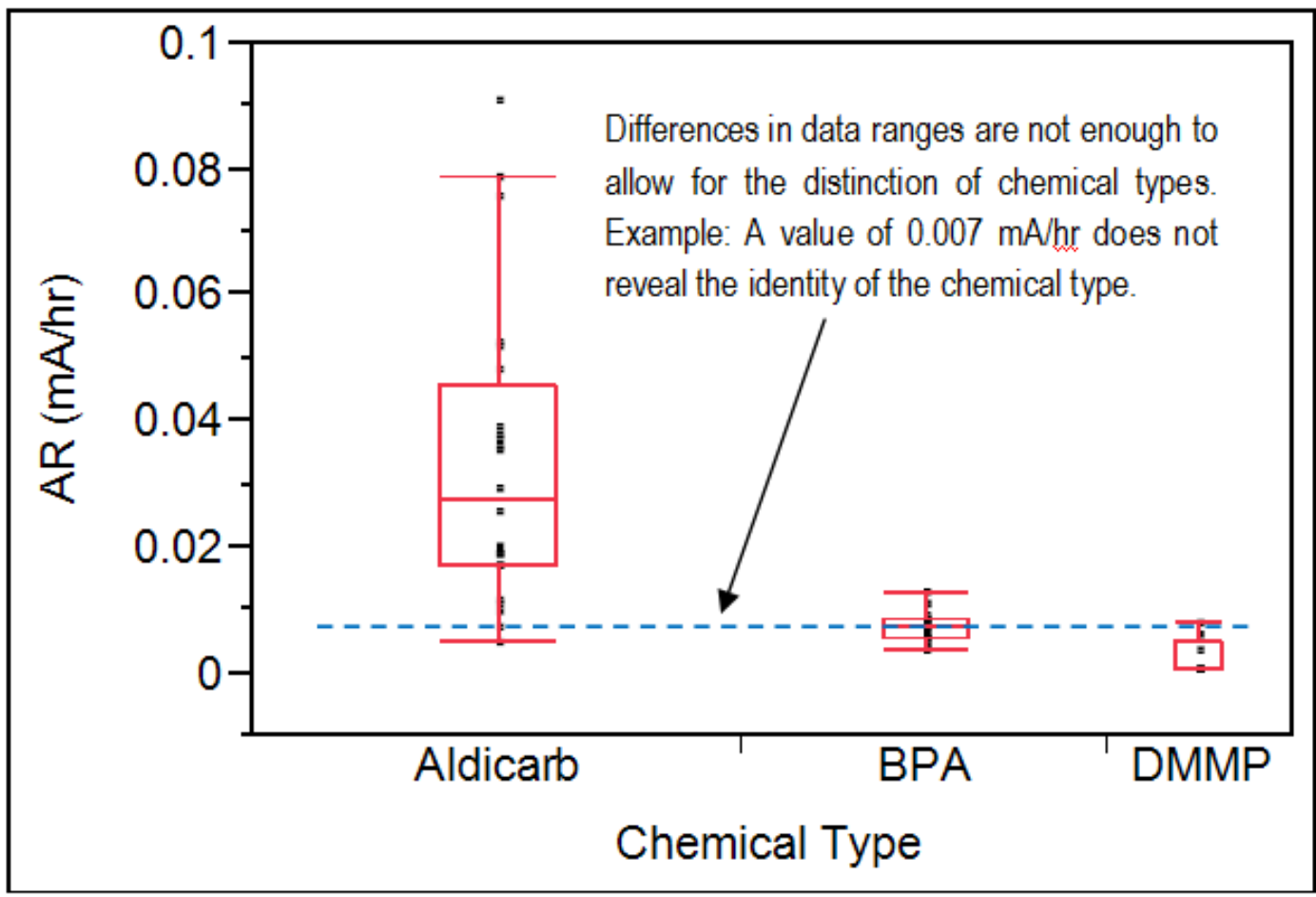


Figure 19. One-way Analysis of AR(mA/hr) by Chemical Type in MFC #5

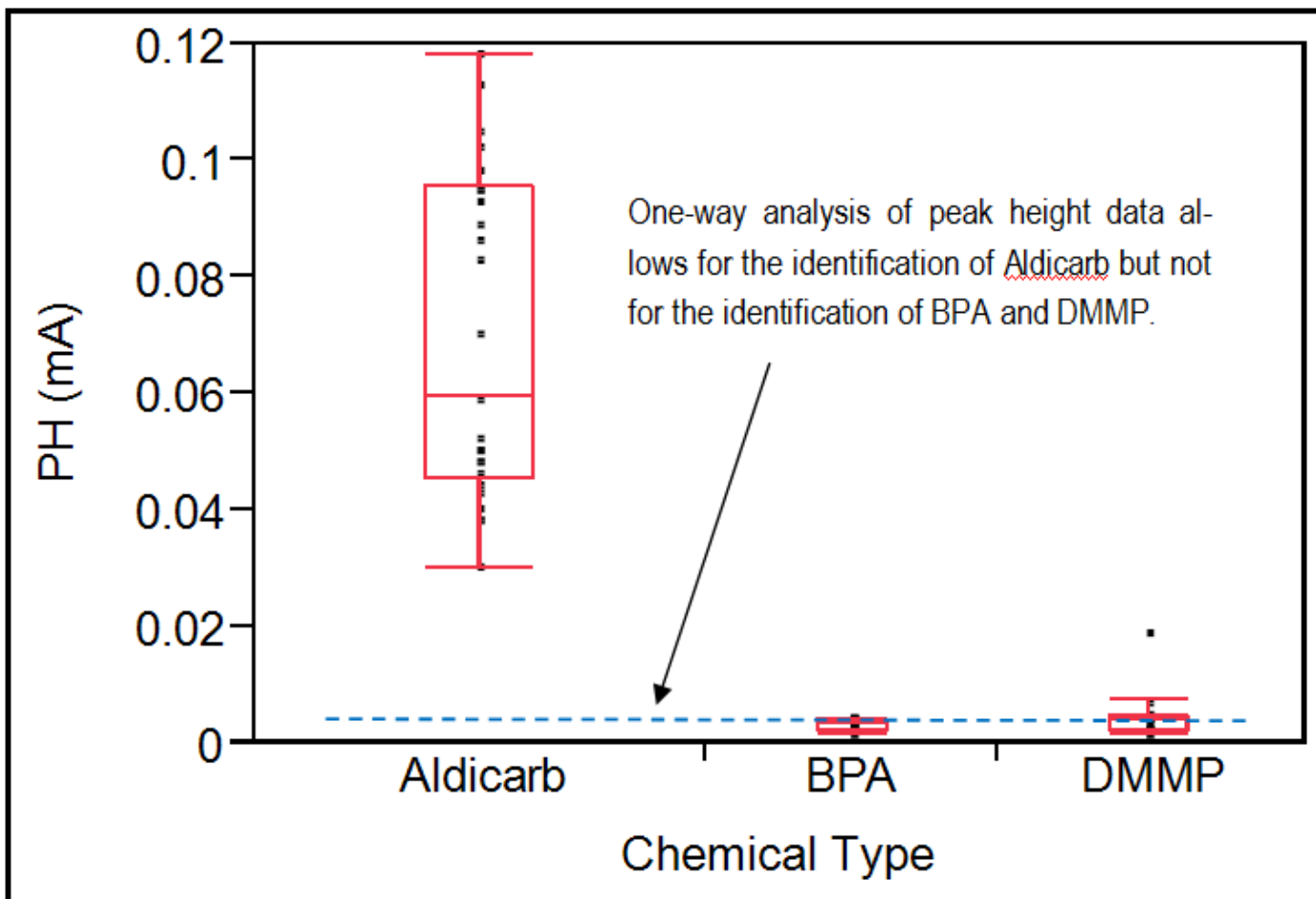


Figure 20. One-way Analysis of PH(mA) by Chemical Type in MFC #10

5.1.2 Integration with ANNs

5.1.2.1 Quantifying Chemicals with ANNs

The data sets at Appendix A and Appendix B were used in the training and development of the ANN. A set of 51 peaks were evaluated for MFC #5 and 58 peaks were in the data set for MFC #10. However, the data used in the ANN for the purpose of quantification was first divided into like groups of chemical type. In this manner the ANN evaluated data inputs from aldicarb only, a separate model was then built and run for BPA, and then another for DMMP. The entire data set was not evaluated simultaneously. Run times for these models averaged less than one minute. Quicker run times are a relative indication of effortless network processing. It appeared that quicker ANN-based correlations were obtained when the data set was smaller. The relationship between data set size and ANN performance is an issue that merits further study.

In each ANN trial, the ANN-derived concentrations were correctly modeled and correlated to the actual concentrations for each combination of metric inputs and for each chemical tested. The ANN-derived concentrations matched the actual concentrations of aldicarb (Figure 21), DMMP (Figure 22), and BPA (Figure 23) for ANN simulations. For each chemical, the ANN was designed to test its effectiveness on model performance with variations of 1-5 hidden layers. The results showed that the model performed as well with 1 hidden layer as it did with 5 hidden layers. This shows that the ANN can convert raw data, even though it was not directly correlated to chemical concentration, into meaningful water quality information. Furthermore, each of the input matrices ([PH, PA, AR, SR], [PH, PA, AR, 10SR], and [PH, PA, AR, FrM]) produced identical results, proving that the new metrics (10SR and FrM) were valid metrics for use in the ANN.

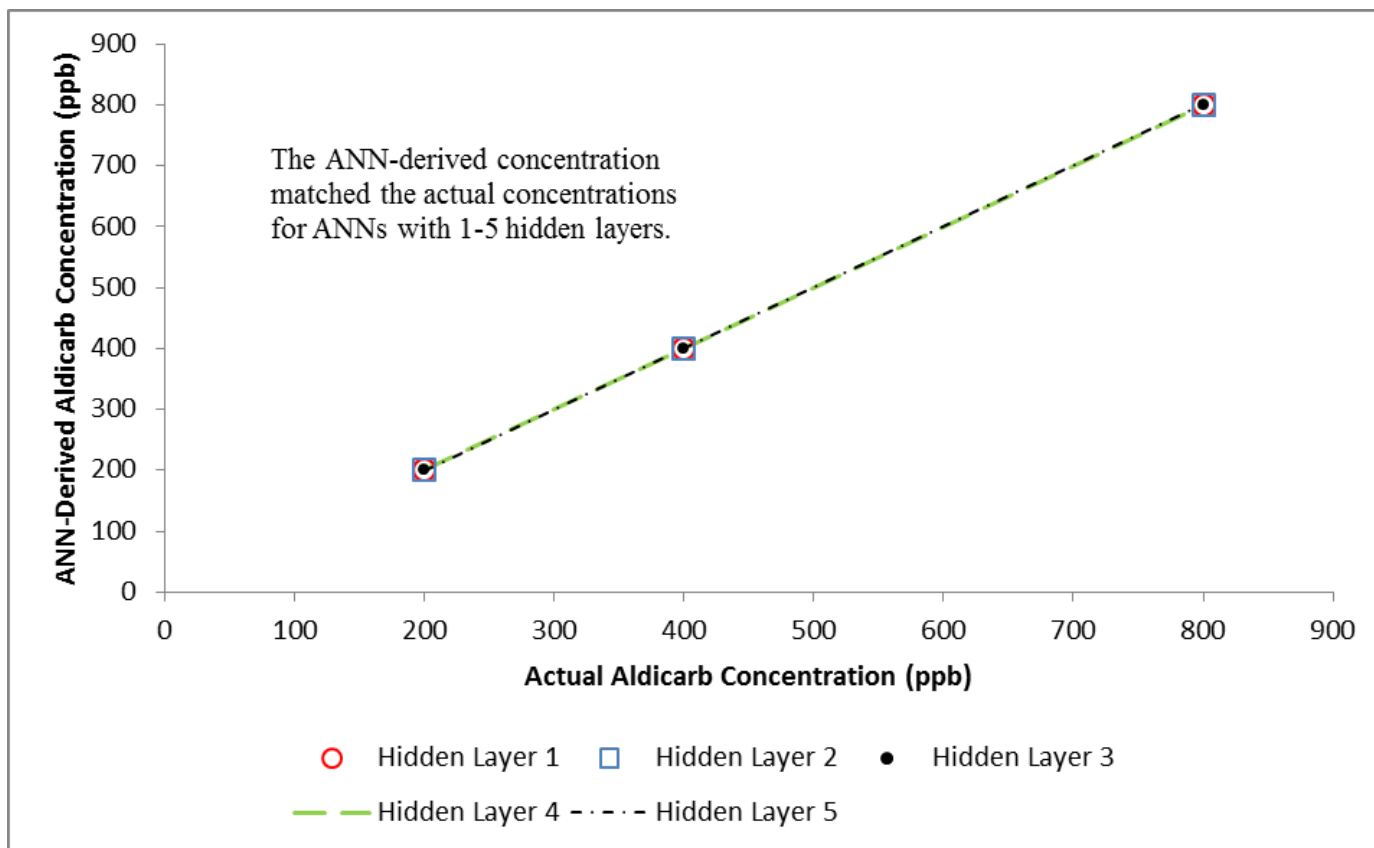


Figure 21. ANN Results for Aldicarb Quantification Tests

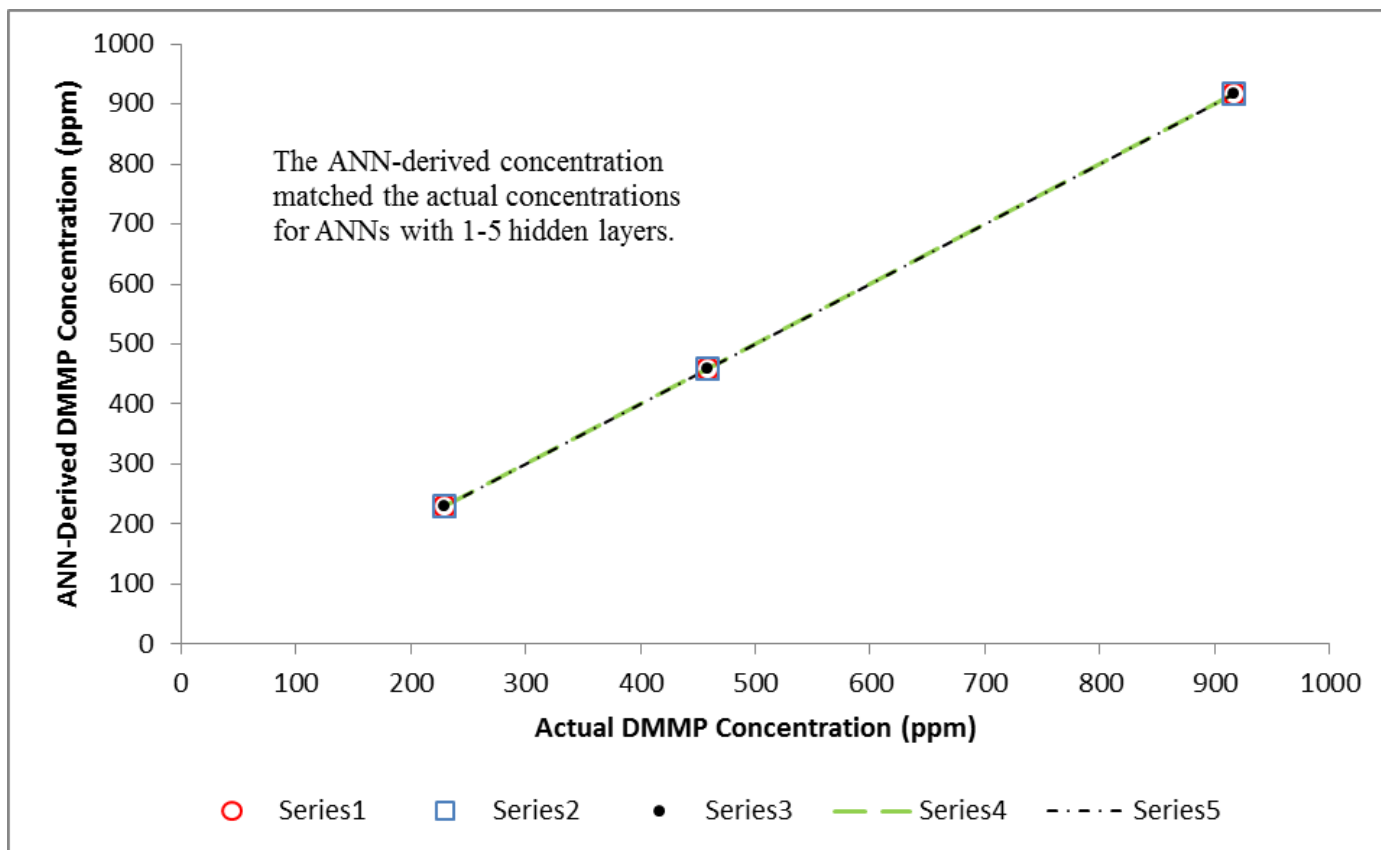


Figure 22. ANN Results for DMMP Quantification Tests

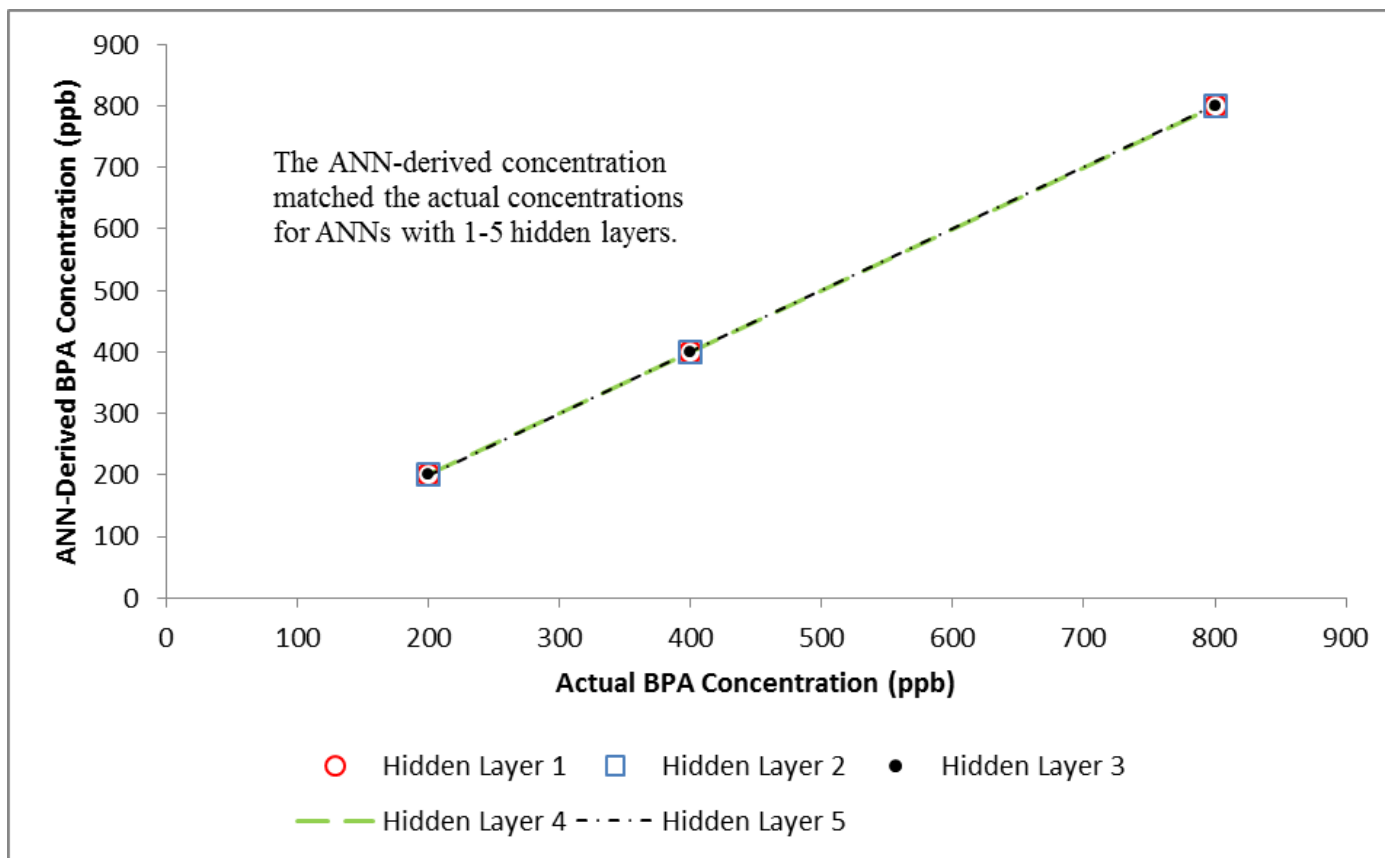


Figure 23. ANN Results for BPA Quantification Tests

5.1.2.2 Identifying Chemicals with ANNs

In the identification of the chemicals a revised ANN was created where the specific chemical was the target of ANN prediction in the output layer instead of chemical concentration. Run times for these models averaged less than one minute as well. As was the case in the previous ANN experiments, the new metrics (10SR and FrM) were incorporated into the input matrices and tested separately. Figure 24 shows that the ANN-derived chemical identities matched the actual identities for 1-5 hidden layers and for every combination of metric input tested in both MFC #5 and MFC #10. As was the case in the quantification experiments, these results also demonstrate that the new metrics (10SR and FrM) are valuable in ANN processing.

This time the data set encompassed all metrics for the three chemicals and over multiple concentration ranges. The fact that the ANN was able to distinguish differences within the entire data set is particularly impressive since the quantitative range of metrics was so diverse. This provides evidence that multi-parameter ANN modeling is highly flexible in differentiating between chemical types and supports its use as a chemical detection device. Furthermore, since the ANN was able to accurately sort out the chemical type amongst the broad range of data inputs, it is conceivable that a more sophisticated model would be able to first determine chemical type, then determine the concentration of the chemical within that type.

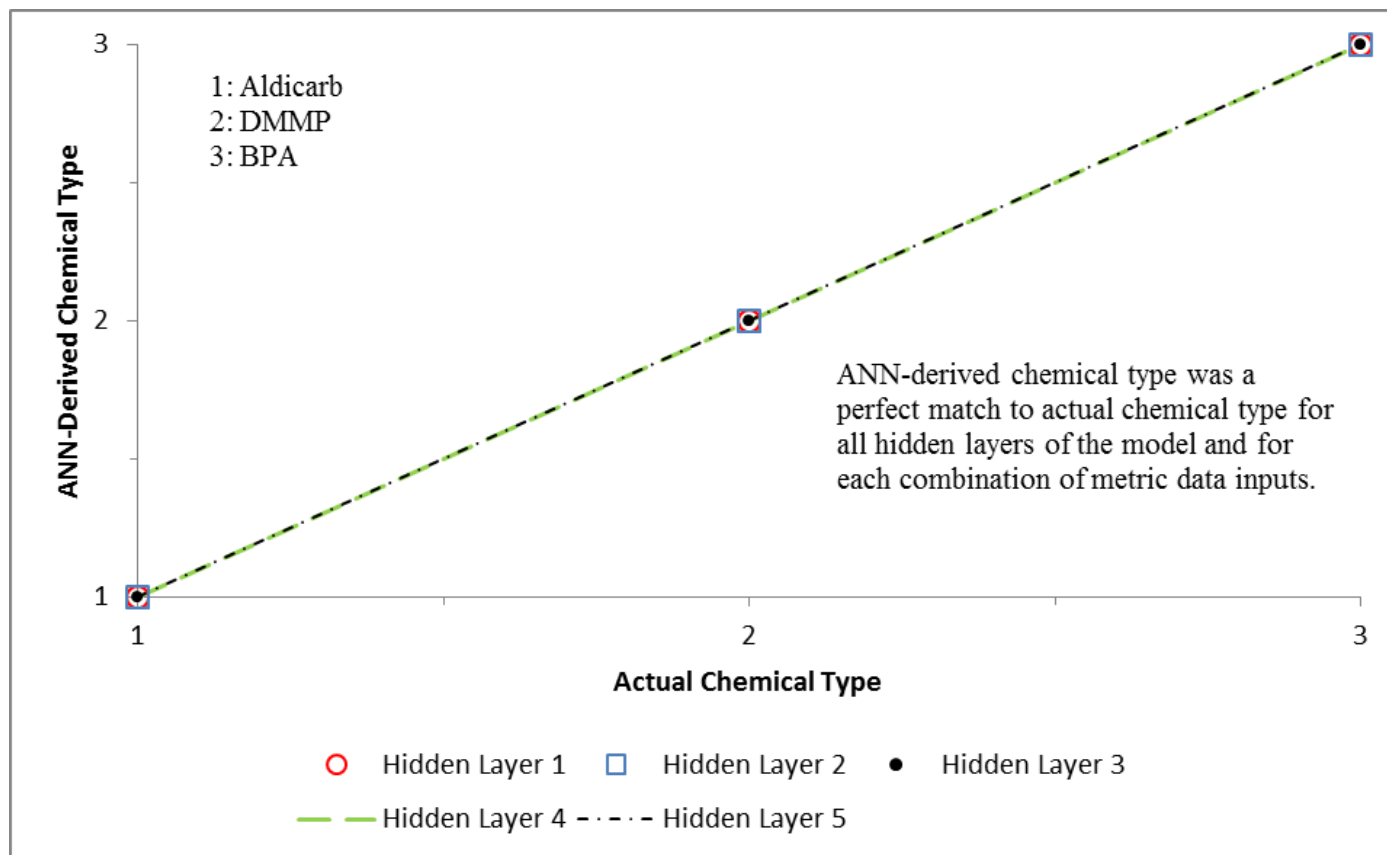


Figure 24. ANN Results for Chemical Identification Tests

5.2 Solvent Effects

5.2.1 The Effect of Solvents on Response Metrics

Figure 25 and Figure 26 show the operating histories for MFC #6 and MFC #7 respectively. Each of the three test chemicals was introduced into the MFCs in aqueous solution and then as part of the acetate-based feed medium. Signals with peak heights greater than 0.3 mA were excluded as described previously. Qualitatively, the response peaks showed the sharp rise and gradual fall that were characteristic of the other experiments. Overall, results were more clearly observed in MFC #7. In Figure 26 DMMP(aq) peaks had PH values < 0.033 mA while DMMP(FM) peaks had PH values of up to 0.145 mA. BPA(aq) peaks had PH values of < 0.019 while BPA(FM) had PH values up to 0.163 mA. Aldicarb(aq) had PH values of up to 0.143 mA while aldicarb(FM) had PH values of up to 0.259 mA. Similar results were observed for MFC #6.

The results show that the peaks with feed medium as the solvent show similarities in both size and shape. Figure 27 displays overlaid images of typical peaks for all three chemicals with the feed medium as the solvent as well as a typical peak from the feed medium by itself. The similarities between peaks suggest that current production is driven by the presence of the acetate-based feed medium and not the presence of the three target chemicals.

Although it was not the focus of the solvent effects testing, an additional experiment was performed in order to observe the effects of using tap water as a solvent for aqueous solutions in lieu of RO water which was used for all aqueous solutions throughout the study. The results for this experiment can be found at Appendix L. The

results revealed that tap water produced a higher PH in all cases. This was expected since reverse osmosis has the capability of filtering out many of the trace metals often needed by bacteria.

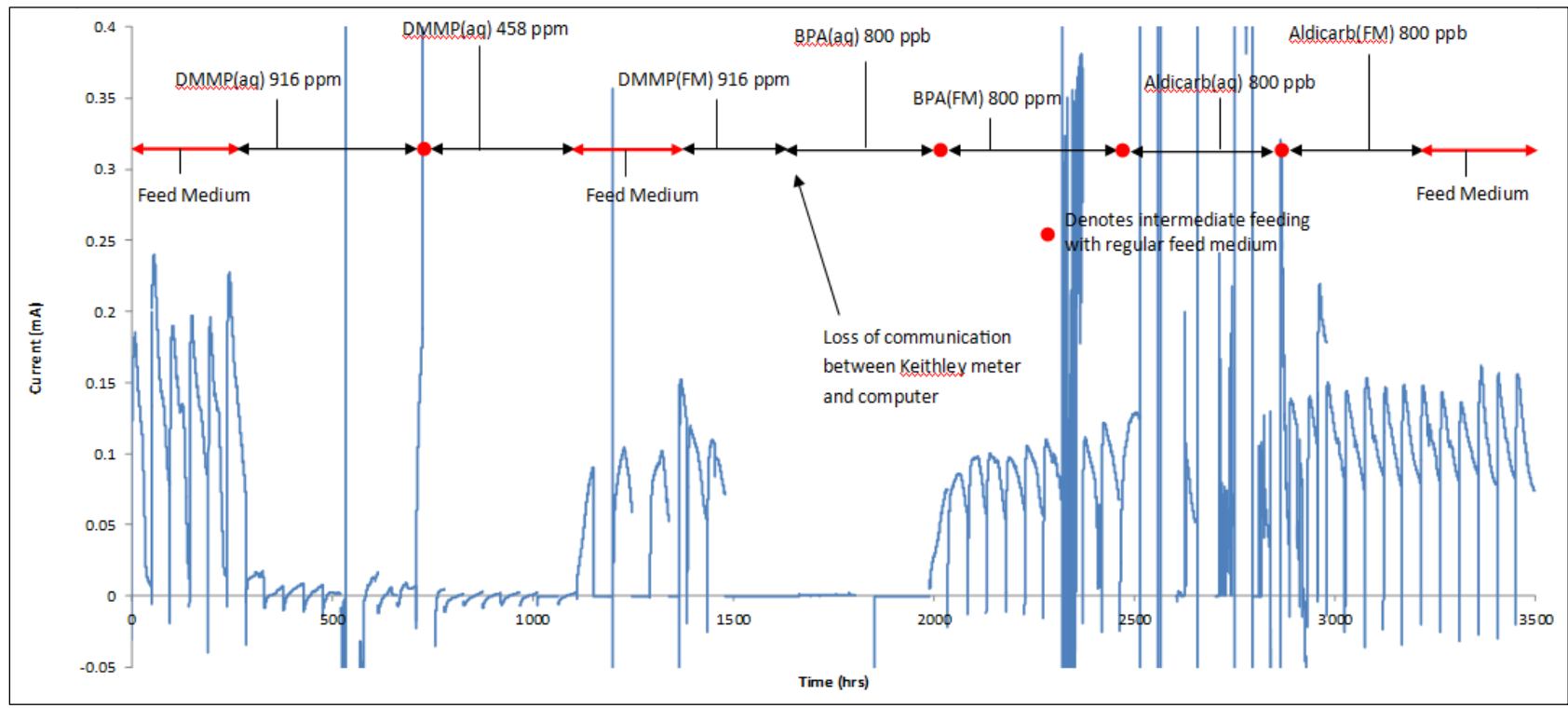


Figure 25. Operating History for MFC #6

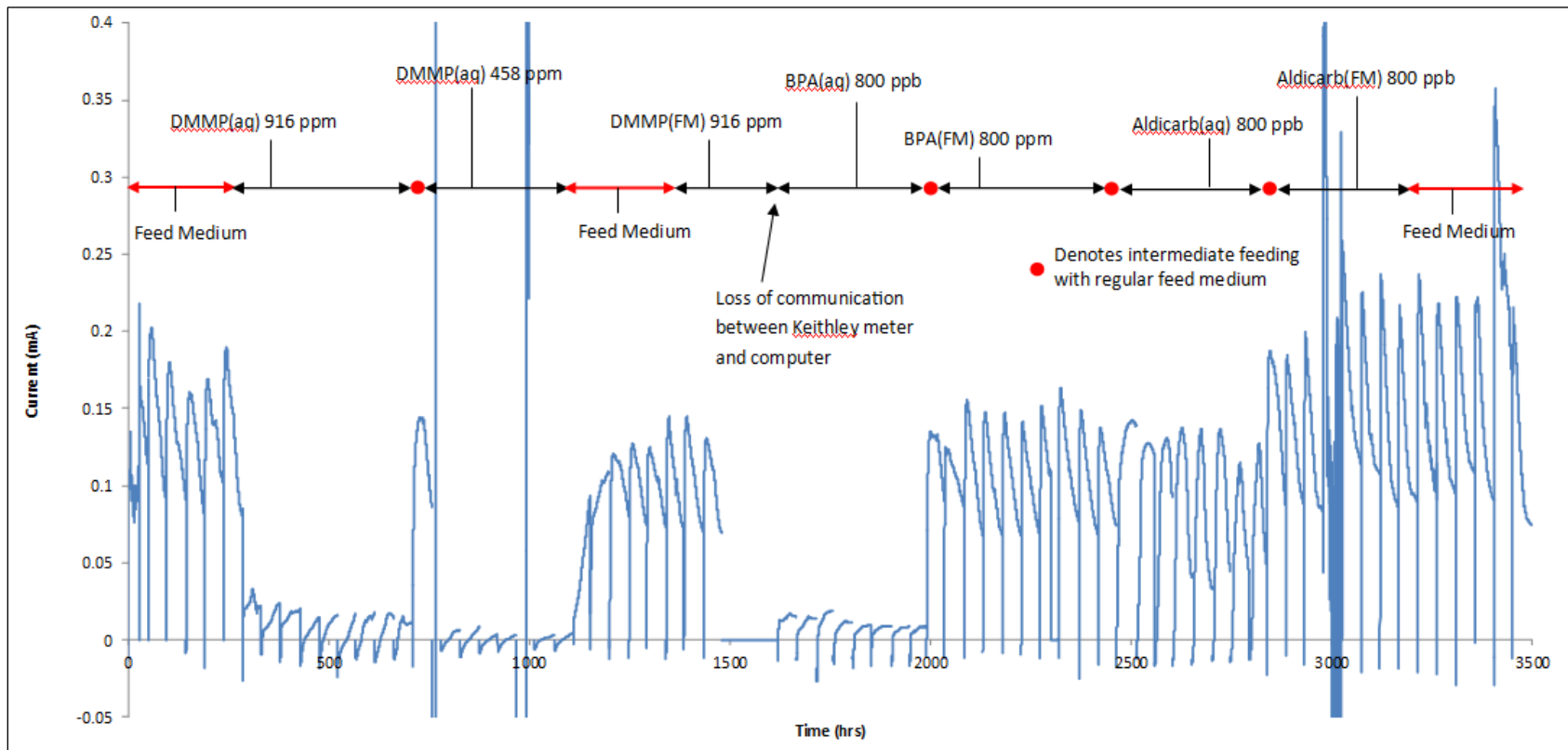


Figure 26. Operating History for MFC #7

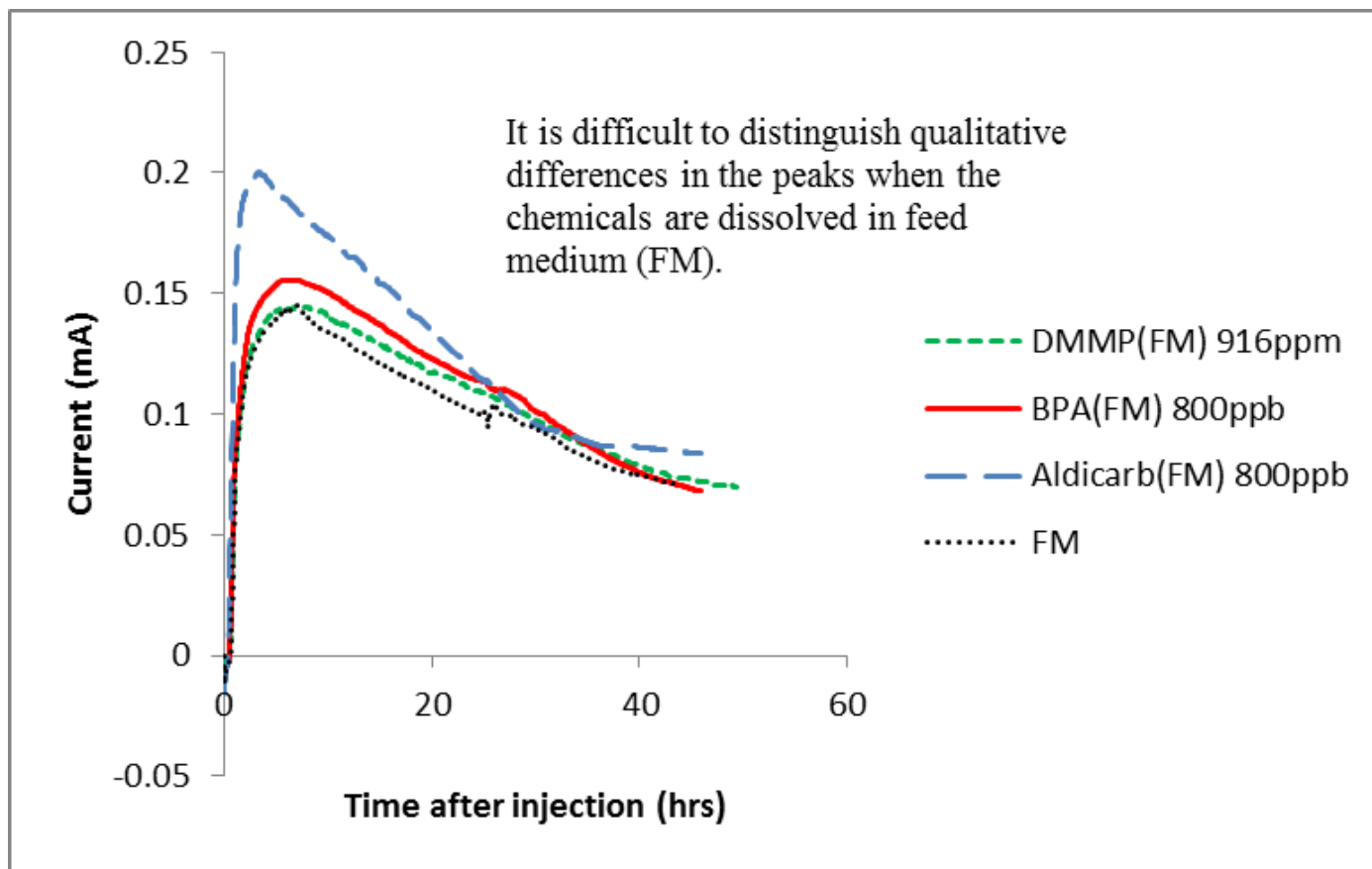


Figure 27. Representative peaks from MFC #7

5.2.2 Using ANNs to Identify Chemicals Dissolved in Feed Medium

The ANN was used to attempt to distinguish the three target chemicals when they were introduced as a solute in the feed medium. All metrics (PH, PA, AR, 10SR, SR, and FrM) were used in the development of the ANN. The input matrices consisted of four metrics at a time constructed in the same fashion as was accomplished in previous tests ([PH, PA, AR, SR], [PH, PA, AR, 10SR], and [PH, PA, AR, FrM]). A total of 15 peaks were evaluated for MFC #6 and 16 peaks were evaluated for MFC #7. The complete data sets can be found at Appendix C and Appendix D.

Figure 28 shows the results from MFC #6 when the matrix [PH, PA, AR, FrM] was used as the input. As can be seen in the figure, the ANN algorithms sorted out differences in the data inputs and correctly determined the chemical type for all three chemicals. However, it should be noted that correct correlations were formulated only when the ANN utilized three, four, and five hidden layers. The number of hidden layers resulting in successful correlations did not vary between combinations metric inputs. This is an indication that neither of the newly-tested metrics (10SR and FrM) served to enhance ANN performance. All ANN outputs from this set of experiments can be found at Appendix K. A higher order of modeling complexity was necessary for the model to create the correlations required to distinguish the small variances between response peaks in this experiment (as shown in Figure 27).

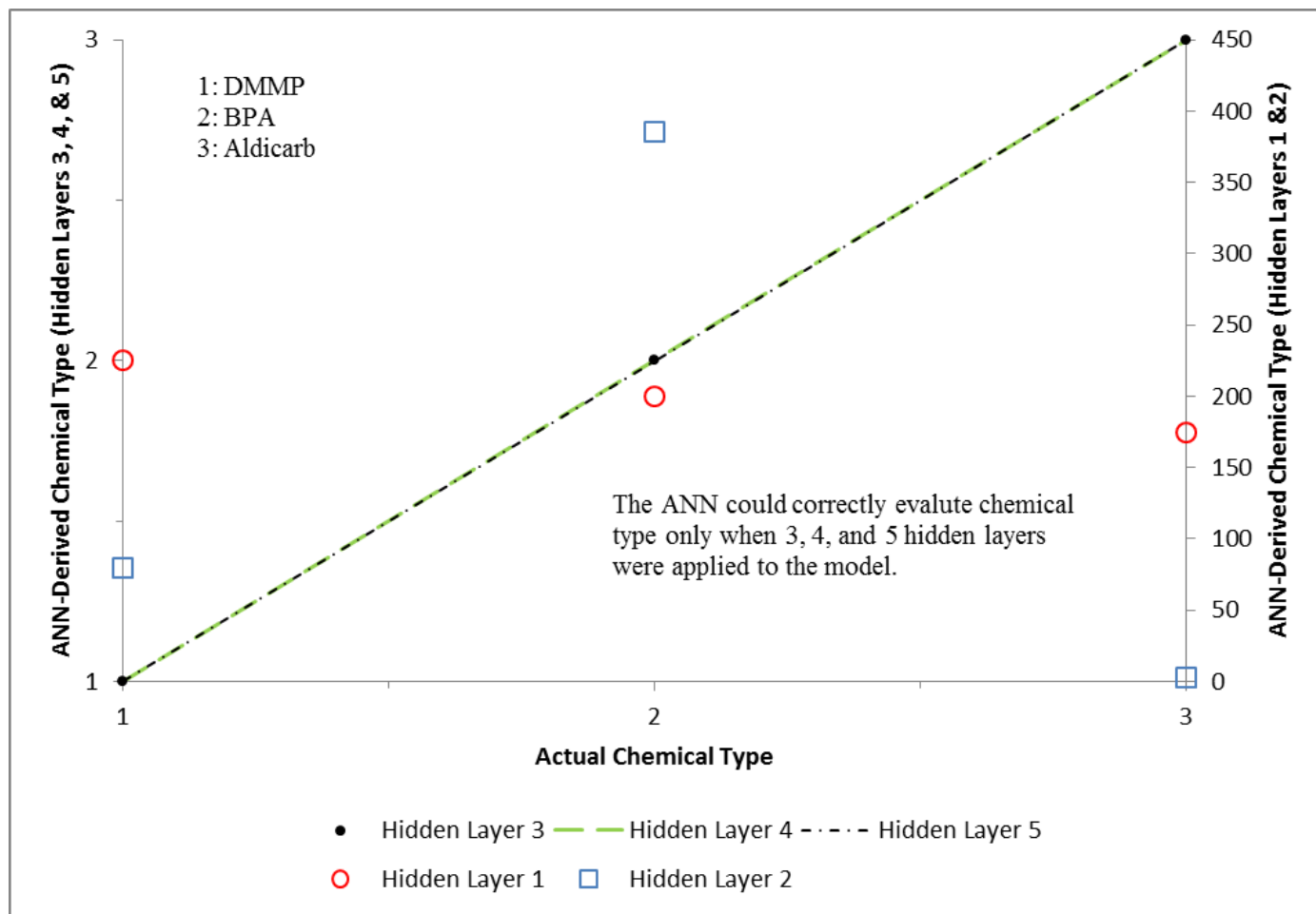


Figure 28. ANN Results for Solvent Effects Testing Using [PH, PA, AR, FrM] as the Input Matrix for MFC #6

5.3 Mixtures

5.3.1 Laboratory Tests

Figure 29 and Figure 30 show the operating histories for MFC #8 and MFC #9, respectively. These two MFCs were subjected to a series of chemical injections in order to determine whether mixtures of the three target chemicals could be distinguished from individual target chemicals. Many of the measured signals from MFC8 were highly dynamic (Figure 29). For example, the aldicarb/BPA signals had PH values that were between 0.026 and 0.063 mA. Only one aldicarb/DMMP peak with a PH of 0.052 mA was recovered due to bad electrode connections and a loss of communication with the computer. The DMMP/BPA signals were relatively stable in size and shape and had PH values that fluctuated around 0.020 mA. Three of the DMMP (only) peaks resembled the DMMP/BPA peaks but not the aldicarb/DMMP peak. The aldicarb (only) peaks were highly variable and had larger PH and PA values than the aldicarb/BPA or aldicarb/DMMP peaks. The BPA (only) peaks had relatively consistent size and shape while being qualitatively different from aldicarb/BPA or DMMP/BPA peaks.

Figure 30 shows more evidence of the dynamic nature of peaks generated by these industrial chemicals (and their mixtures). The aldicarb/BPA signals had PH values that were between 0.017 and 0.079 mA. This time, only two aldicarb/DMMP signals were recovered because of the communication loss with the computer. These peaks had PH values that were approximately 0.03 mA. The DMMP/BPA signals were highly dynamic, they showed negative voltages, and lacked the well-organized structure that is needed to facilitate retrieval of response metrics. Only three of these peaks provided usable metrics for the ANN. The peaks associated with the individual chemicals were

also highly dynamic. These results show that the qualitative differences in the shapes of the response peaks are not as obvious as what was observed in the quantitative and qualitative tests.

The same difficulties that were obvious in the other data sets also exist in this data set with regard to establishing correlations within the raw data. For example, Figure 31 describes an example of a single-metric evaluation using SR in the data set for MFC #8. Once again, in this figure outlier box plots help to highlight the data ranges. In this case, SR values are not unique to chemical mixtures. None of the raw metrics enabled the distinction of all chemical types simultaneously. The results show that direct correlations with raw data does not easily allow for the determination of unique chemical mixtures. All one-way correlations for MFC #8 and MFC #9 can be found at Appendix J.

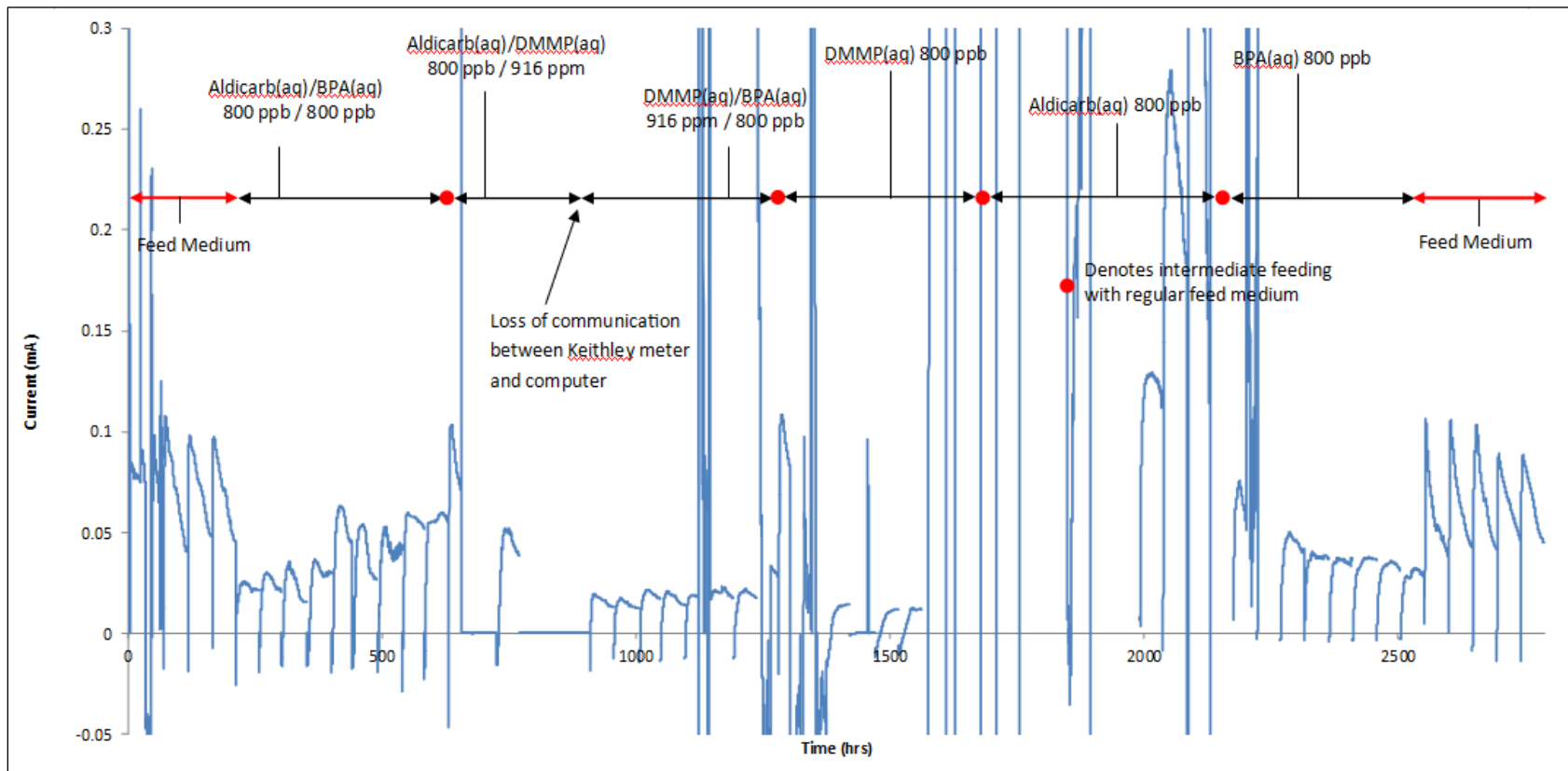


Figure 29. Operating History for MFC #8

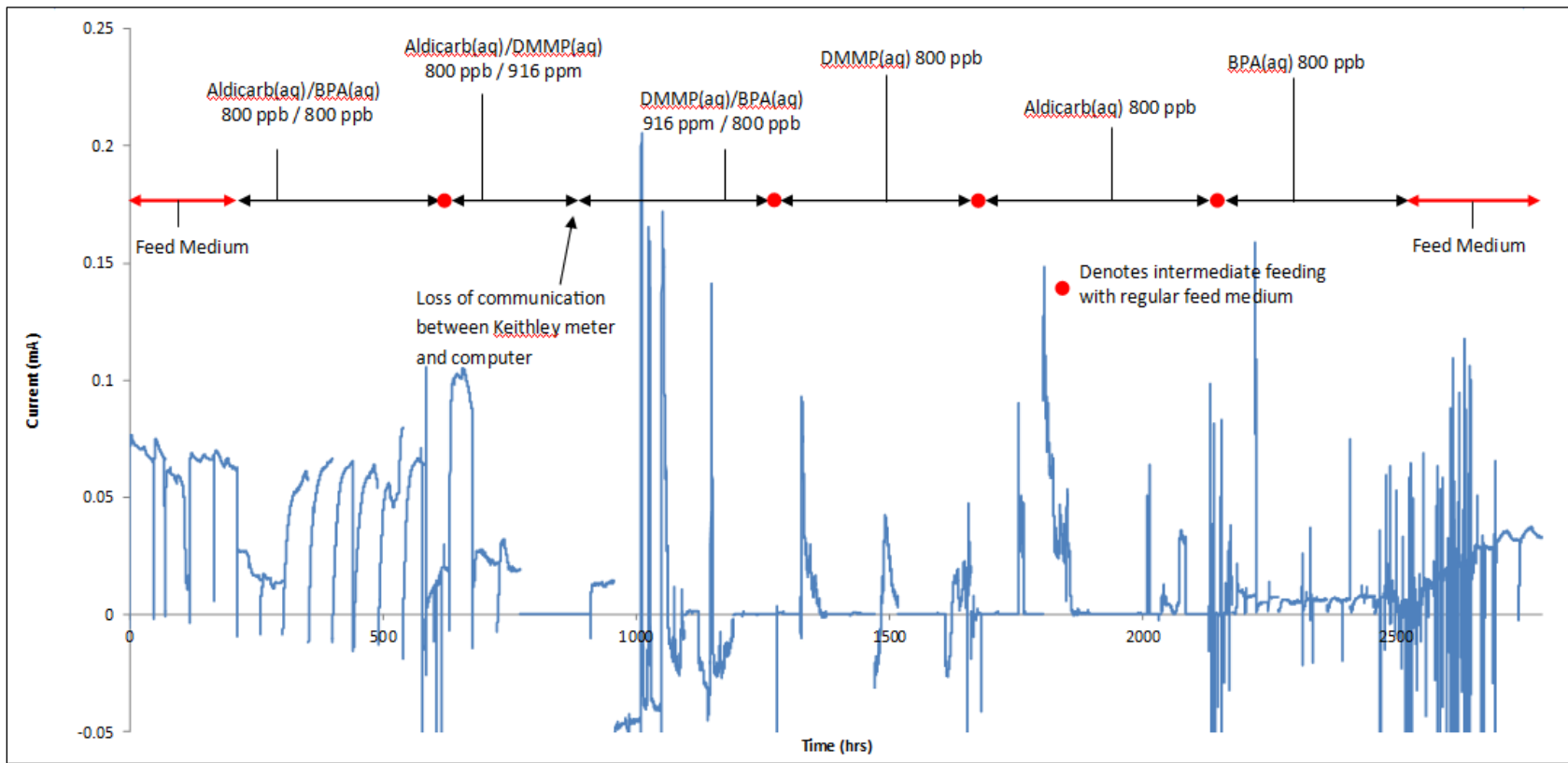


Figure 30. Operating History for MFC #9

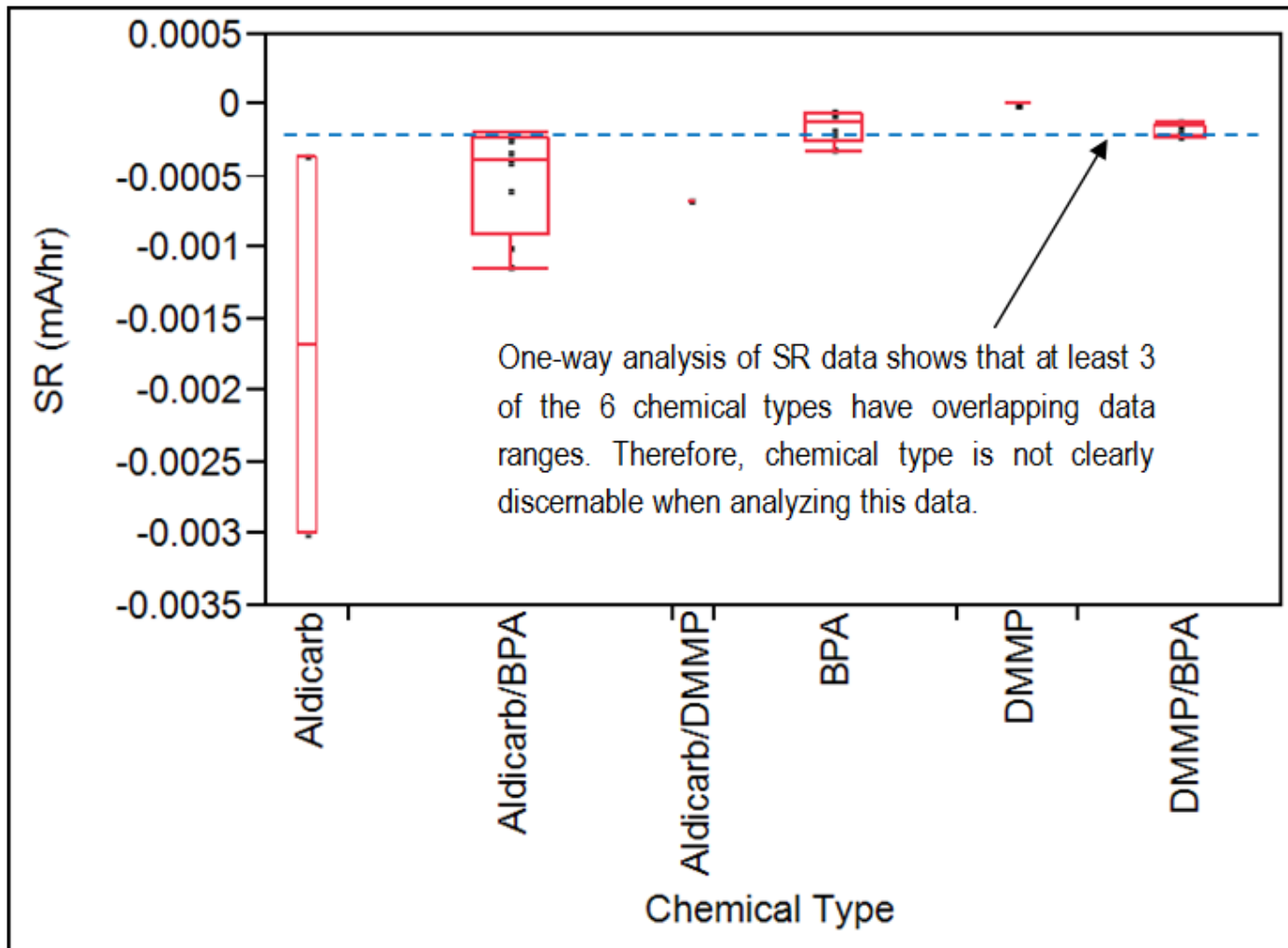


Figure 31. One-way Analysis of SR (mA/hr) By Chemical Type for MFC #8

5.3.2 Integration with ANNs

All metrics (PH, PA, AR, 10SR, SR, and FrM) were obtained from the data set in the analysis of mixtures. Since not all peaks were useful for generating metric information, only 51% of the response peaks for MFC #8 and 47% of the peaks from MFC #9 were used in the ANN. A total of 25 peaks were evaluated in the data set for MFC #8 and 23 were in the data set for MFC #9. These data sets can be found at Appendix E and Appendix F. Figure 32 shows that the ANN correctly identified all mixtures and individual chemicals using any number of hidden layers. Additionally, this was the case for each set of input matrices tested in both MFC #5 and MFC #10. 10SR and FrM were useful metrics for use in the ANN. Also, ANNs are highly capable in the determination of chemical type even when the input metrics are dynamic in nature. Clearly, ANNs can be used in water quality monitoring applications.

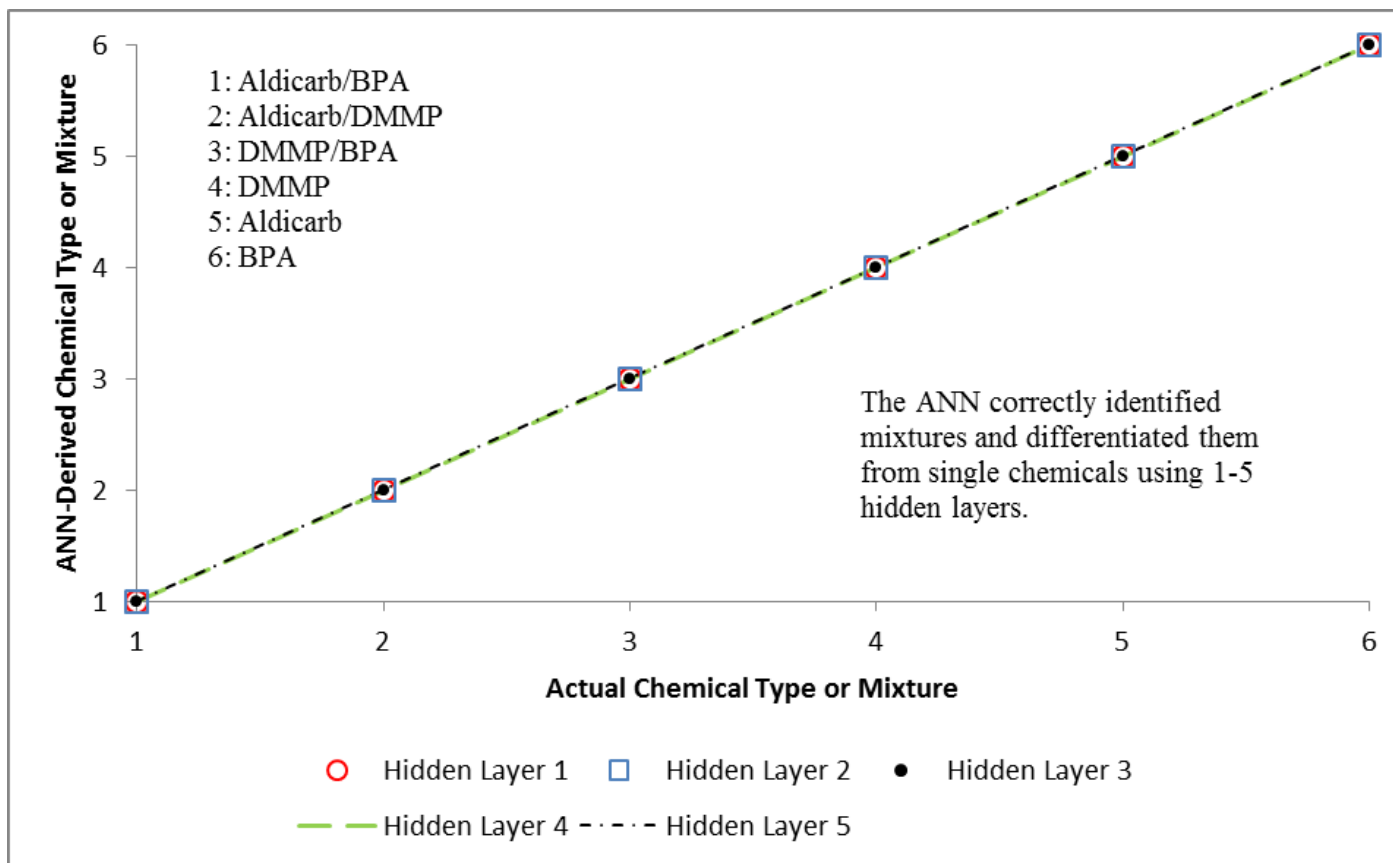


Figure 32. ANN Results for Mixtures Testing

VI. Conclusion

This study has provided an evaluation of the use of MFC-based biosensing for the detection of three specific organic pollutants. A variety of quantitative metrics were derived from electronic response signals for all three chemicals over a range of concentrations and experimental conditions. These metrics were correlated with water quality data using direct regressions and also via computer modeling with an ANN.

The direct correlation of raw metrics with water quality data proved to be ineffective in the distinction of chemical type or concentration. Non-linear correlations of large data sets generated low coefficients of determination ($0.02 \leq R^2 \leq 0.64$) that were unreliable in the prediction of relevant outputs. Additionally, basic one-way analysis of the raw metric data proved to have limited application.

Three sets of experiments revealed the flexibility and utility of the ANN in MFC-based biosensing. In the first experiment, the use of the artificial neural network enabled the identification of chemical type and concentration with only one hidden layer of neurons. In the second experiment, when the standard feed medium was used as a solvent only small qualitative and quantitative differences in the response peaks were observed. The ANN, however, correctly derived the identity of each chemical with a model using three hidden layers. In the third experiment, chemical mixtures were correctly identified and differentiated from individual chemicals using an ANN with one hidden layer. Finally, two metrics that have never been used before, 10SR and FrM, proved to be equally as useful as metrics previously used in MFC research.

This study proves that MFC-based biosensing, when used in conjunction with ANNs, can successfully be applied to the detection and quantification of organic

pollutants. This report is the first to integrate ANNs and MFC-based biosensing for the detection of organic pollutants that are toxic and only partially biodegradable. It is also the first study to evaluate the utility of 10SR and FrM as metrics. The study also provides insight into the application of MFC-based biosensing with regard to limits of detection and in scenarios where chemical mixtures and unique solvents are involved. These findings have wide-ranging implications for the field of water quality monitoring as they suggest that MFC-based biosensing is flexible enough to be used in a variety of scenarios and under various conditions. It is even conceivable that MFCs can someday be used as both a power source and a water quality monitoring device simultaneously (e.g. use at wastewater treatment plants).

VII. Future Work

This study has shown that MFC-based biosensing coupled with ANN processing has legitimate applications in the field of water quality monitoring. However, issues exist that should be addressed either to improve this approach or to answer questions that might remain. Future work should address the following issues:

- Field trials that apply the technology to surface water sources like ponds and rivers where microbial populations and other water parameters are likely to be very dynamic
- Long-term field trials in outdoor environments to determine the effects of weather and atmospheric conditions on MFC response peaks
- Continuous-flow MFCs that can be used in real-time water quality monitoring applications
- More sophisticated ANN models that have the ability to perform multiple functions either in stepwise phases or simultaneously (e.g. identify then quantify)
- Monitoring experiments with other analytes of concern in water quality monitoring (e.g. regulated contaminants)
- Alternative MFC designs including smaller anodes for faster response times and materials that are substantial enough to endure outdoor weather conditions
- The use of electrode-reducing microorganisms that are engineered or enriched for enhanced current production

Appendix A. Raw ANN Data for MFC #5

Table A1. Data for MFC #5

Date	Input Matrix Data						Output Matrix Data			
	PH (mA)	PA (mA-hr)	AR (mA/hr)	10SR (mA/hr)	SR (mA/hr)	FrM	[Aldicarb] (ppb)	[DMMP] (ppm)	[BPA] (ppb)	MFC No.
9-Apr-13	0.055	2.146	0.036970	-0.00171	-0.00009	52.86966	800	0	0	5
11-Apr-13	0.054	1.817	0.025690	-0.00139	-0.00073	43.94673	800	0	0	5
15-Apr-13	0.045	1.447	0.028820	-0.00049	-0.00033	33.52991	800	0	0	5
17-Apr-13	0.047	1.654	0.017140	-0.00048	-0.00028	43.07422	800	0	0	5
19-Apr-13	0.055	1.645	0.016620	-0.00057	-0.00089	36.98571	800	0	0	5
27-Apr-13	0.065	2.099	0.007400	-0.00118	-0.00076	49.79976	800	0	0	5
29-Apr-13	0.082	2.596	0.01869	-0.00106	-0.00087	52.76811	800	0	0	5
1-May-13	0.117	3.784	0.018480	-0.00312	-0.00160	84.9971	800	0	0	5
3-May-13	0.195	5.178	0.051550	-0.00692	-0.00349	96.92441	800	0	0	5
5-May-13	0.202	6.407	0.075680	-0.00400	-0.00299	131.3494	800	0	0	5
7-May-13	0.178	5.618	0.052120	-0.00355	-0.00227	421.2728	800	0	0	5
9-May-13	0.143	4.973	0.048180	-0.00208	-0.00195	103.4949	800	0	0	5
13-May-13	0.076	0.194	0.011350	-0.00148	-0.00092	50.28361	400	0	0	5
19-May-13	0.194	6.672	0.035840	-0.00291	-0.00276	146.2349	400	0	0	5
21-May-13	0.076	2.016	0.019980	0.00207	-0.00217	36.67929	400	0	0	5
23-May-13	0.054	1.414	0.018570	-0.00057	-0.00058	4668.855	400	0	0	5
25-May-13	0.046	1.604	0.009670	-0.00070	-0.00051	38.0894	400	0	0	5
29-May-13	0.048	1.541	0.01093	-0.00106	-0.00045	35.84498	400	0	0	5
2-Jun-13	0.179	3.542	0.07889	-0.00118	-0.0014	40.4991	200	0	0	5
4-Jun-13	0.157	6.097	0.03552	-0.00055	-0.00144	136.5657	200	0	0	5
6-Jun-13	0.17	6.246	0.03755	-0.00246	-0.00215	136.7935	200	0	0	5
8-Jun-13	0.17	5.931	0.0387	-0.00259	-0.00171	128.3959	200	0	0	5
12-Jun-13	0.202	6.965	0.09055	-0.00118	-0.00225	145.7877	200	0	0	5
16-Jun-13	0.18	6.662	0.00458	-0.0019	-0.00216	146.9971	200	0	0	5
30-Jun-13	0.019	0.711	0.00756	-0.00039	0.00003	17.71667	0	916	0	5
2-Jul-13	0.014	0.421	0.00366	0	0	10.08737	0	916	0	5
22-Jul-13	0.003	-0.046	0.00062	0	0.000	0.436	0	458	0	5
26-Jul-13	0.003	-0.017	0.0005	0	0.000	0.734	0	458	0	5
28-Jul-13	0.002	-0.046	0.0056	0	0.000	0.641	0	458	0	5
5-Aug-13	0.003	0.124	0.00042	0	0.000	3.17	0	229	0	5
7-Aug-13	0.003	-0.027	0.0005	0	0.000	0.637	0	229	0	5
17-Aug-13	0.002	0.005	0.00018	0	0.000	0.708	0	229	0	5
19-Aug-13	0.002	0.02	0.00021	0	0.000	0.91	0	229	0	5
23-Aug-13	0.006	0.281	0.00407	0	0.000	7.35	0	0	800	5
25-Aug-13	0.006	0.204	0.00772	0	0.000	5.22	0	0	800	5
2-Sep-13	0.009	0.262	0.01235	0	0.000	6.73	0	0	800	5
6-Sep-13	0.006	0.227	0.00408	0	0	5.303	0	0	800	5
14-Sep-13	0.005	0.192	0.00783	0	0	4.66	0	0	400	5
16-Sep-13	0.005	0.202	0.00807	0	0	5.353	0	0	400	5
18-Sep-13	0.005	0.188	0.00695	-0.00004	-0.00004	4.714	0	0	400	5
20-Sep-13	0.005	0.198	0.00579	-0.00002	-0.00002	4.986	0	0	400	5
22-Sep-13	0.005	0.206	0.00646	-0.00006	-0.00009	5.004	0	0	400	5
24-Sep-13	0.005	0.192	0.00516	0	-0.00005	4.704	0	0	400	5
28-Sep-13	0.007	0.274	0.00893	-0.00003	-0.00002	6.37	0	0	200	5
30-Sep-13	0.007	0.236	0.00822	-0.00013	-0.00004	5.545	0	0	200	5
2-Oct-13	0.004	0.157	0.01083	-0.00002	-0.00005	3.48	0	0	200	5
4-Oct-13	0.004	0.16	0.00737	-0.00004	-0.00007	3.502	0	0	200	5
6-Oct-13	0.004	0.164	0.01073	-0.00001	-0.00005	3.816	0	0	200	5
8-Oct-13	0.004	0.13	0.0054	-0.00014	-0.00011	2.488	0	0	200	5
10-Oct-13	0.004	0.119	0.00522	-0.00003	-0.00008	2.306	0	0	200	5
12-Oct-13	0.004	0.136	0.00325	-0.00008	-0.0001	2.769	0	0	200	5

Appendix B. Raw ANN Data for MFC #10

Table B1. Data for MFC #10

Date	Input Matrix Data						Output Matrix Data			
	PH (mA)	PA (mA-hr)	AR (mA/hr)	10SR (mA/hr)	SR (mA/hr)	FrM	[Aldicarb] (ppb)	[DMMP] (ppm)	[BPA] (ppb)	MFC No.
9-Apr-13	0.048	1.540	0.03216	-0.00193	-0.00044	35.73824	800	0	0	10
15-Apr-13	0.050	1.615	0.01142	-0.00100	-0.00103	37.76086	800	0	0	10
17-Apr-13	0.044	1.609	0.01327	-0.00038	-0.00069	37.53825	800	0	0	10
19-Apr-13	0.052	1.581	0.01432	-0.00089	-0.00076	32.10609	800	0	0	10
21-Apr-13	0.038	1.330	0.00357	-0.00089	-0.00043	32.58294	800	0	0	10
23-Apr-13	0.038	1.107	0.00463	-0.00115	-0.00054	22.98566	800	0	0	10
25-Apr-13	0.040	1.142	0.00825	-0.00128	-0.00052	23.14054	800	0	0	10
27-Apr-13	0.059	1.547	0.00812	-0.00277	-0.00094	31.71992	800	0	0	10
29-Apr-13	0.050	1.390	0.00838	-0.00145	-0.00078	27.10321	800	0	0	10
1-May-13	0.089	2.621	0.01202	-0.00266	-0.00183	54.78257	800	0	0	10
5-May-13	0.095	2.879	0.02704	-0.00245	-0.00143	58.92710	800	0	0	10
7-May-13	0.105	3.283	0.02974	-0.00165	-0.00289	63.86678	800	0	0	10
9-May-13	0.070	2.491	0.01480	-0.00224	-0.00162	54.59157	800	0	0	10
13-May-13	0.048	1.497	0.00457	-0.00149	-0.00950	34.04088	400	0	0	10
17-May-13	0.043	1.540	0.00701	-0.00081	-0.00040	35.66350	400	0	0	10
19-May-13	0.113	4.478	0.01465	-0.00038	-0.00051	106.94750	400	0	0	10
21-May-13	0.046	1.399	0.00706	-0.00117	-0.00087	29.59246	400	0	0	10
29-May-13	0.030	0.913	0.01505	-0.00090	-0.00106	20.13369	400	0	0	10
4-Jun-13	0.083	2.517	0.01290	-0.00182	-0.00246	49.45327	200	0	0	10
6-Jun-13	0.098	2.840	0.09870	-0.00406	-0.00259	60.01716	200	0	0	10
8-Jun-13	0.095	3.132	0.01250	-0.00061	-0.00213	66.74736	200	0	0	10
10-Jun-13	0.102	3.906	0.01557	-0.00061	-0.00091	88.18084	200	0	0	10
12-Jun-13	0.086	3.226	0.01633	-0.00072	-0.00121	70.13469	200	0	0	10
14-Jun-13	0.118	5.282	0.05673	-0.00092	-0.00075	132.88120	200	0	0	10
16-Jun-13	0.093	3.756	0.02501	-0.00018	-0.00050	89.14399	200	0	0	10
30-Jun-13	0.019	0.743	0.00842	-0.00054	0.00006	18.60927	0	916	0	10
18-Jul-13	0.007	0.243	0.00650	0.00000	0	6.03	0	458	0	10
20-Jul-13	0.005	0.092	0.00081	0.00000	0	2.96	0	458	0	10
22-Jul-13	0.004	-0.003	0.00103	0.00000	0	0.61	0	458	0	10
24-Jul-13	0.004	0.061	0.00054	0.00000	0	1.9	0	458	0	10
26-Jul-13	0.004	0.007	0.00098	0.00000	0	1.02	0	458	0	10
28-Jul-13	0.005	0.061	0.00105	0.00000	0	2.21	0	458	0	10
30-Jul-13	0.004	0.024	0.00116	0.00000	0	1.3	0	458	0	10
1-Aug-13	0.003	0.011	0.00090	0.00000	0	0.81	0	458	0	10
5-Aug-13	0.004	0.109	0.00378	0.00000	0	3.4	0	229	0	10
7-Aug-13	0.003	-0.013	0.00125	0.00000	0	0.63	0	229	0	10
9-Aug-13	0.002	0.009	0.00053	0.00000	0	0.91	0	229	0	10
11-Aug-13	0.002	-0.003	0.00050	0.00000	0	0.69	0	229	0	10
13-Aug-13	0.001	-0.020	0.00047	0.00000	0	0.39	0	229	0	10
15-Aug-13	0.002	-0.018	0.00039	0.00000	0	0.48	0	229	0	10
17-Aug-13	0.002	-0.026	0.00044	0.00000	0	0.46	0	229	0	10
19-Aug-13	0.001	-0.046	0.00050	0.00000	0	0.11	0	229	0	10
23-Aug-13	0.004	0.172	0.01322	0.00000	0	4.5	0	0	800	10
25-Aug-13	0.004	0.120	0.00881	0.00000	0	3.12	0	0	800	10
27-Aug-13	0.004	0.088	0.00623	0.00000	0	2.43	0	0	800	10
29-Aug-13	0.004	0.111	0.00831	0.00000	0	3.33	0	0	800	10
31-Aug-13	0.004	0.108	0.00819	0.00000	0	3.45	0	0	800	10
2-Sep-13	0.003	0.008	0.00699	0.00000	0	2.26	0	0	800	10
4-Sep-13	0.002	0.076	0.00729	0.00000	0	2.22	0	0	800	10
6-Sep-13	0.003	0.067	0.00329	0	0	1.895	0	0	800	10
12-Sep-13	0.004	0.128	0.00677	0	0	3.3	0	0	400	10
14-Sep-13	0.003	0.086	0.00497	0	0	2.215	0	0	400	10
16-Sep-13	0.003	0.092	0.00461	0	0	2.566	0	0	400	10
18-Sep-13	0.003	0.086	0.00434	0	0	2.234	0	0	400	10
20-Sep-13	0.003	0.096	0.00429	0	0	2.424	0	0	400	10
24-Sep-13	0.001	0.037	0.00081	0	0	0.871	0	0	400	10
28-Sep-13	0.002	0.081	0.00046	-0.00001	-0.00001	2.073	0	0	200	10
30-Sep-13	0.001	0.023	0.00006	0	0	0.57	0	0	200	10

Appendix C. Raw ANN Data for MFC #6

Table C1. Data for MFC #6

Date	Input Matrix Data						Output Matrix Data			
	PH (mA)	PA (mA-hr)	AR (mA/hr)	10SR (mA/hr)	SR (mA/hr)	FrM	DV1*	DV2*	DV3*	Chemical Type**
30-Jun-13	0.119	4.454	0.05951	-0.00099	-0.00171	98.77941	0	0	0	1
2-Jul-13	0.11	4	0.04107	-0.00157	-0.00123	86.13739	0	0	0	1
5-Aug-13	0.086	3.678	0.03437	-0.00131	-0.00177	93	0	0	0	2
7-Aug-13	0.099	3.818	0.373	-0.00155	-0.00231	85.1	0	0	0	2
9-Aug-13	0.1	4.08	0.04699	-0.00036	-0.00247	93.3	0	0	0	2
11-Aug-13	0.098	3.871	0.05066	-0.00034	-0.00171	85.7	0	0	0	2
13-Aug-13	0.106	4.033	0.05504	-0.0005	-0.00226	86.7	0	0	0	2
15-Aug-13	0.11	4.317	0.0636	-0.00072	-0.00264	95.5	0	0	0	2
19-Aug-13	0.111	3.447	0.10097	-0.0013	-0.0015	77.1	0	0	0	2
14-Sep-13	0.15	5.307	0.1682	-0.00209	-0.00153	113.9559	0	0	0	3
16-Sep-13	0.144	5.299	0.11394	-0.00182	-0.00155	114.5259	0	0	0	3
18-Sep-13	0.153	5.346	0.12371	-0.00253	-0.00163	112.3191	0	0	0	3
20-Sep-13	0.146	5.008	0.11922	-0.0025	-0.00172	104.138	0	0	0	3
22-Sep-13	0.149	5.115	0.13498	-0.00228	-0.00173	107.0792	0	0	0	3
24-Sep-13	0.148	5.202	0.11126	-0.0024	-0.00148	113.2197	0	0	0	3

* DV denotes the use of a dummy variable in the matrix
 ** Chemical type codes for solutions where the feed medium was used as the solvent are: 1) DMMP; 2) BPA; 3) Aldicarb

Appendix D. Raw ANN Data for MFC #7

Table D1. Data for MFC #7

Date	Input Matrix Data						Output Matrix Data			
	PH (mA)	PA (mA-hr)	AR (mA/hr)	10SR (mA/hr)	SR (mA/hr)	FrM	DV1*	DV2*	DV3*	Chemical Type**
30-Jun-13	0.145	5.16	0.11468	-0.0022	-0.00192	111.6439	0	0	0	1
2-Jul-13	0.131	4.537	0.12796	-0.00134	-0.00187	90.25503	0	0	0	1
5-Aug-13	0.125	5.215	0.18039	-0.00011	-0.00077	125	0	0	0	2
7-Aug-13	0.156	5.124	0.17698	-0.00237	-0.00243	102	0	0	0	2
9-Aug-13	0.148	5.015	0.16145	-0.00292	-0.00192	105.8	0	0	0	2
11-Aug-13	0.147	4.859	0.16956	-0.00271	-0.00207	98.3	0	0	0	2
13-Aug-13	0.142	4.746	0.18454	-0.00224	-0.00182	97.6	0	0	0	2
17-Aug-13	0.163	5.779	0.24813	-0.00265	-0.00191	123.9	0	0	0	2
19-Aug-13	0.149	5.004	0.20621	-0.00242	-0.00195	103.7	0	0	0	2
10-Sep-13	0.185	5.951	0.20889	-0.00262	-0.00252	119.522	0	0	0	3
12-Sep-13	0.2	5.768	0.17359	-0.0038	-0.00297	111.131	0	0	0	3
16-Sep-13	0.259	7.952	0.2286	-0.00495	-0.0032	165.599	0	0	0	3
18-Sep-13	0.226	6.76	0.16769	-0.00509	-0.00273	137.514	0	0	0	3
20-Sep-13	0.237	6.465	0.18254	-0.00509	-0.00379	121.461	0	0	0	3
22-Sep-13	0.217	6.044	0.17768	-0.00572	-0.0029	119.208	0	0	0	3
24-Sep-13	0.237	7.007	0.14942	-0.00534	-0.00319	139.8	0	0	0	3

* DV denotes the use of a dummy variable in the matrix

** Chemical type codes for solutions where the feed medium was used as the solvent are: 1) DMMP; 2) BPA; 3) Aldicarb

Appendix E. Raw ANN Data for MFC #8

Table E1. Data for MFC #8

Date	Input Matrix Data						Output Matrix Data			
	PH (mA)	PA (mA-hr)	AR (mA/hr)	10SR (mA/hr)	SR (mA/hr)	FrM	DV1*	DV2*	DV3*	Chemical Type**
12-Jun-13	0.03	1.01	0.00404	-0.00029	-0.00035	21.52317	0	0	0	1
14-Jun-13	0.035	1.104	0.00694	-0.0005	-0.00061	23.97951	0	0	0	1
16-Jun-13	0.036	1.263	0.00517	-0.00042	-0.00023	27.49795	0	0	0	1
18-Jun-13	0.063	1.895	0.00882	-0.00086	-0.001	37.97976	0	0	0	1
20-Jun-13	0.054	1.744	0.00745	-0.00098	-0.00115	36.04927	0	0	0	1
22-Jun-13	0.053	1.79	0.00762	-0.00109	-0.00026	41.972	0	0	0	1
24-Jun-13	0.6	2.215	0.01147	-0.00023	-0.0002	47.1617	0	0	0	1
26-Jun-13	0.06	2.484	0.01217	-0.00033	-0.00042	60.67105	0	0	0	1
2-Jul-13	0.052	1.659	0.00529	-0.00084	-0.00068	35.374	0	0	0	2
18-Jul-13	0.02	0.698	0.01396	-0.00022	-0.00017	15.1	0	0	0	3
20-Jul-13	0.017	0.668	0.00935	-0.00026	-0.00013	16.3	0	0	0	3
22-Jul-13	0.021	0.708	0.01261	-0.00017	-0.00021	14.7	0	0	0	3
24-Jul-13	0.021	0.747	0.00852	-0.00024	-0.00024	17.3	0	0	0	3
30-Jul-13	0.022	0.737	0.01032	-0.00021	-0.00021	16.6	0	0	0	3
7-Aug-13	0.015	0.291	0.00254	0	0	9.05	0	0	0	4
11-Aug-13	0.012	0.249	0.00092	0	0	2	0	0	0	4
13-Aug-13	0.013	0.271	0.00091	0	0	6.55	0	0	0	4
2-Sep-13	0.129	5.206	0.06241	0	-0.00036	122.74	0	0	0	5
4-Sep-13	0.28	10.896	0.23015	-0.0038	-0.003	248.54	0	0	0	5
14-Sep-13	0.05	1.92	0.01036	-0.0004	-0.00032	46.075	0	0	0	6
16-Sep-13	0.04	1.688	0.011	-0.00025	-0.00005	41.501	0	0	0	6
18-Sep-13	0.038	1.496	0.0087	-0.00004	-0.00007	35.862	0	0	0	6
20-Sep-13	0.038	1.478	0.00749	-0.00007	-0.00007	36.274	0	0	0	6
22-Sep-13	0.036	1.419	0.00789	-0.00014	-0.00024	34.965	0	0	0	6
24-Sep-13	0.032	1.265	0.00626	-0.00026	-0.00019	31.176	0	0	0	6

* DV denotes the use of a dummy variable in the matrix
 ** Chemical type codes for aqueous chemical mixtures and individual aqueous chemical solutions are: 1) Aldicarb/BPA; 2) Aldicarb/DMMP; 3) DMMP/BPA; 4) DMMP; 5) Aldicarb; 6) BPA

Appendix F. Raw ANN Data for MFC #9

Table F1. Data for MFC #9

Date	Input Matrix Data						Output Matrix Data			
	PH (mA)	PA (mA-hr)	AR (mA/hr)	10SR (mA/hr)	SR (mA/hr)	FrM	DV1*	DV2*	DV3*	Chemical Type**
10-Jun-13	0.028	0.993	0.02055	-0.00003	-0.00036	20.29798	0	0	0	1
12-Jun-13	0.017	0.591	0.00938	-0.00022	-0.00008	12.68642	0	0	0	1
14-Jun-13	0.061	2.348	0.00302	0	0	67.43188	0	0	0	1
16-Jun-13	0.067	2.404	0.00766	0	0	63.08373	0	0	0	1
18-Jun-13	0.066	2.096	0.00564	0	0	48.95272	0	0	0	1
20-Jun-13	0.064	2.299	0.00441	-0.00133	-0.00133	61.56813	0	0	0	1
22-Jun-13	0.079	2.282	0.00536	0	0	60.28423	0	0	0	1
24-Jun-13	0.066	2.369	0.00564	-0.00053	-0.00028	57.34818	0	0	0	1
30-Jun-13	0.028	1.091	0.01239	-0.00025	-0.00019	27.453	0	0	0	2
2-Jul-13	0.032	0.908	0.00398	-0.0012	-0.00036	19.155	0	0	0	2
18-Jul-13	0.015	0.574	0.01119	0	0	13.447	0	0	0	3
24-Jul-13	0.172	0.557	0.1169	-0.01584	-0.03068	-8.291	0	0	0	3
28-Jul-13	0.141	-0.615	0.26026	-0.01556	-0.04695	-0.01283	0	0	0	3
7-Aug-13	0	0.007	0.00003	0	0	0.1812	0	0	0	4
9-Aug-13	0	0.016	0.00008	-0.00002	-0.00001	0.323	0	0	0	4
13-Aug-13	0	0.012	0.00003	-0.00002	-0.00001	0.319	0	0	0	4
27-Aug-13	0.054	0.27	0.05163	-0.00468	-0.01531	1.38	0	0	0	5
14-Sep-13	0.006	0.246	0.00086	-0.00004	-0.00002	6.063	0	0	0	6
16-Sep-13	0.006	0.279	0.00087	0.00004	0	7.131	0	0	0	6
18-Sep-13	0.007	0.272	0.00067	0.00007	0	6.878	0	0	0	6
20-Sep-13	0.008	0.305	0.00071	0.00007	0.00001	7.99	0	0	0	6
22-Sep-13	0.008	0.284	0.00095	0.00002	0.0001	7.28	0	0	0	6
24-Sep-13	0.006	0.196	0.00089	0.0001	0.00002	4.8	0	0	0	6

* DV denotes the use of a dummy variable in the matrix
 ** Chemical type codes for aqueous chemical mixtures and individual aqueous chemical solutions are: 1) Aldicarb/BPA; 2) Aldicarb/DMMP; 3) DMMP/BPA; 4) DMMP; 5) Aldicarb; 6) BPA

Appendix G. Sample ANN Code using MATLAB

Actual code used for MFC #10 in aldicarb quantification tests (format shown here was the same for all ANN runs):

```
%The format for the input matrix is: ['PH' 'PA' 'AR' '10SR']
%The format for the output matrix is: ['dummy' 'dummy' 'dummy' 'cell_number']

tstart = clock;

inputs = [0.048 1.540 0.03216 -0.00193; 0.050 1.615 0.01142 -0.00100; 0.044 1.609 0.01327
-0.00038;
0.052 1.581 0.01432 -0.00089; 0.038 1.330 0.00357 -0.00089; 0.038 1.107 0.00463 -
0.00115;
0.040 1.142 0.00825 -0.00128; 0.059 1.547 0.00812 -0.00277; 0.050 1.390 0.00838 -
0.00145;
0.089 2.621 0.01202 -0.00266; 0.095 2.879 0.02704 -0.00245; 0.105 3.283 0.02974 -
0.00165;
0.070 2.491 0.01480 -0.00224; 0.048 1.497 0.00457 -0.00149; 0.043 1.540 0.00701 -
0.00081;
0.113 4.478 0.01465 -0.00038; 0.046 1.399 0.00706 -0.00117; 0.030 0.913 0.01505 -
0.00090;
0.083 2.517 0.01290 -0.00182; 0.098 2.840 0.09870 -0.00406; 0.095 3.132 0.01250 -
0.00061;
0.102 3.906 0.01557 -0.00061; 0.086 3.226 0.01633 -0.00072; 0.118 5.282 0.05673 -
0.00092;
0.093 3.756 0.02501 -0.00018];

targets = [800 0 0 10; 800 0 0 10; 800 0 0 10;
800 0 0 10; 800 0 0 10; 800 0 0 10;
800 0 0 10; 800 0 0 10; 800 0 0 10;
800 0 0 10; 400 0 0 10; 400 0 0 10;
400 0 0 10; 400 0 0 10; 400 0 0 10;
200 0 0 10; 200 0 0 10; 200 0 0 10;
200 0 0 10; 200 0 0 10; 200 0 0 10;
200 0 0 10];

%preallocate the plotting matrix (PM)
PM = zeros(25,5);

%the variable is interest is vv - this is the column number in the target
%matrix
vv = 1;
countt = 1;

for count = 1:1:5
% Create a Fitting Network
hiddenLayerSize = count;
```



```

net = fitnet(hiddenLayerSize);
% Set up Division of Data for Training, Validation, Testing
net.divideParam.trainRatio = 80/100;
net.divideParam.valRatio = 10/100;
net.divideParam.testRatio = 10/100;
% Train the Network
[net,tr] = train(net,inputs,targets);
% Test the Network
outputs = net(inputs);
errors = gsubtract(outputs,targets);
performance = perform(net,targets,outputs);
% View the Network
% view(net)
plotperf(tr)

Outputs = net(inputs);
% trOut = Outputs(tr.trainInd);
% vOut = Outputs(tr.valInd);
% tsOut = Outputs(tr.testInd);
% trTarg = Outputs(tr.trainInd);
% vTarg = targets(tr.valInd);
% tsTarg = targets(tr.testInd);
% figure (98)
% plotregression(trTarg,trOut,'Train',vTarg,vOut,'Validation',tsTarg,tsOut,'Testing');

PM(:,countt) = Outputs(:,vv);
countt = countt +1;
end

figure(1)
plot(targets(:,vv),PM(:,1),'ro',targets(:,vv),PM(:,2),'go',targets(:,vv),PM(:,3),'ko',
targets(:,vv),PM(:,4),'m--',targets(:,vv),PM(:,5),'k-')
title('MFC10 Aldicarb Conc using 10-hr SR')
xlabel('Aldicarb Conc')
ylabel('ANN-Derived Aldicarb Conc')
legend('One','Two','Three','Four','Five')

% figure(2)
% plot(targets(:,vv),PM(:,6),'ko',targets(:,vv),PM(:,7),'b-',targets(:,vv),PM(:,8),'--
m+',targets(:,vv),PM(:,9),'bd',targets(:,vv),PM(:,10),'kx')
% title('Model performance for identical simulations')
% xlabel('MFC Number')
% ylabel('ANN-Derived MFC Number')
% legend('Run_6','Run_7','Run_8','Run_9','Run_10')

tstop = clock;
runtime = etime(tstop,tstart)/60;
disp('length of run in minutes:')
disp(runtime)

```

Appendix H. One-way Analysis Plots for MFC #5 and MFC #10

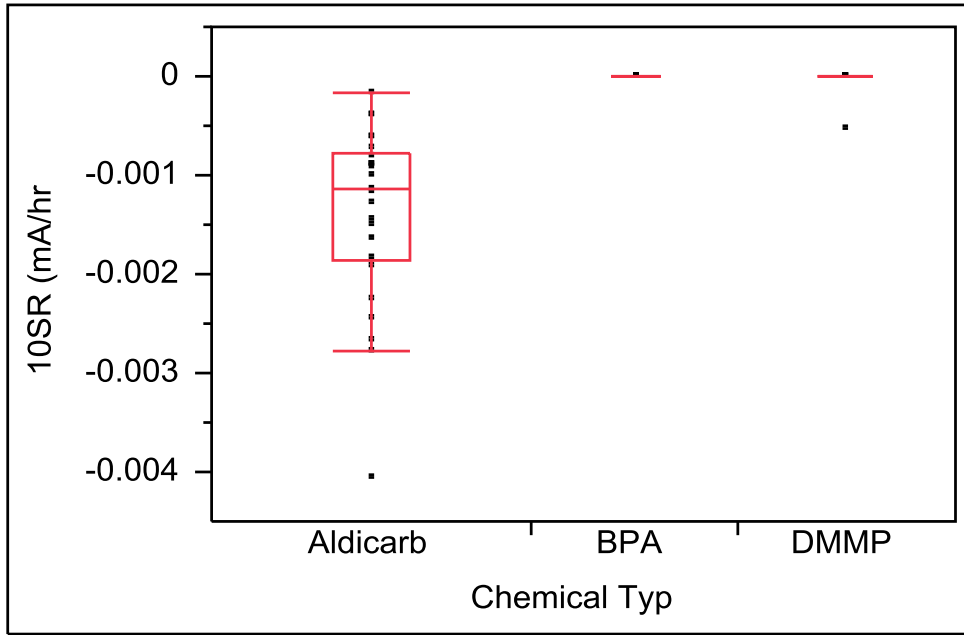


Figure H1. One-way Analysis of 10SR (mA/hr) By Chemical Type in MFC #10

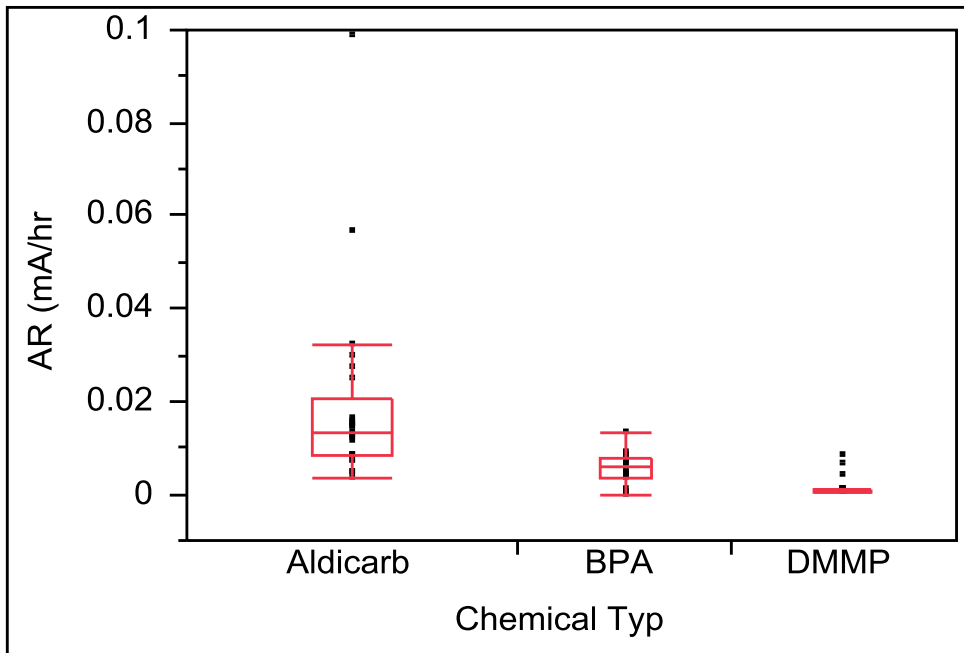


Figure H2. One-way Analysis of AR (mA/hr) By Chemical Type in MFC #10

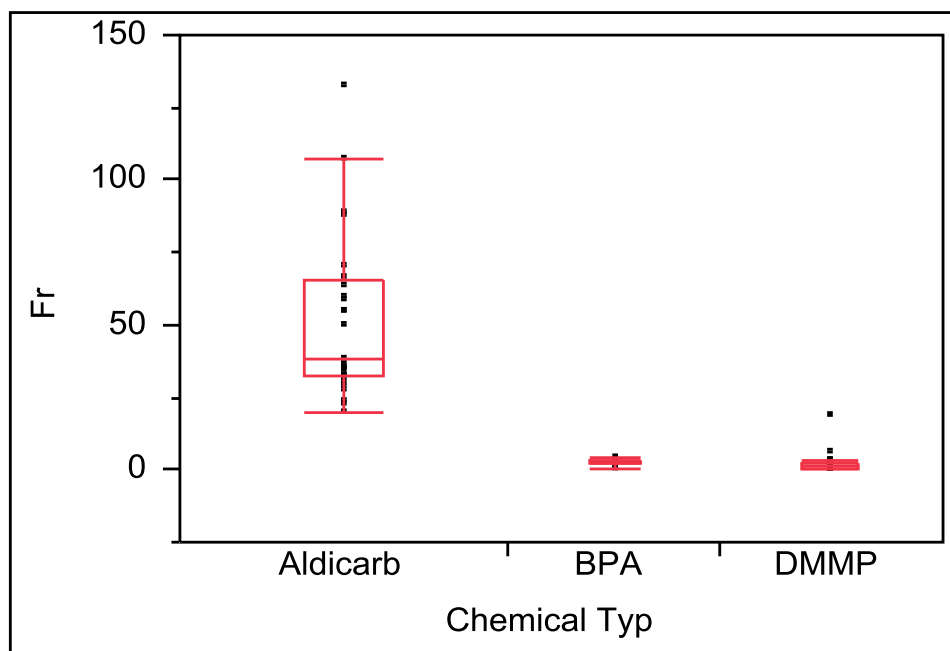


Figure H3. One-way Analysis of FrM By Chemical Type in MFC #10

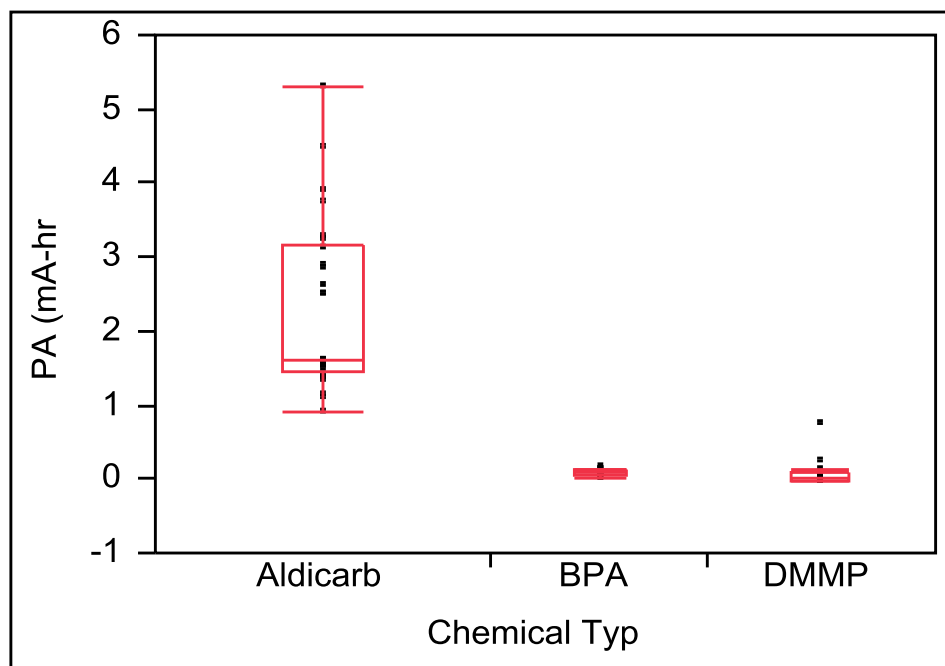


Figure H4. One-way Analysis of PA (mA-hr) By Chemical Type in MFC #10

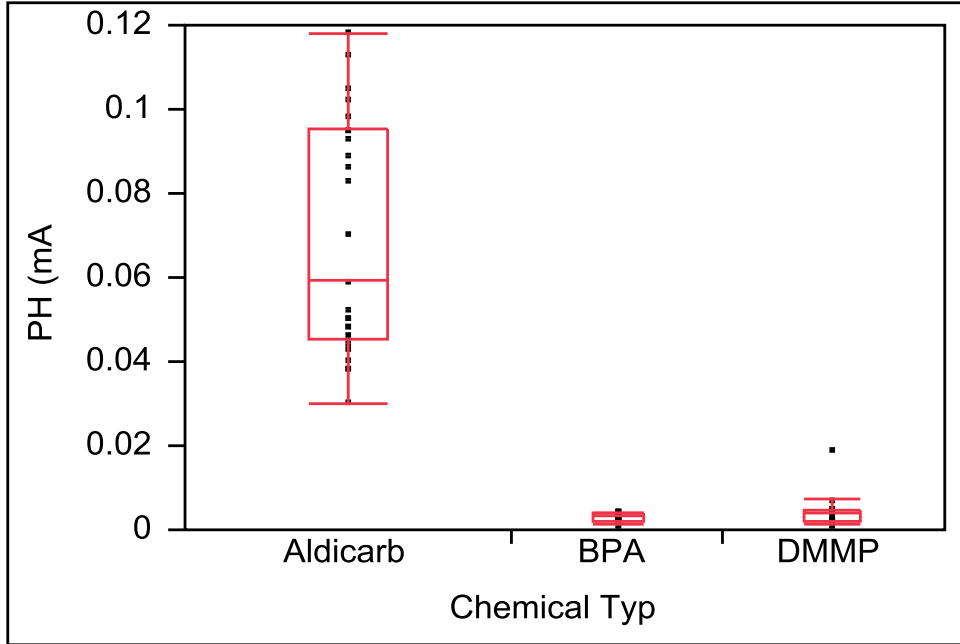


Figure H5. One-way Analysis of PH (mA) By Chemical Type in MFC #10

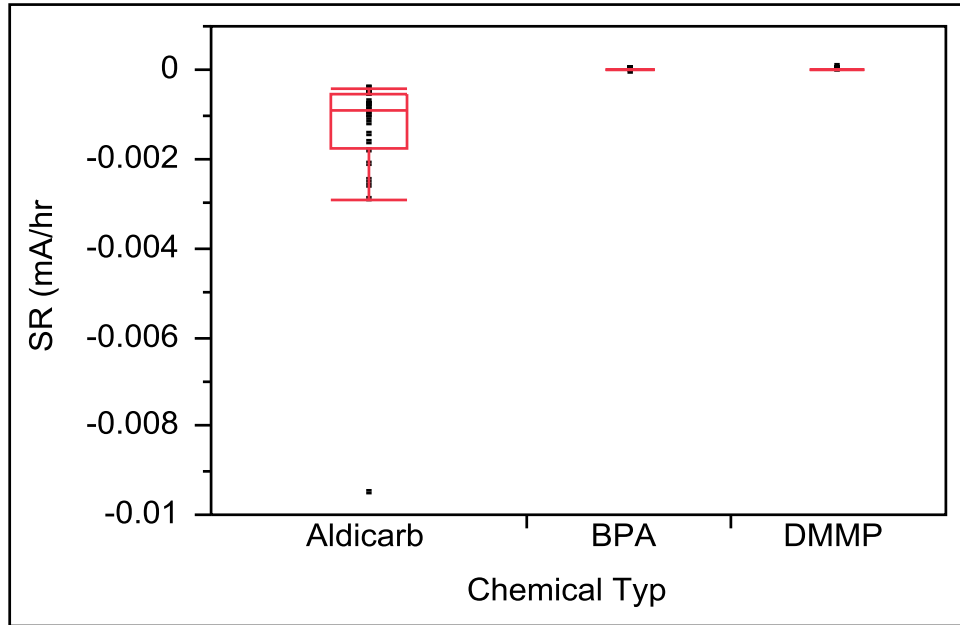


Figure H6. One-way Analysis of SR (mA/hr) By Chemical Type in MFC #10

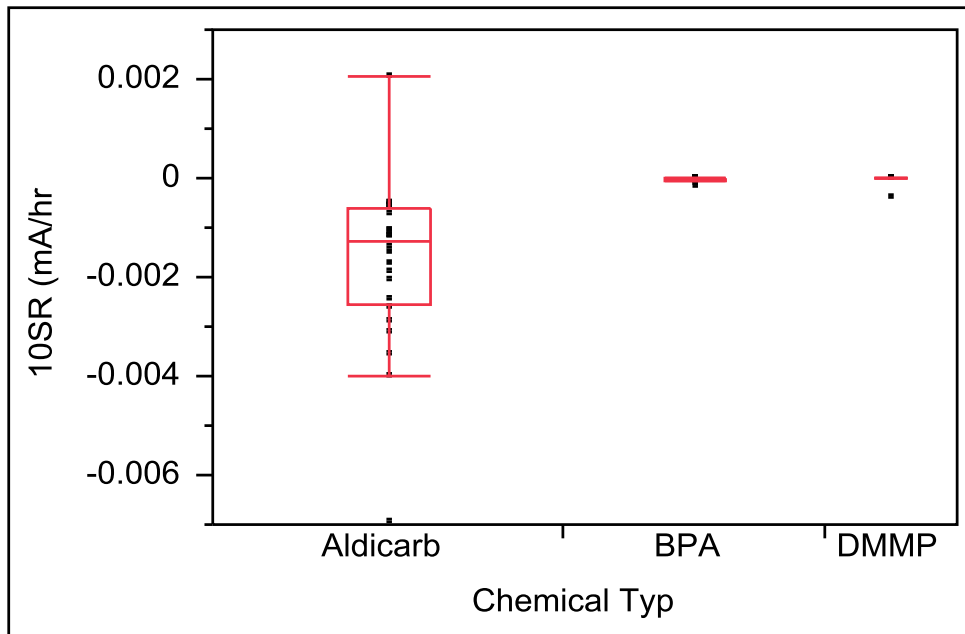


Figure H7. One-way Analysis of 10SR (mA/hr) By Chemical Type in MFC #5

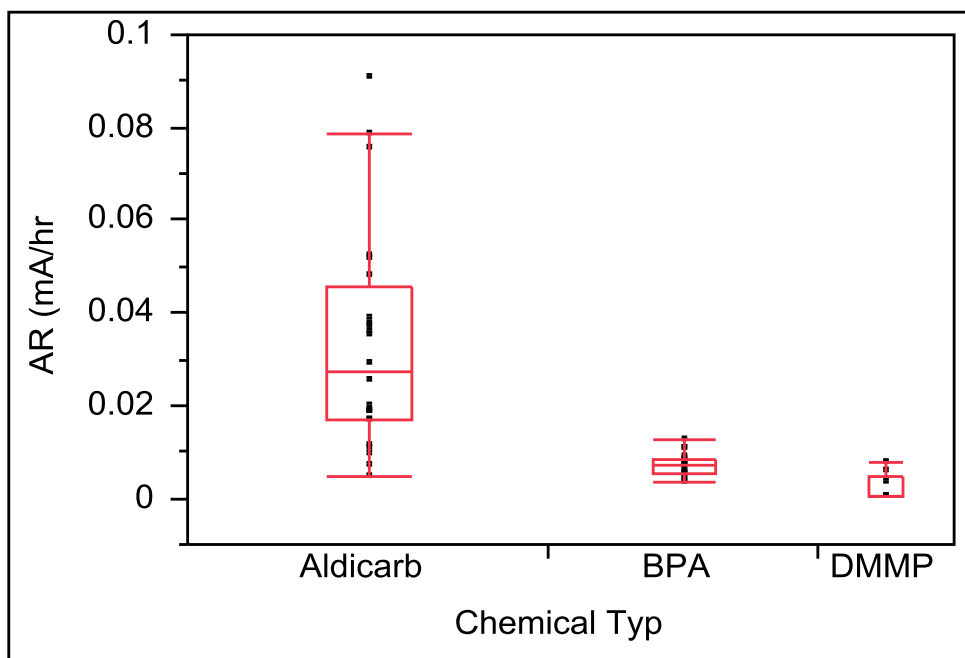


Figure H8. One-way Analysis of AR (mA/hr) By Chemical Type in MFC #5

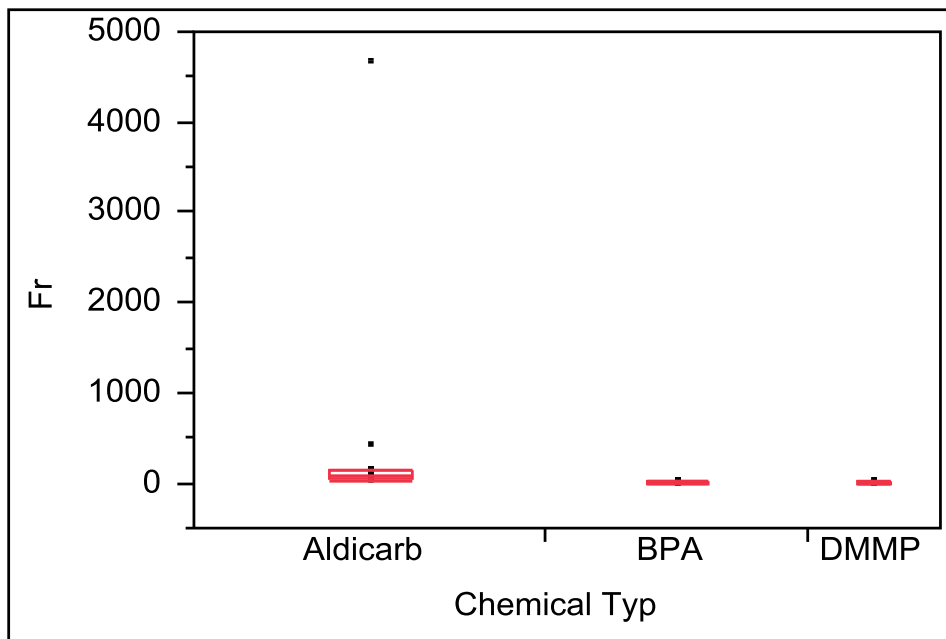


Figure H9. One-way Analysis of FrM By Chemical Type in MFC #5

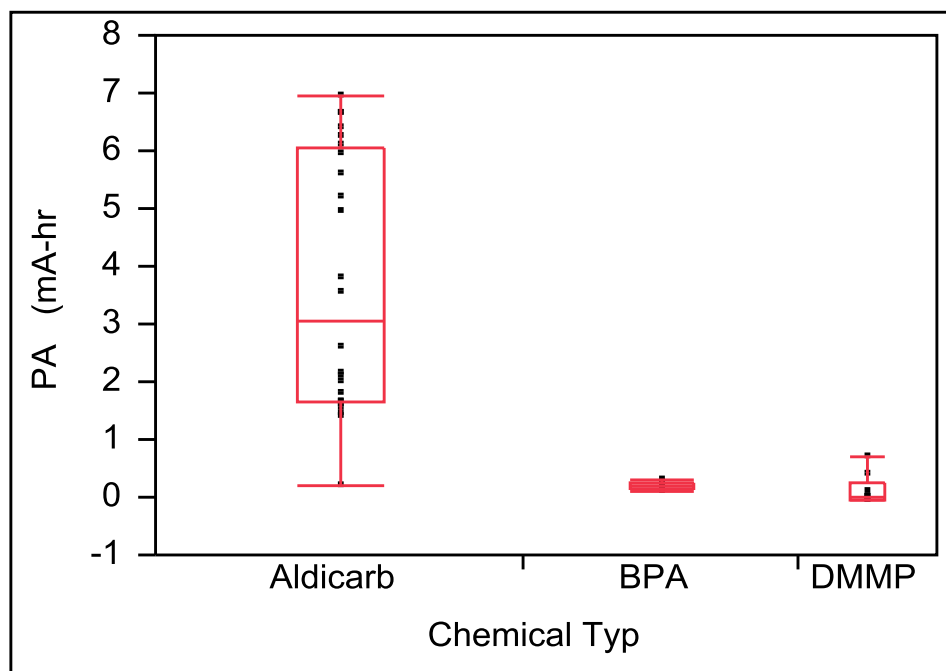


Figure H10. One-way Analysis of PA (mA-hr) By Chemical Type in MFC #5

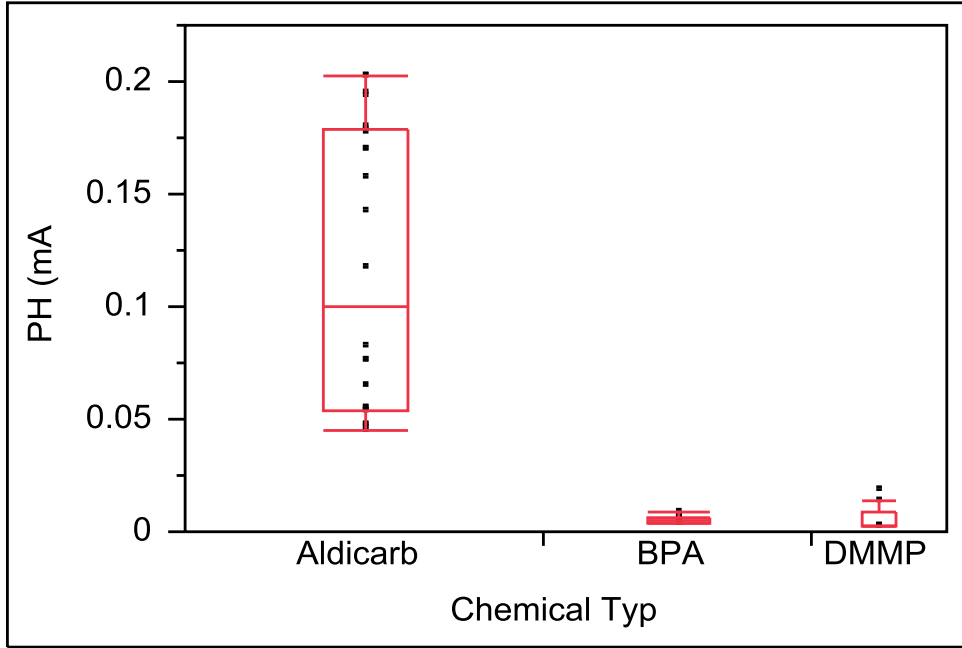


Figure H11. One-way Analysis of PH (mA) By Chemical Type in MFC #5

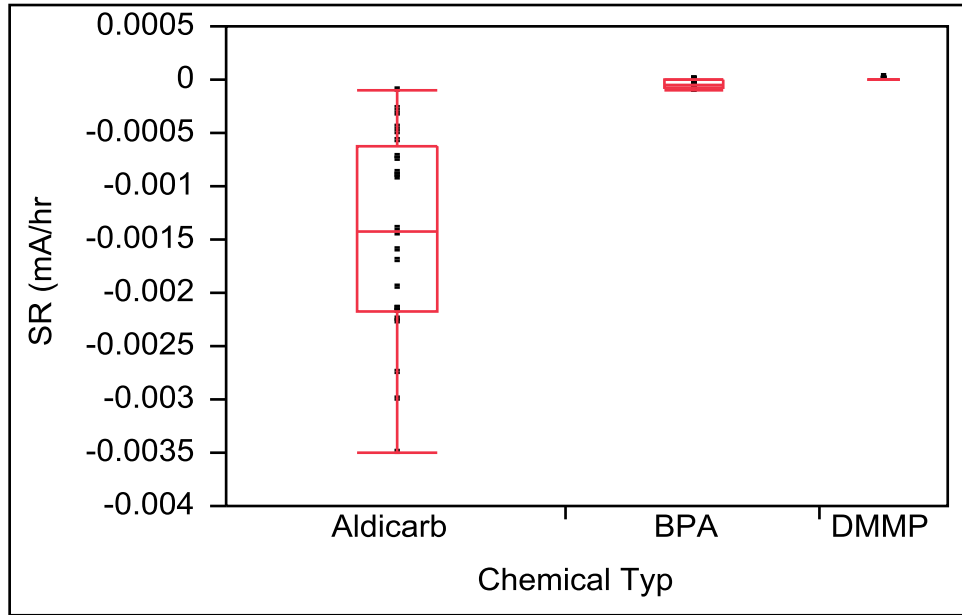


Figure H12. One-way Analysis of SR (mA/hr) By Chemical Type in MFC #5

Appendix I. MFC #5 & MFC #10 Metric Correlations for Quantification

Experiments

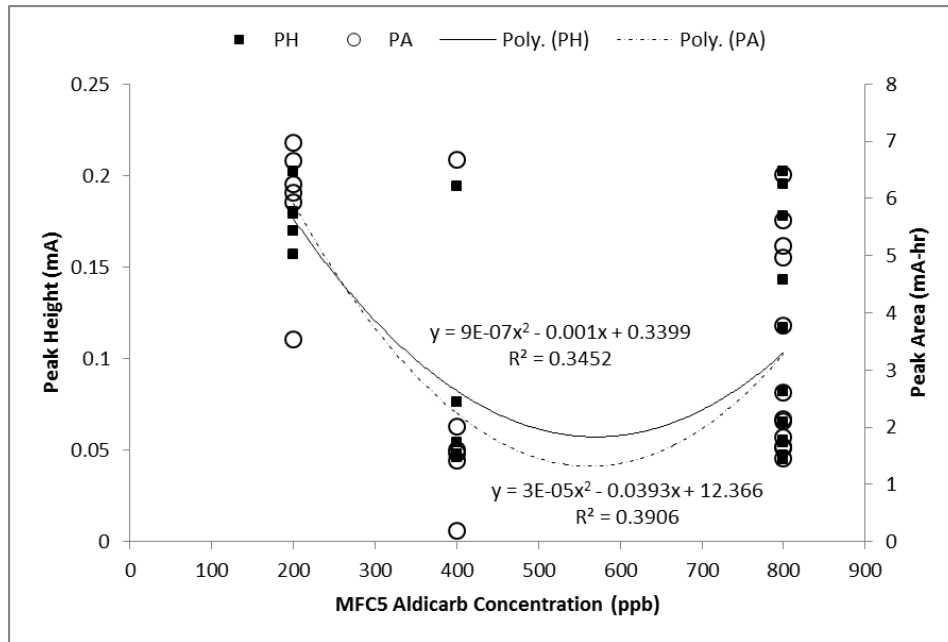


Figure I1. PH and PA Correlations with Aldicarb Concentrations in MFC #5

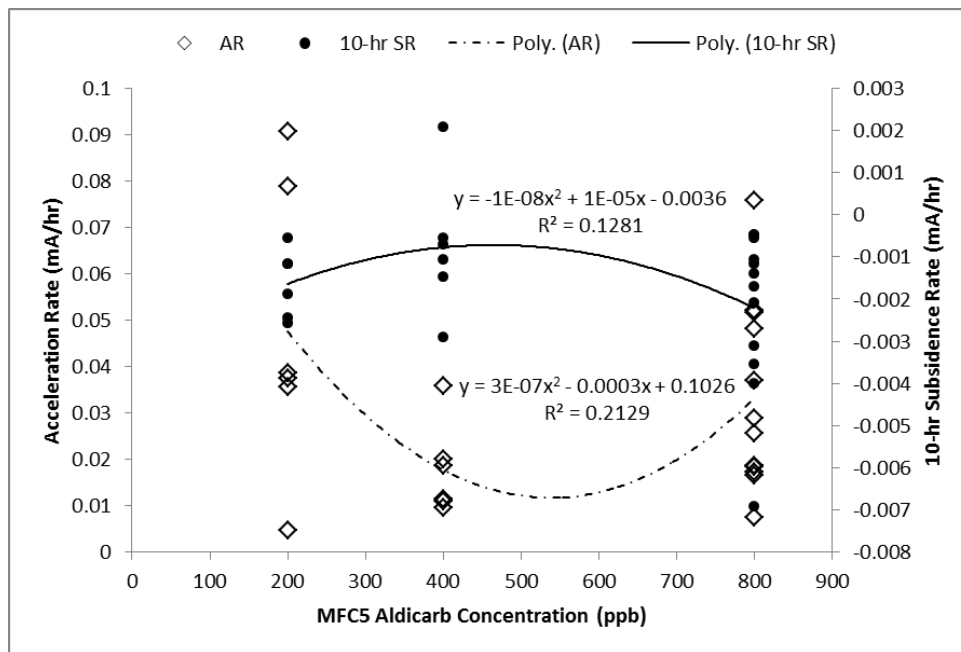


Figure I2. AR and 10SR Correlations with Aldicarb Concentrations in MFC #5

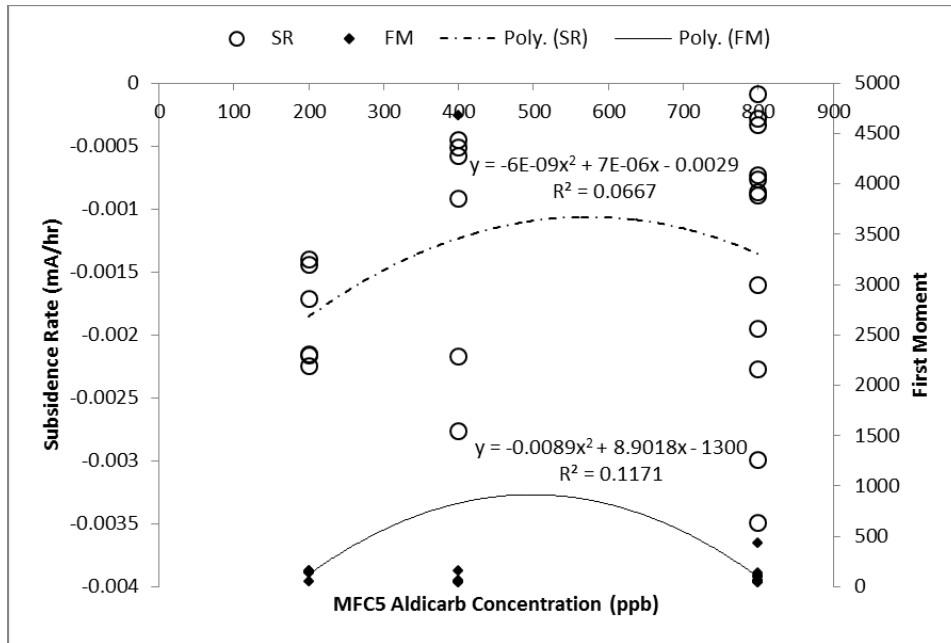


Figure I3. SR and FrM Correlations with Aldicarb Concentrations in MFC #5

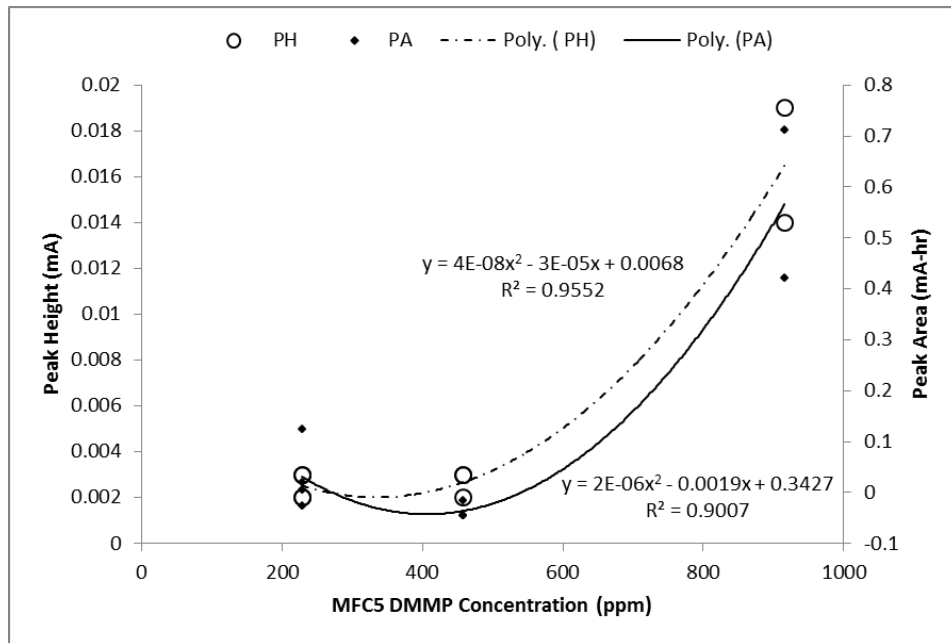


Figure I4. PH and PA Correlations with DMMP Concentrations in MFC #5

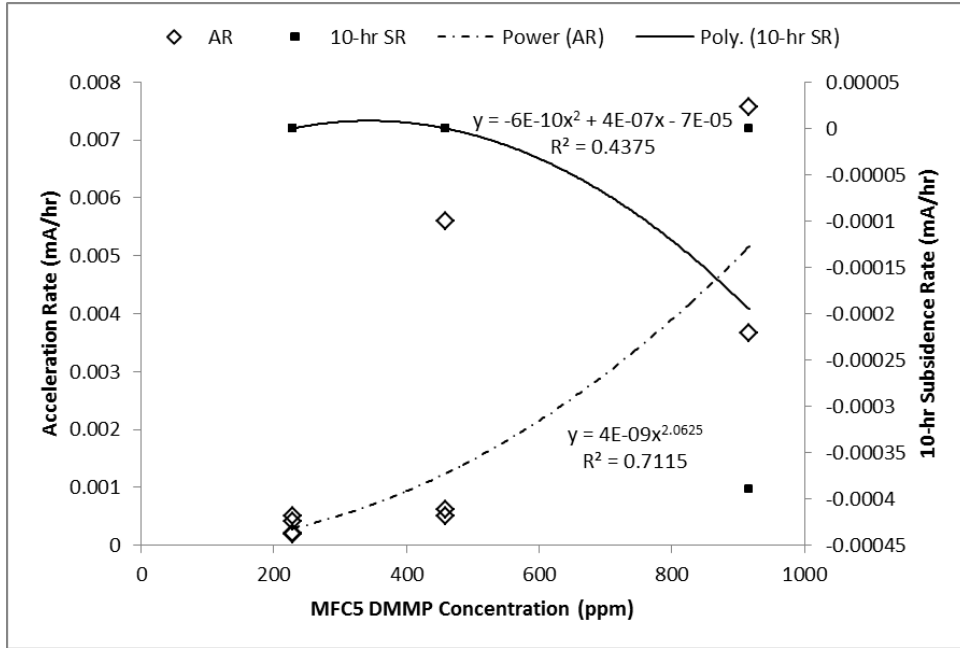


Figure I5. AR and 10SR Correlations with DMMP Concentrations in MFC #5

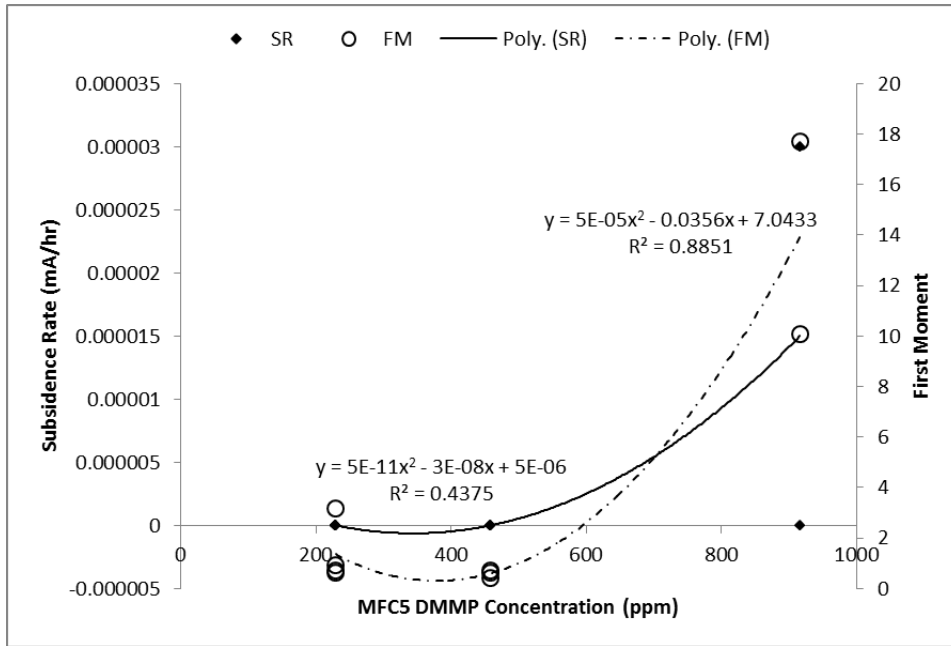


Figure I6. SR and FrM Correlations with DMMP Concentrations in MFC #5

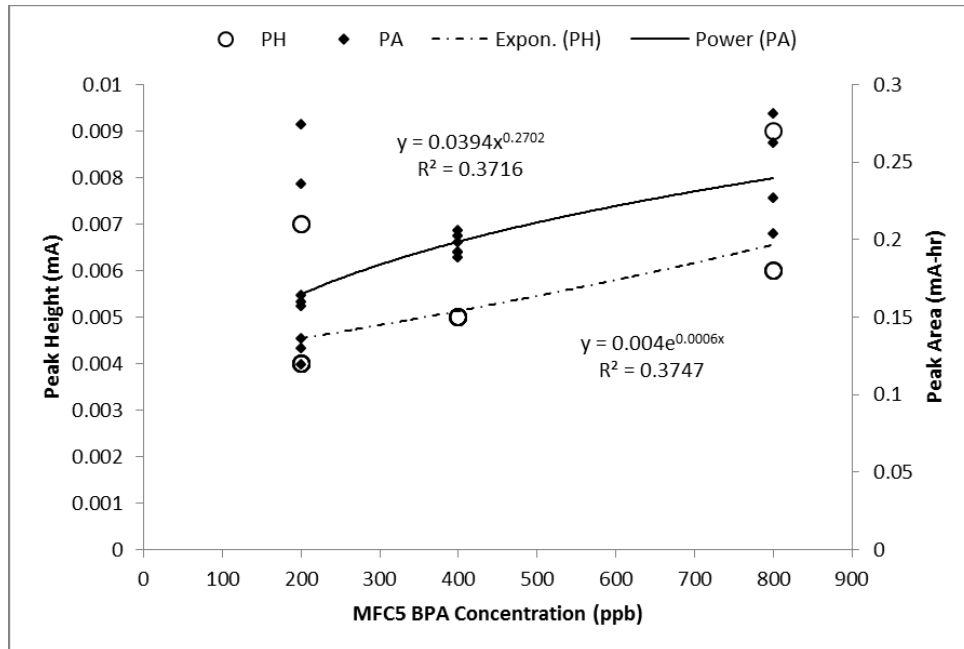


Figure 17. PH and PA Correlations with BPA Concentrations in MFC #5

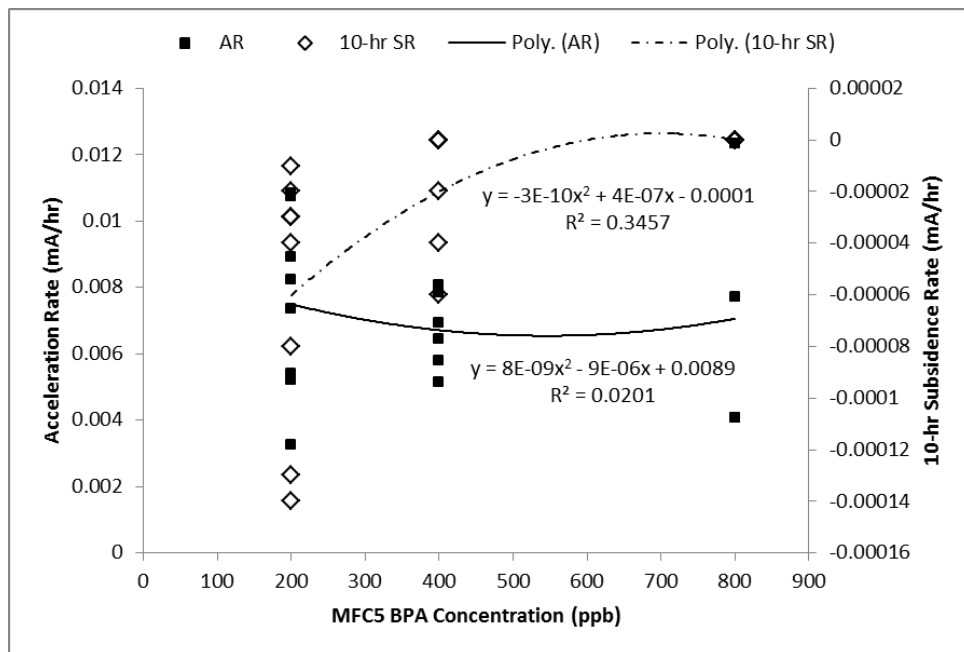


Figure 18. AR and 10SR Correlations with BPA Concentrations in MFC #5

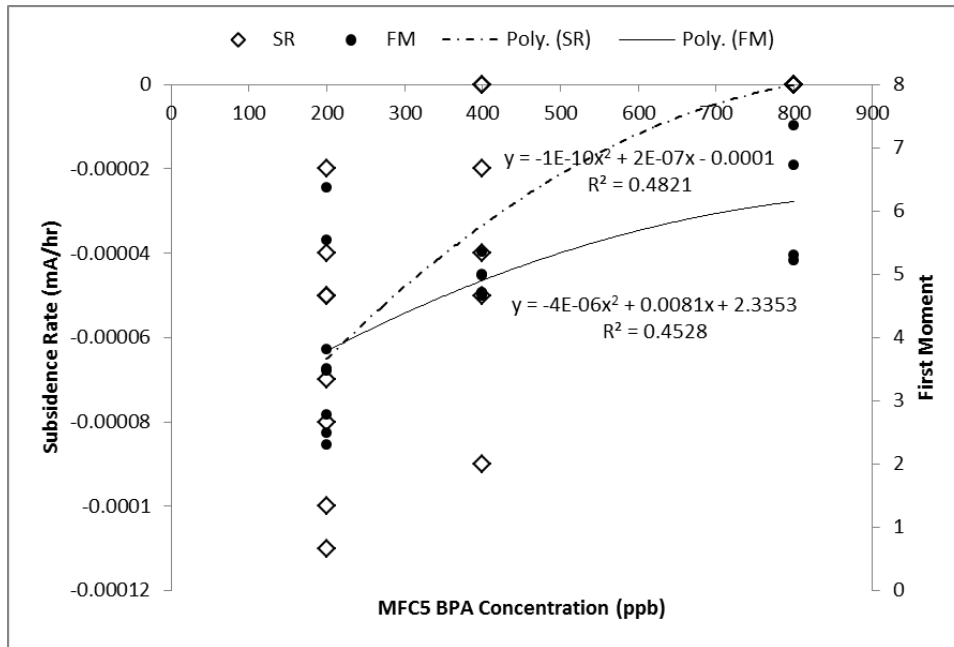


Figure I9. SR and FrM Correlations with BPA Concentrations in MFC #5

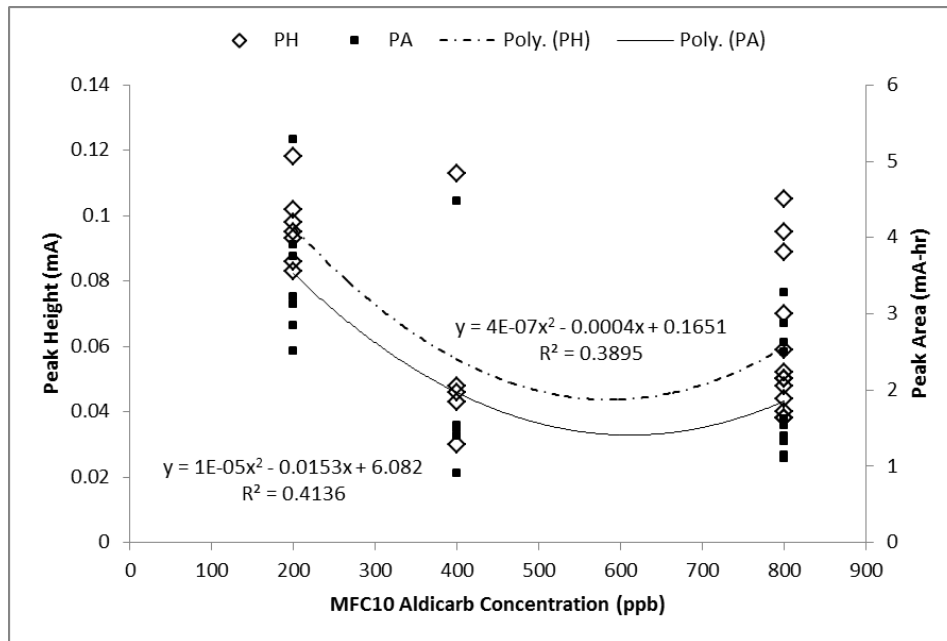


Figure I10. PH and PA Correlations with Aldicarb Concentrations in MFC #10

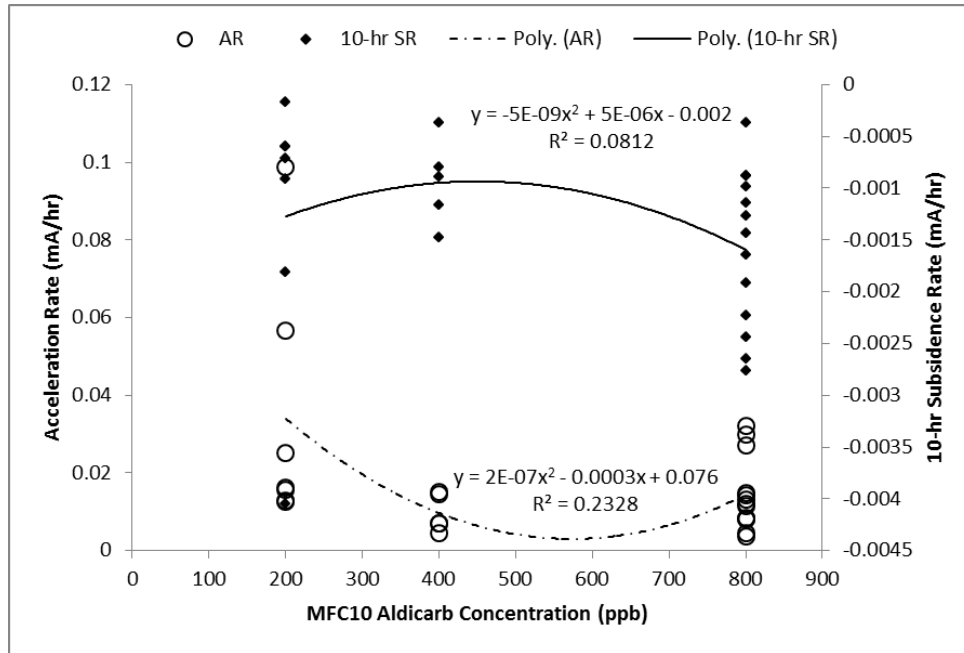


Figure I11. AR and 10SR Correlations with Aldicarb Concentrations in MFC #10

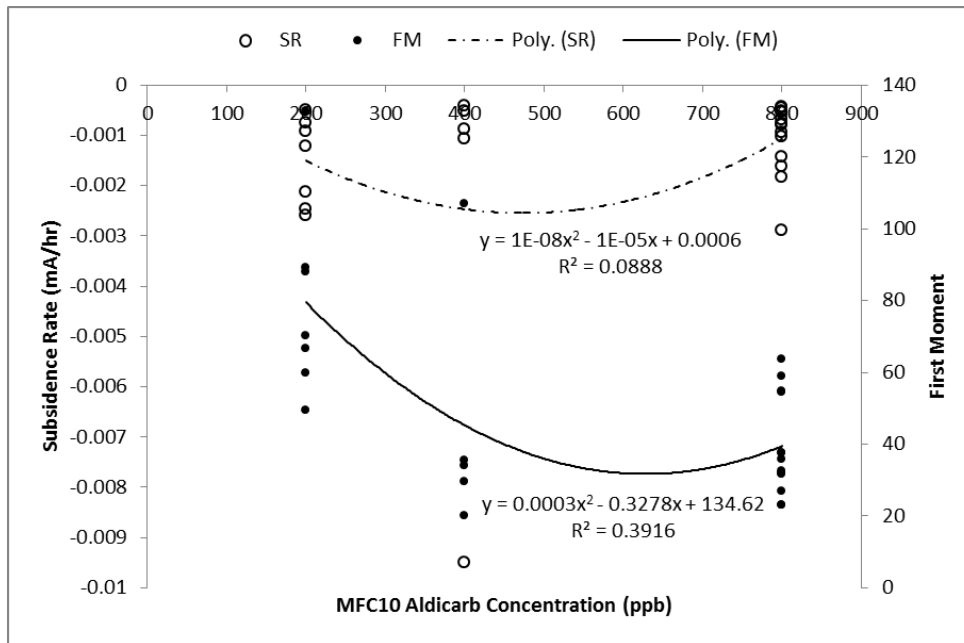


Figure I12. SR and FrM Correlations with Aldicarb Concentrations in MFC #10

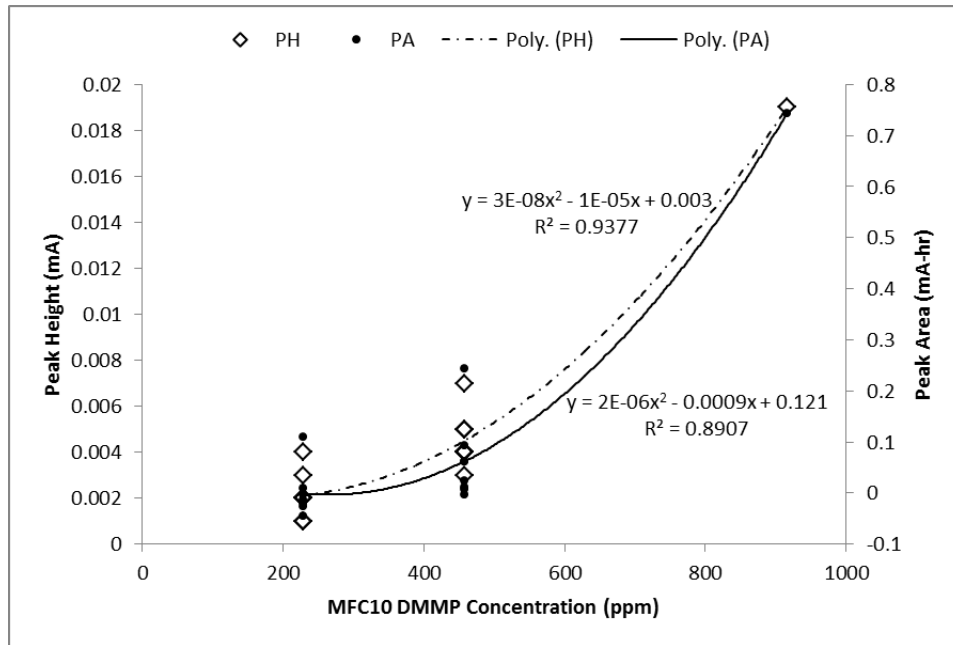


Figure I13. PH and PA Correlations with DMMP Concentrations in MFC #10

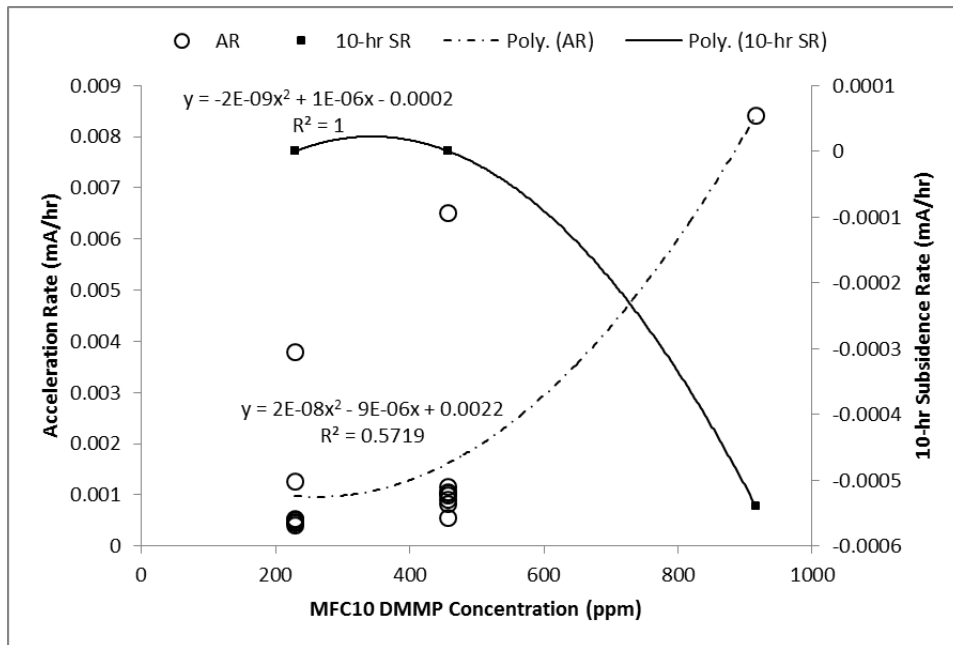


Figure I14. AR and 10SR Correlations with DMMP Concentrations in MFC #10

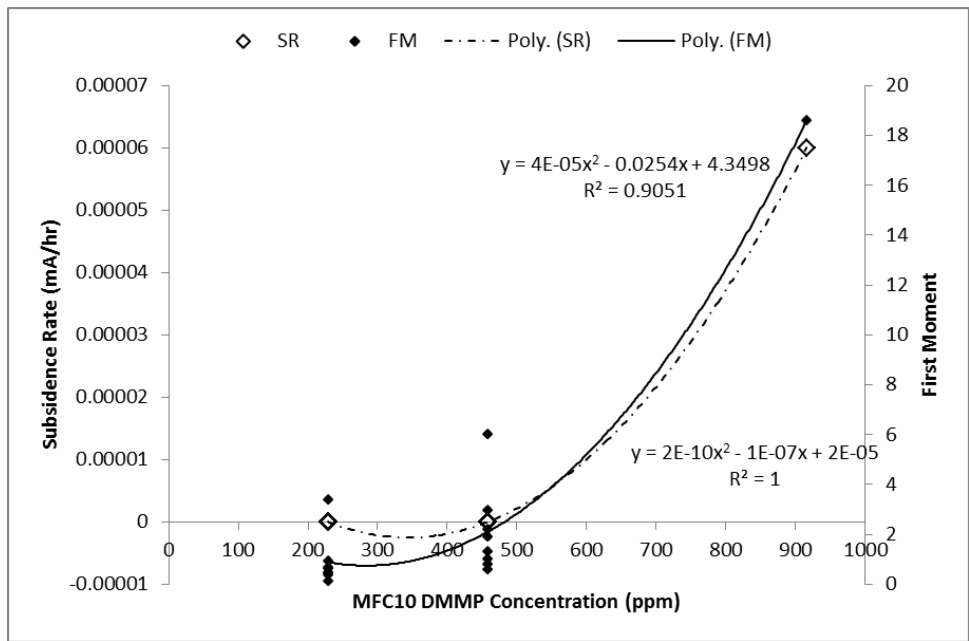


Figure I15. SR and FrM Correlations with DMMP Concentrations in MFC #10

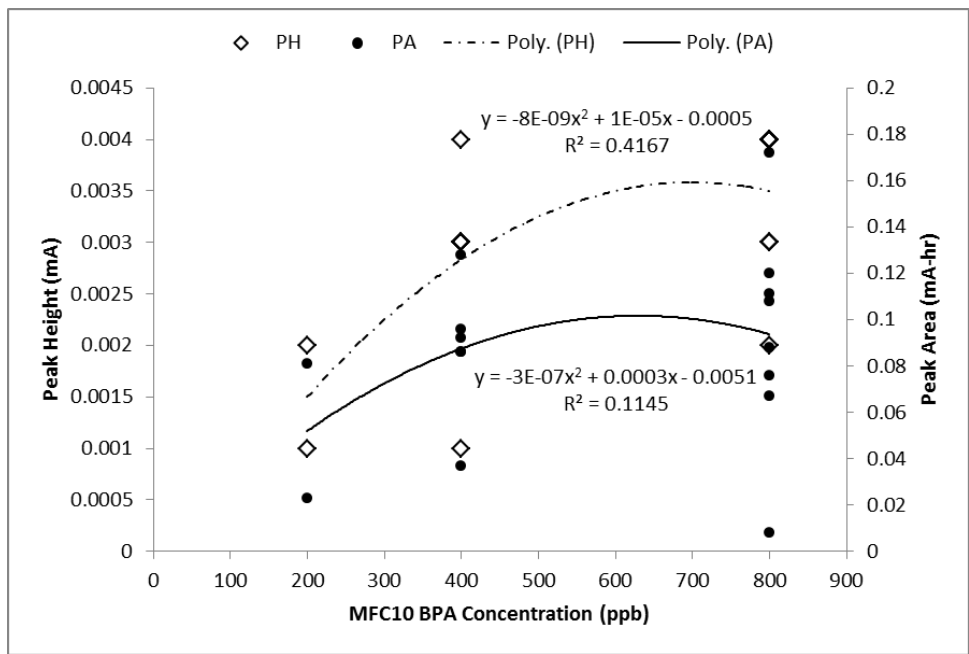


Figure I16. PH and PA Correlations with BPA Concentrations in MFC #10

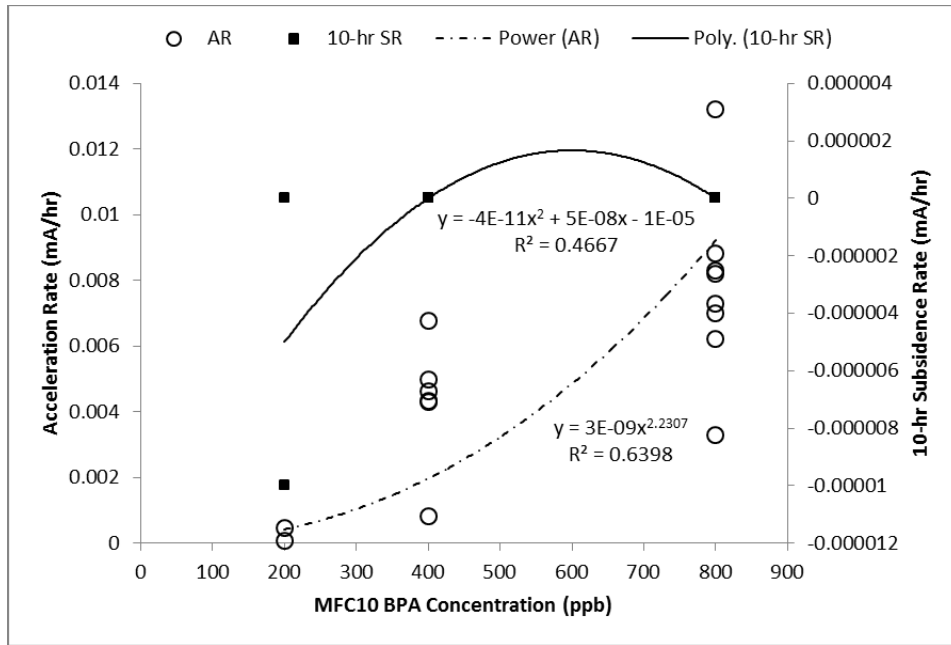


Figure I17. AR and 10SR Correlations with BPA Concentrations in MFC #10

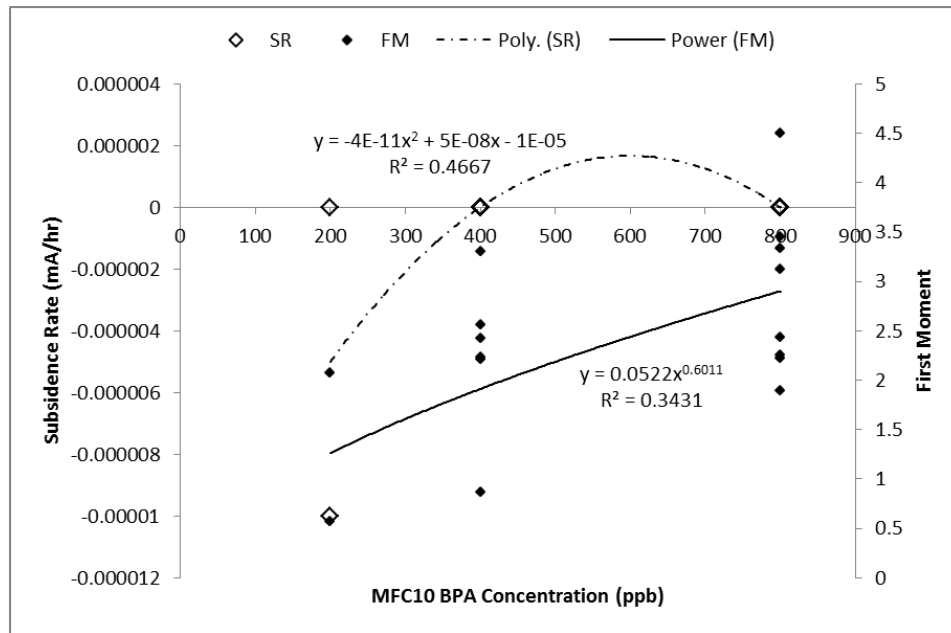


Figure I18. SR and FrM Correlations with BPA Concentrations in MFC #10

Appendix J. One-way Analysis Plots for MFC #8 and MFC #9

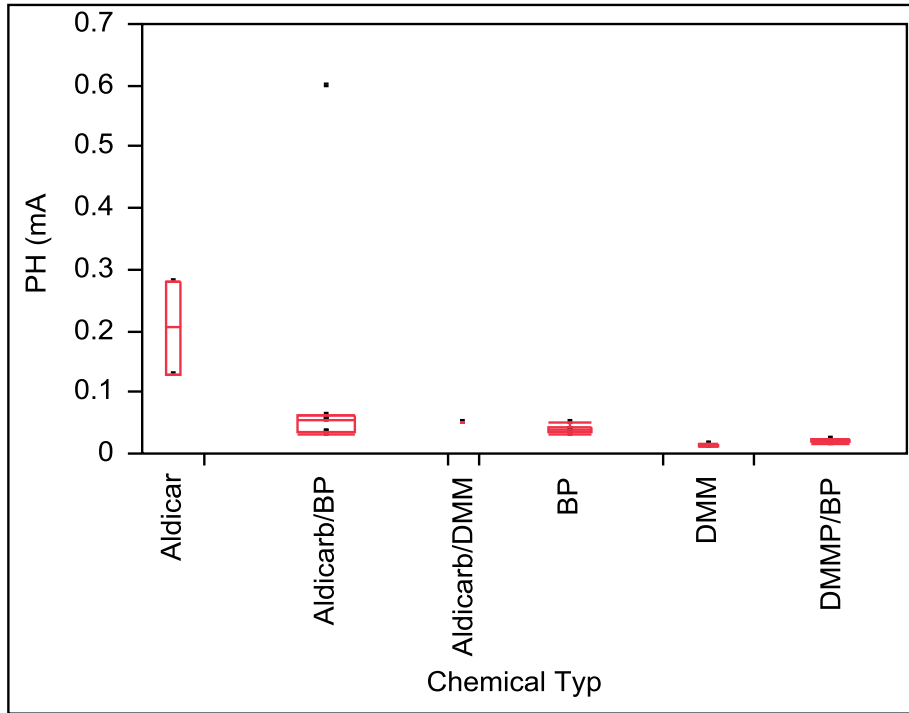


Figure J1. One-way Analysis of PH (mA) By Chemical Type for MFC #8

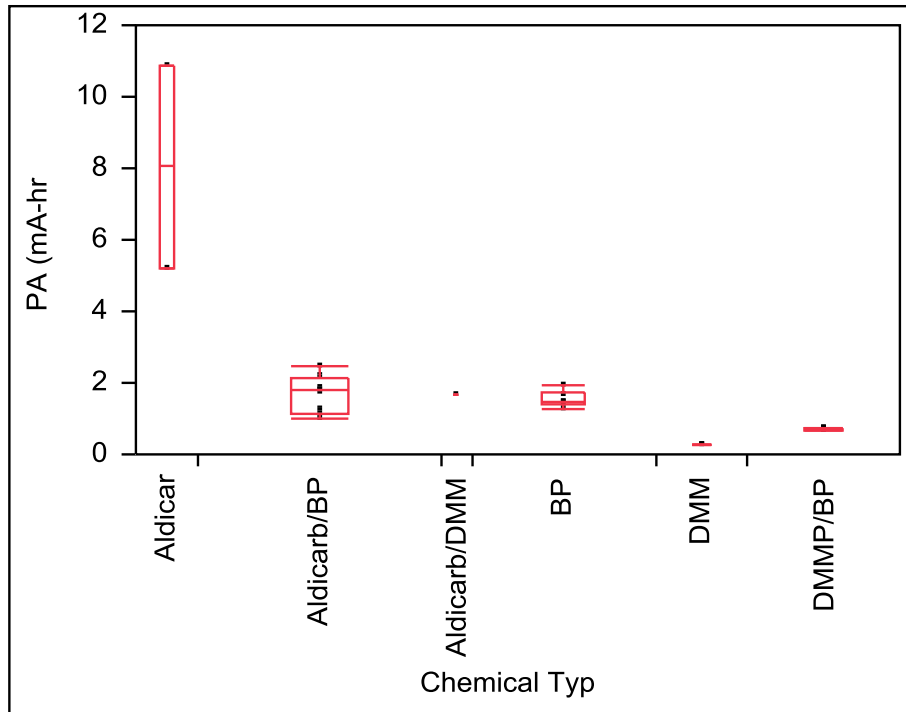


Figure J2. One-way Analysis of PA (mA-hr) By Chemical Type for MFC #8

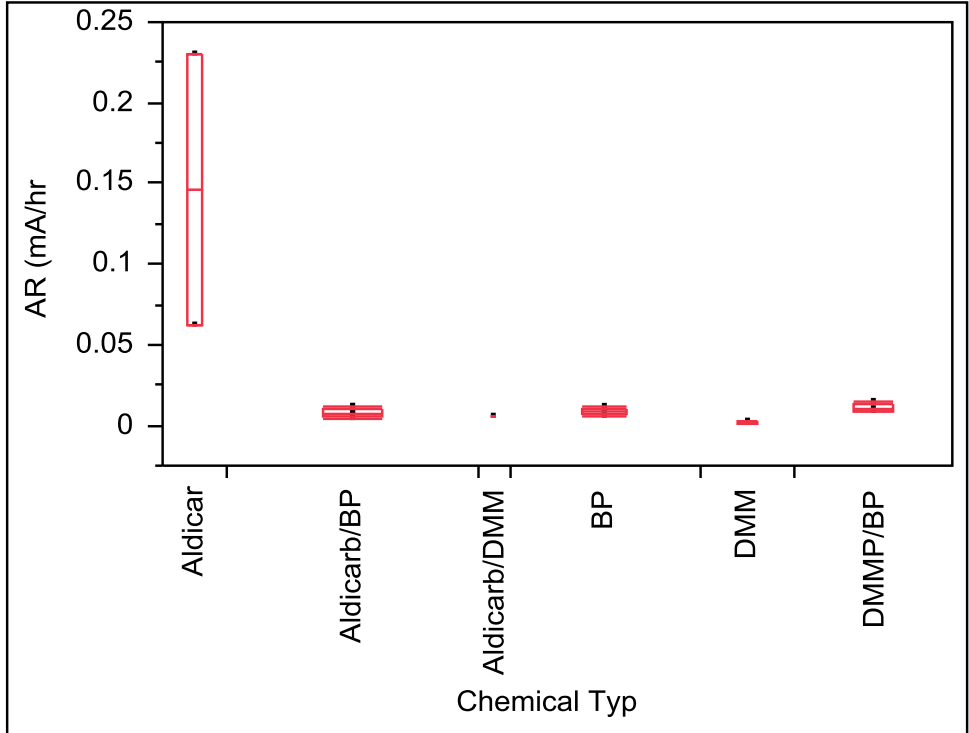


Figure J3. One-way Analysis of AR (mA/hr) By Chemical Type for MFC #8

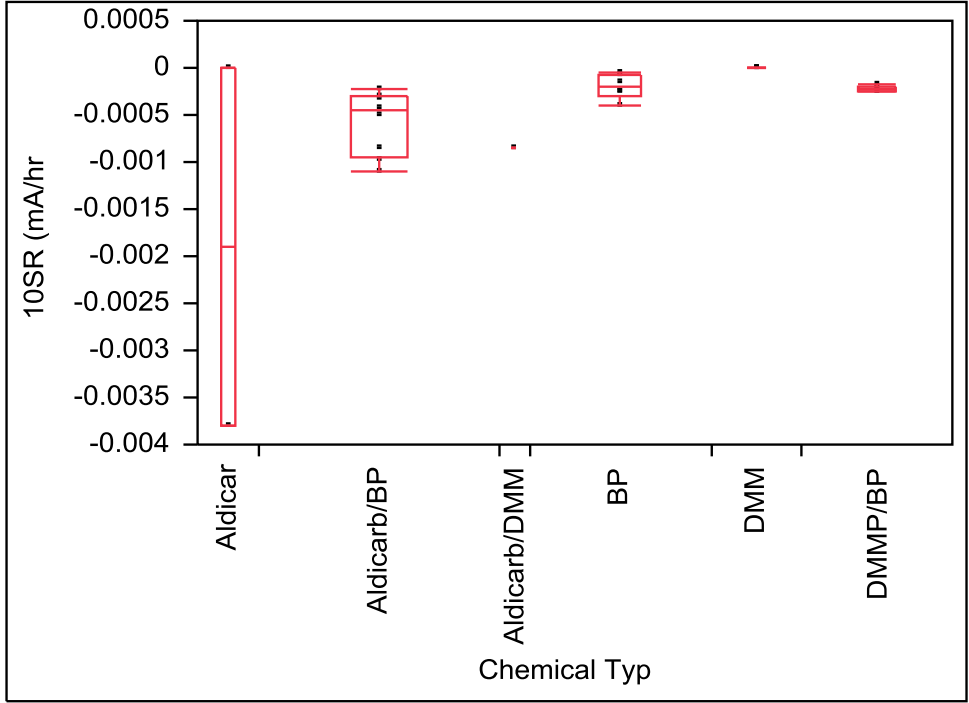


Figure J4. One-way Analysis of 10SR (mA/hr) By Chemical Type for MFC #8

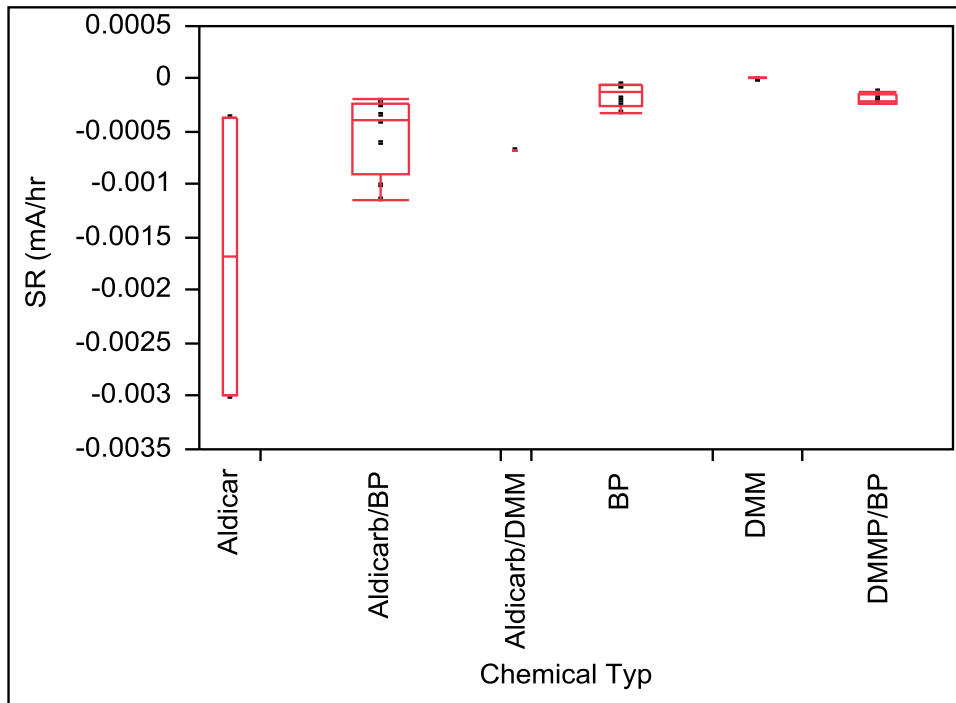


Figure J5. One-way Analysis of SR (mA/hr) By Chemical Type for MFC #8

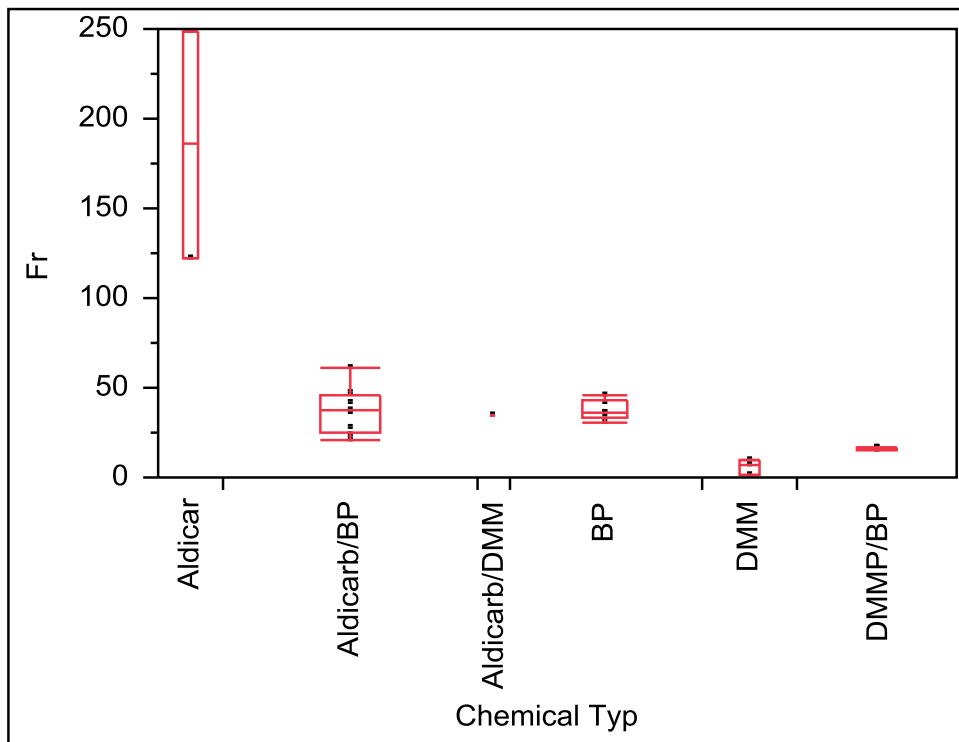


Figure J6. One-way Analysis of FrM By Chemical Type for MFC #8

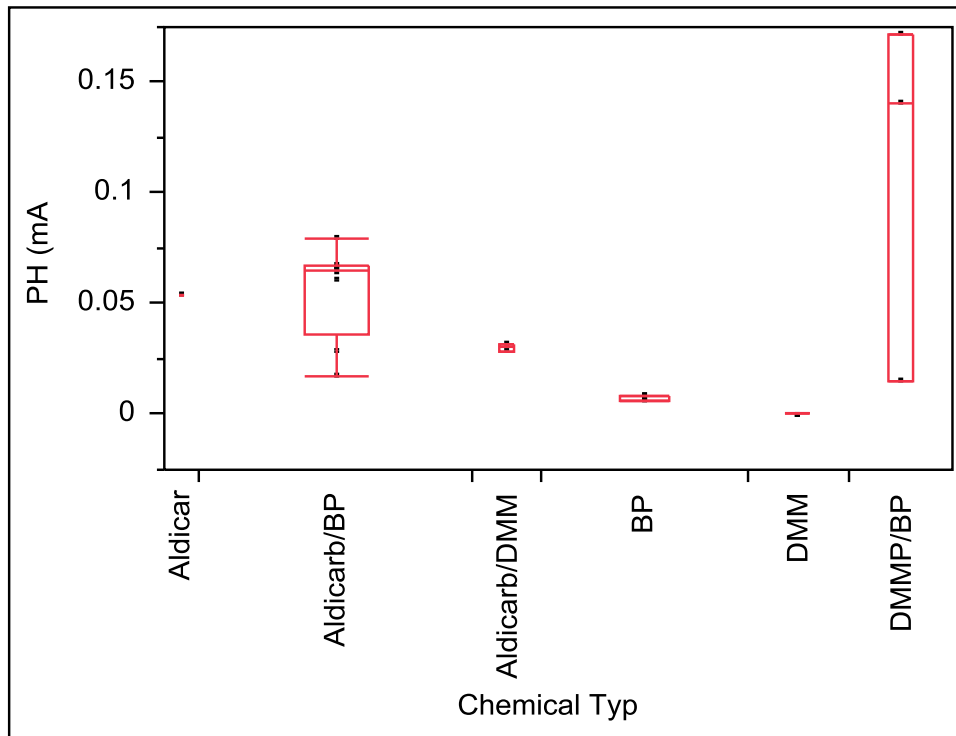


Figure J7. One-way Analysis of PH (mA) By Chemical Type for MFC #9

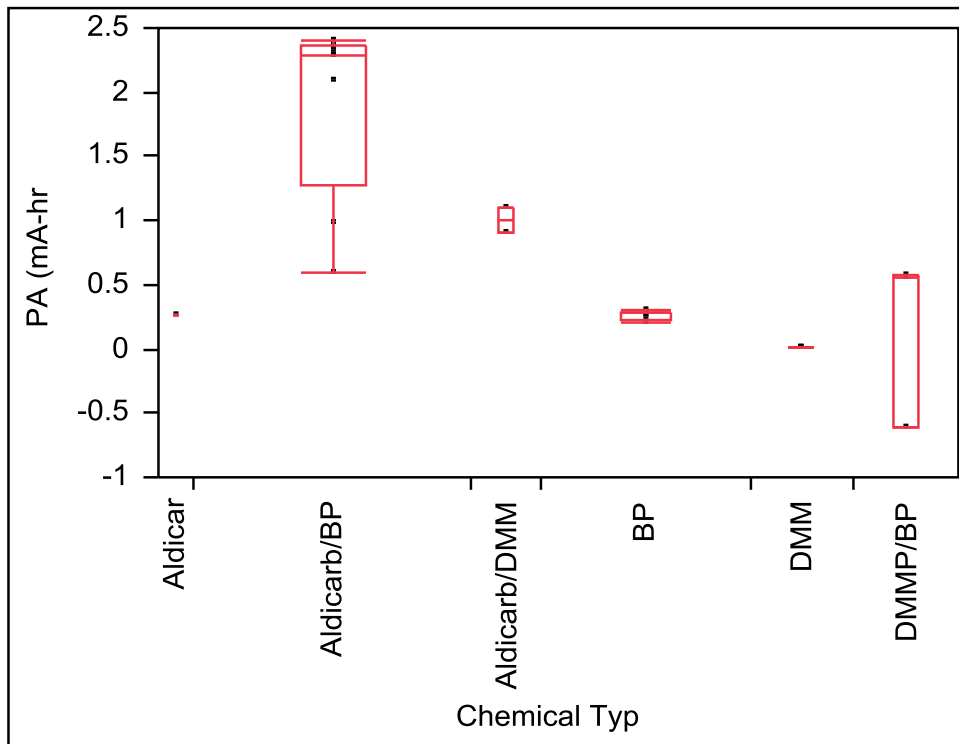


Figure J8. One-way Analysis of PA (mA-hr) By Chemical Type for MFC #9

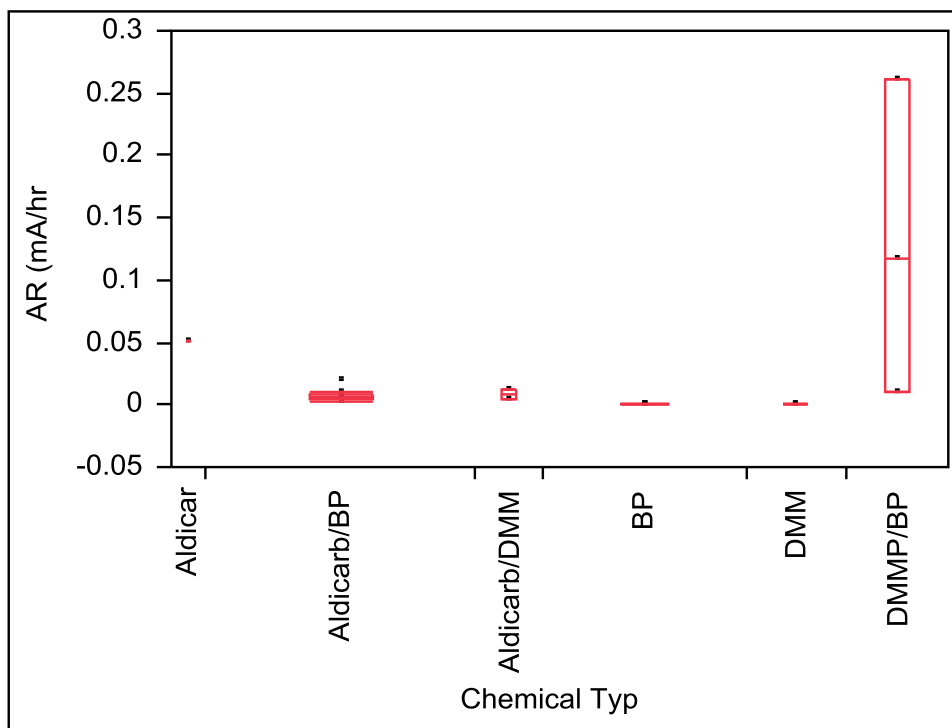


Figure J9. One-way Analysis of AR (mA/hr) By Chemical Type for MFC #9

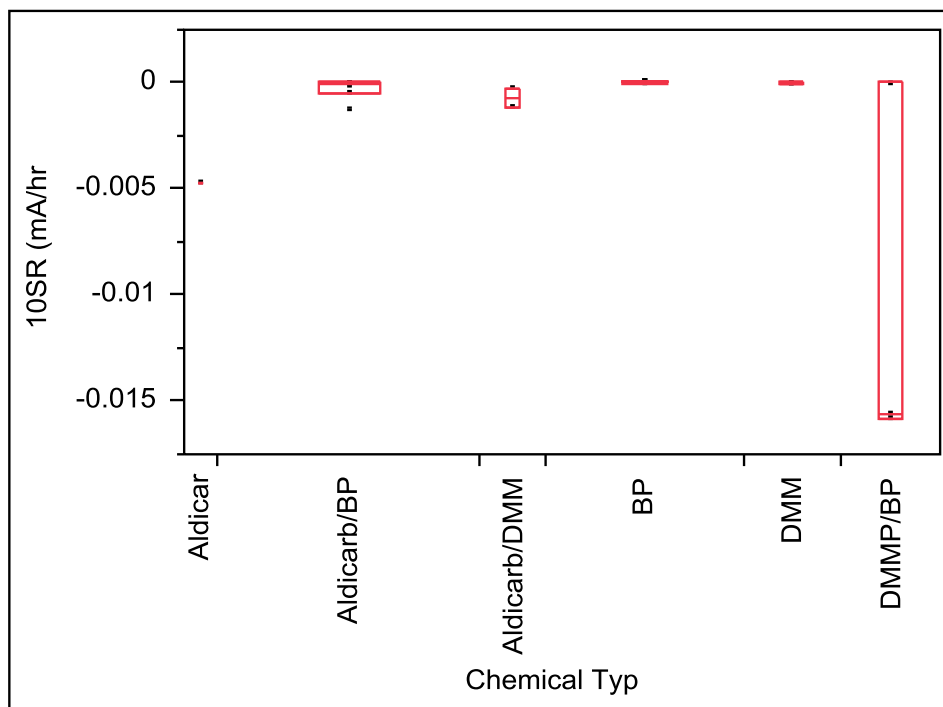


Figure J10. One-way Analysis of 10SR (mA/hr) By Chemical Type for MFC #9

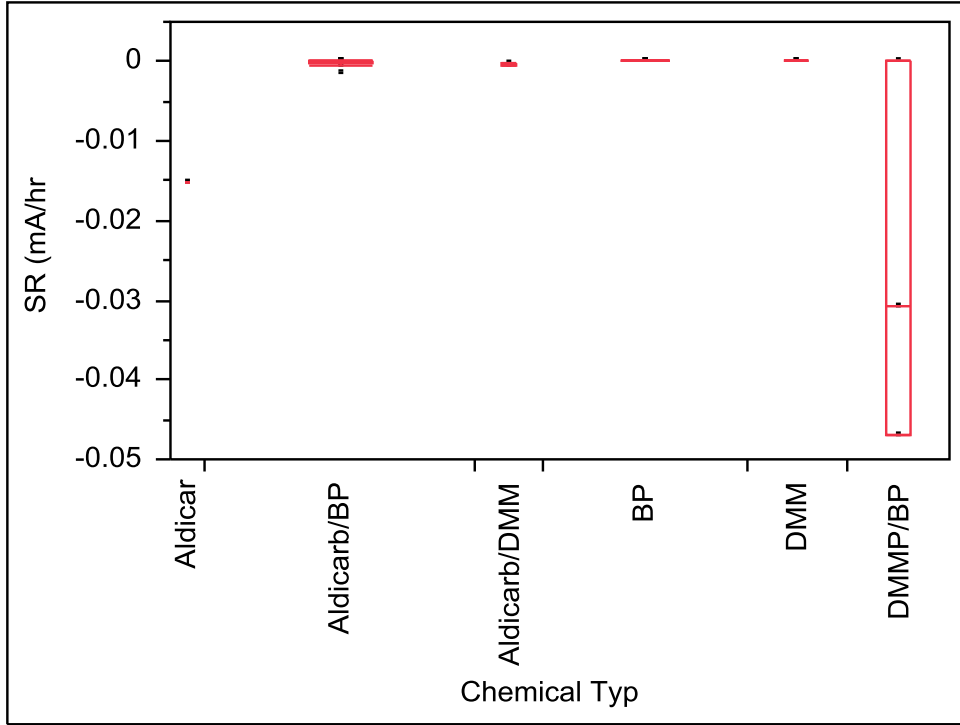


Figure J11. One-way Analysis of SR (mA/hr) By Chemical Type for MFC #9

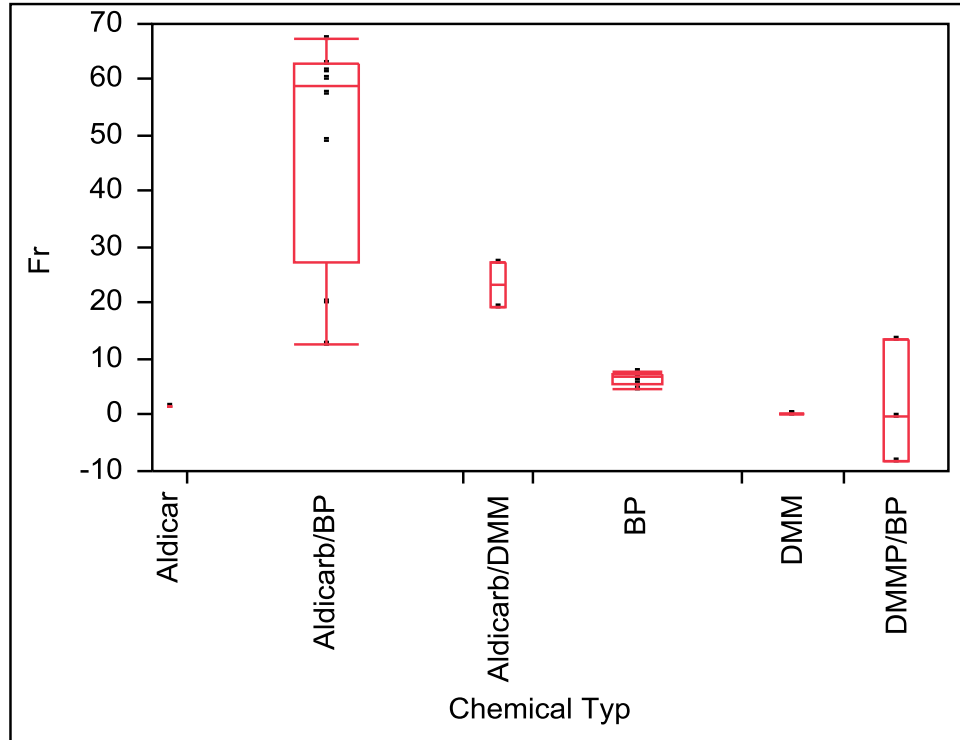


Figure J12. One-way Analysis of FrM By Chemical Type for MFC #9

Appendix K. ANN Outputs for Solvent Effects Testing

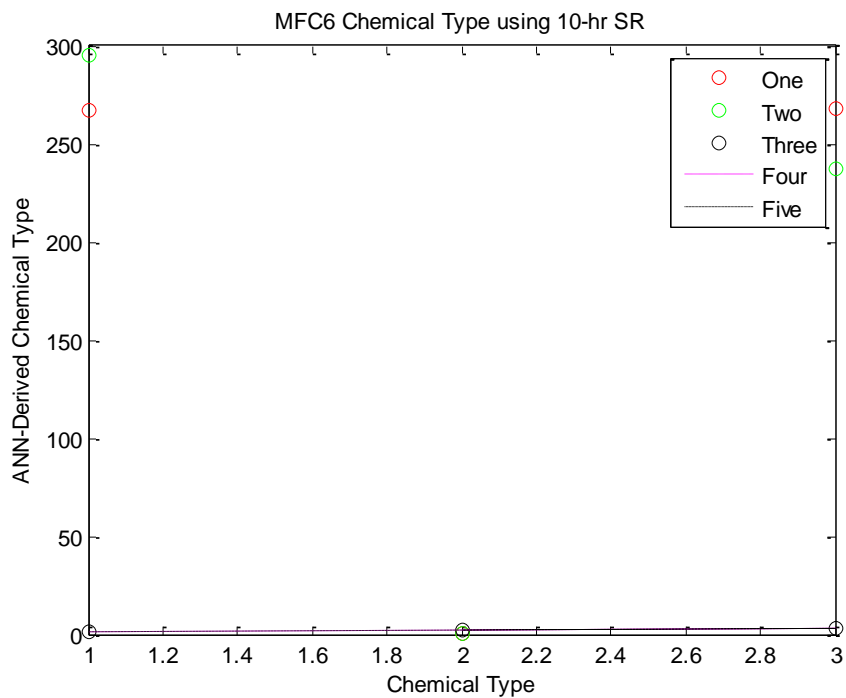


Figure K1. ANN Results Using [PH, PA, AR, 10SR] as the Input Matrix for MFC #6

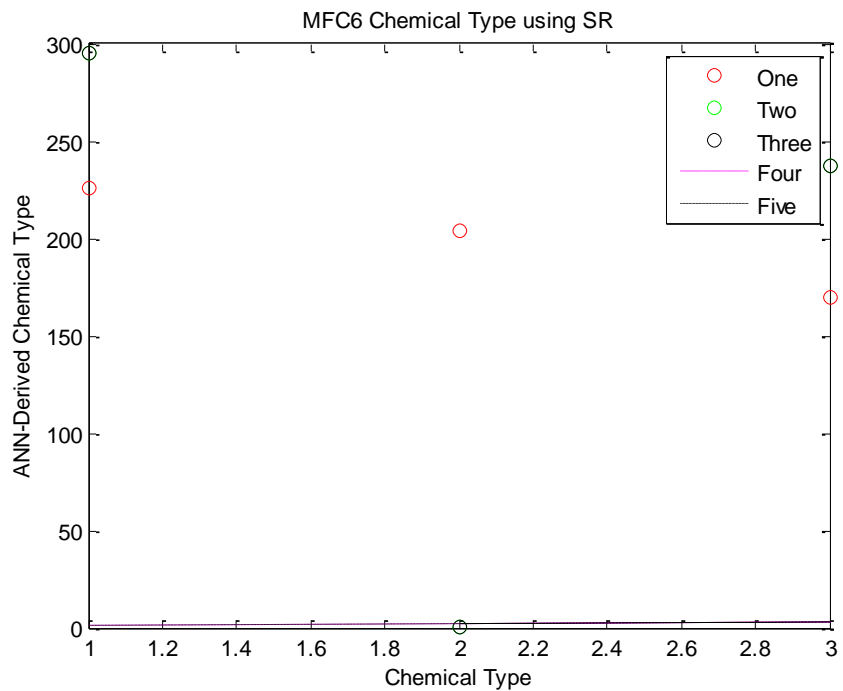


Figure K2. ANN Results Using [PH, PA, AR, SR] as the Input Matrix for MFC #6

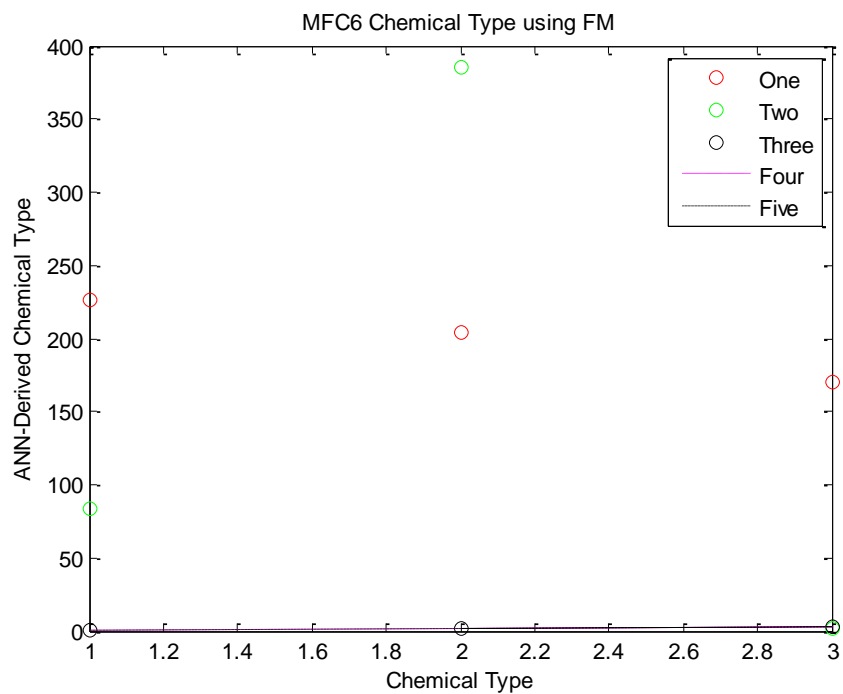


Figure K3. ANN Results Using [PH, PA, AR, FrM] as the Input Matrix for MFC #6

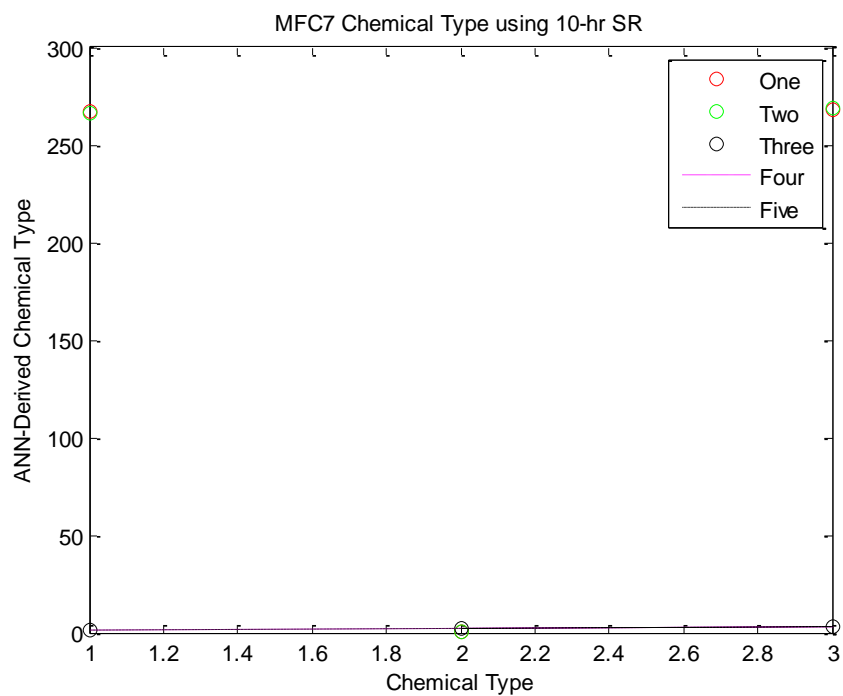


Figure K4. ANN Results Using [PH, PA, AR, 10SR] as the Input Matrix for MFC #7

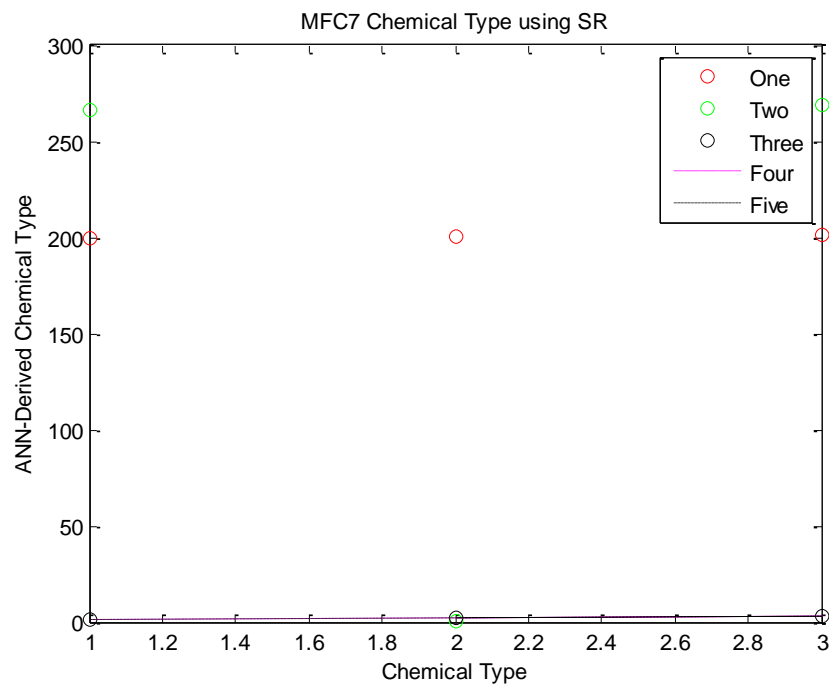


Figure K5. ANN Results Using [PH, PA, AR, SR] as the Input Matrix for MFC #7

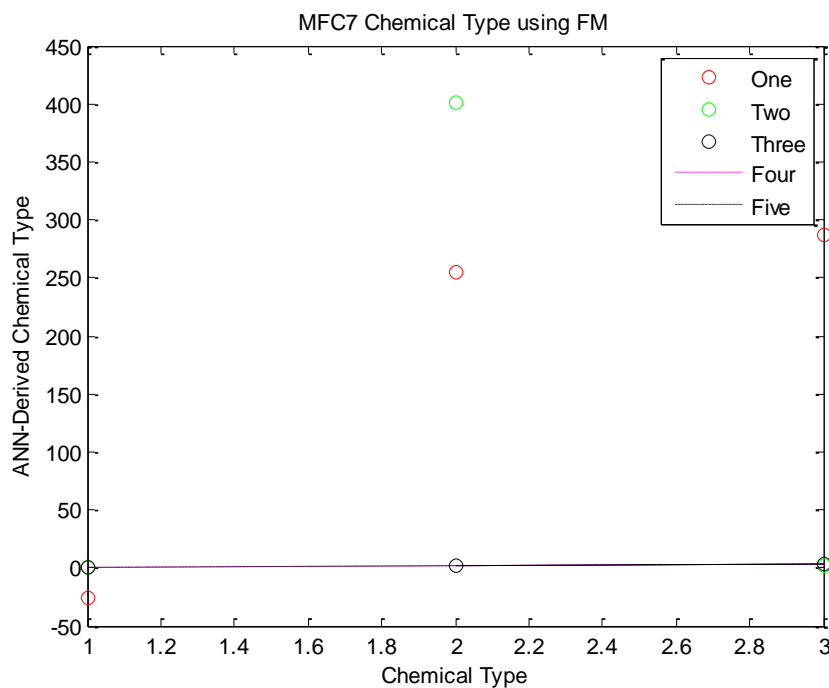


Figure K6. ANN Results Using [PH, PA, AR, FrM] as the Input Matrix for MFC #7

Appendix L. Results for Tap Water Experiments

For this experiment MFCs that were previously exposed to an aqueous solution of chemical (in RO water) were selected to be fed the same chemical dissolved in tap water. The MFCs were exposed to the tap water solutions for three consecutive feedings. Feeding intervals were 48 hours to be consistent with the rest of the study. The results are shown in Table L1 and Figures L1, L2, and L3 below. All relevant PH data was averaged in Table L1 to highlight the increased charges exhibited by the tap water solutions. Figures L1, L2, and L3 show actual response peaks that are representative of the average results. The tap water contributed to a higher charge (i.e. higher PH) for each of the three chemicals tested (BPA, DMMP and aldicarb). This is an expected result since reverse osmosis has the potential to filter out trace metals and other minerals needed by the bacteria.

Table L1. Peak Height (PH) Data from Tap Water Experiments

Date	BPA (MFC #6)	DMMP (MFC #7)	Aldicarb (MFC #8)
8-Oct-13	0.029	0.043	0.228
10-Oct-13	0.024	0.043	0.285
12-Oct-13	0.025	0.027	0.321
Ave in Tap H ₂ O	0.026	0.038	0.278
Ave in RO H ₂ O (previous experiments)	0.001	0.019	0.205

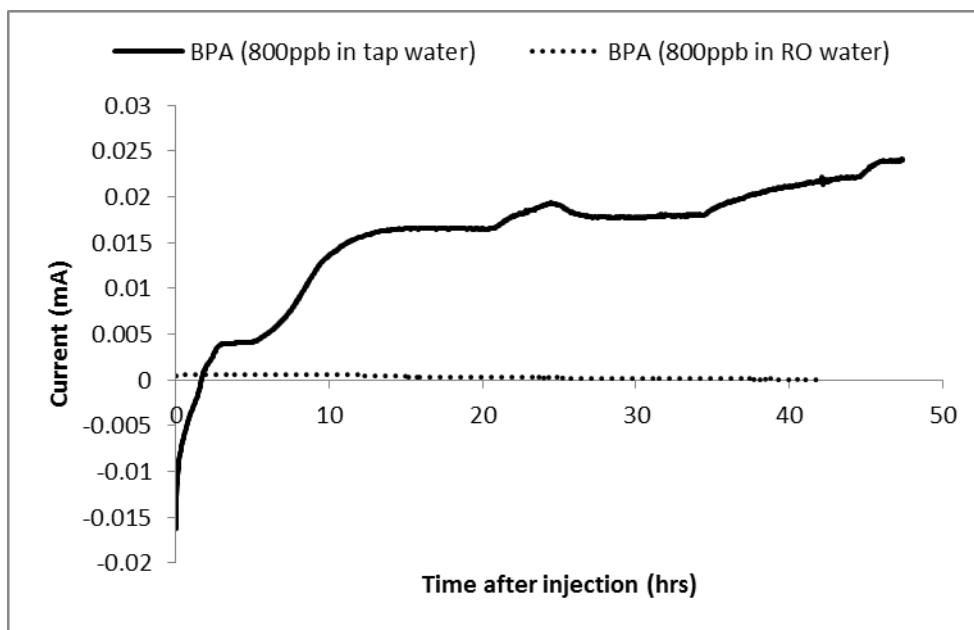


Figure L1. Typical Responses (MFC #6) for BPA(aq) in Tap Water vs. RO Water

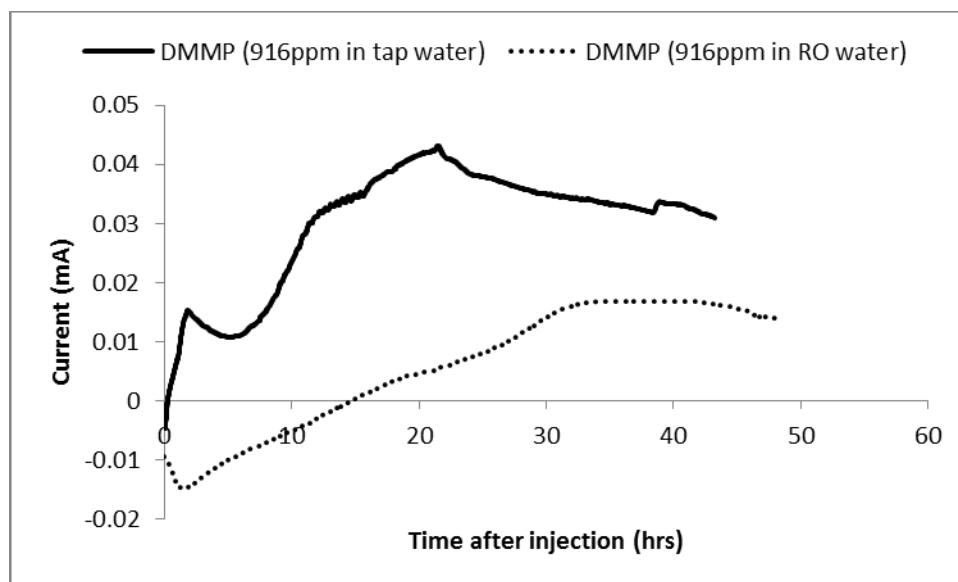


Figure L2. Typical Responses (MFC #7) for DMMP(aq) in Tap Water vs. RO Water

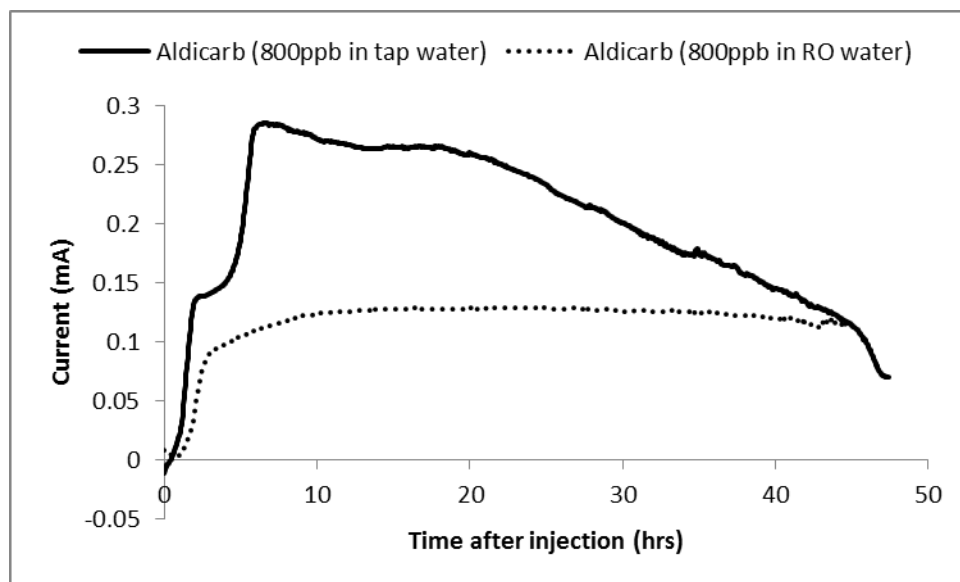


Figure L3. Typical Responses (MFC #8) for Aldicarb(aq) in Tap Water vs. RO Water

Appendix M. The Effect of Training Ratio on ANN Performance

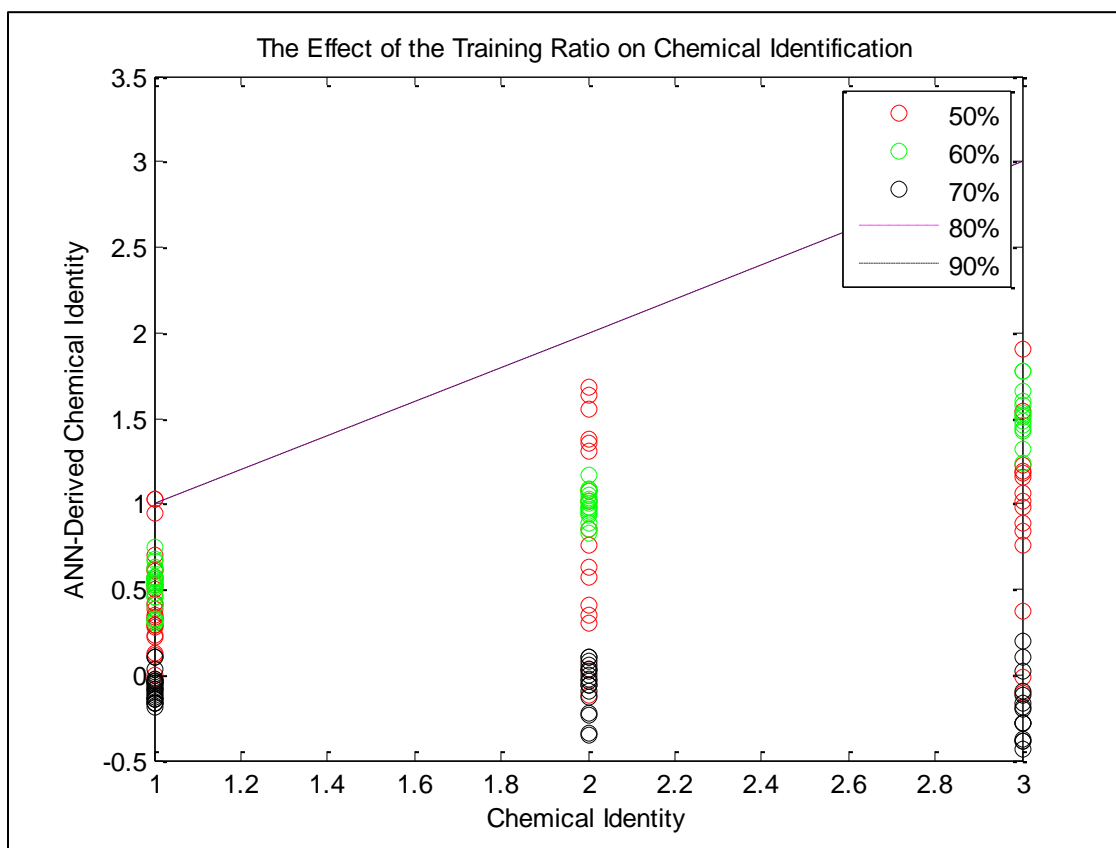


Figure M1. Figure showing the effect of the training fraction on ANN performance.

Using 80% of the data for training the model worked better than 50, 60, or 70%.

Bibliography

- Aulenta, F., Catervi, A., Majone, M., Panero, S., Reale, P., & Rossetti, S. (2007). Electron transfer from a solid-state electrode assisted by methyl viologen sustains efficient microbial reductive dechlorination of ICE. *Environmental Science & Technology*, 41(7), 2554-2559. Retrieved from <http://search.ebscohost.com/login.aspx?direct=true&db=a9h&AN=24813607&site=ehost-live>
- Bennett G.M. and W.G. Philip (1928). *J Chem Soc*, pp. 1930-7.
- Biffinger, J. C., Byrd, J. N., Dudley, B. L., & Ringeisen, B. R. (2008). Oxygen exposure promotes fuel diversity for shewanella oneidensis microbial fuel cells. *Biosensors and Bioelectronics*, 23(6), 820-826. doi:<http://dx.doi.org/10.1016/j.bios.2007.08.021>
- Bond, D. R., Holmes, D. E., Tender, L. M., & Lovley, D. R. (2002). Electrode-reducing microorganisms that harvest energy from marine sediments. *Science*, 295(5554), 483-485. Retrieved from <http://search.ebscohost.com/login.aspx?direct=true&db=a9h&AN=6061751&site=ehost-live>
- Chae, K., Choi, M., Kim, K., Ajayi, F. F., Park, W., Kim, C., & Kim, I. S. (2010). Methanogenesis control by employing various environmental stress conditions in two-chambered microbial fuel cells. *Bioresource Technology*, 101(14), 5350-5357. doi:<http://dx.doi.org/10.1016/j.biortech.2010.02.035>
- Cheng, S., & Logan, B. E. (2007). Ammonia treatment of carbon cloth anodes to enhance power generation of microbial fuel cells. *Electrochemistry Communications*, 9(3), 492-496. doi:10.1016/j.elecom.2006.10.023
- Cheng, S., & Logan, B. E. (2011). Increasing power generation for scaling up single-chamber air cathode microbial fuel cells. *Bioresource Technology*, 102(6), 4468-4473. doi:<http://dx.doi.org/10.1016/j.biortech.2010.12.104>
- Choi, S., & Chae, J. (2013). Optimal biofilm formation and power generation in a micro-sized microbial fuel cell (MFC). *Sensors and Actuators A: Physical*, 195(0), 206-212. doi:<http://dx.doi.org/10.1016/j.sna.2012.07.015>
- Clauwaert, P., Mulenga, S., Aelterman, P., & Verstraete, W. (2009). Litre-scale microbial fuel cells operated in a complete loop. *Applied Microbiology & Biotechnology*, 83(2), 241-247. doi:10.1007/s00253-009-1876-0

- Dekker, A., Heijne, A. T., Saakes, M., Hamelers, H. V. M., & Buisman, C. J. N. (2009). *Analysis and improvement of a scaled-up and stacked microbial fuel cell*. Retrieved from <http://search.ebscohost.com/login.aspx?direct=true&db=a9h&AN=47027107&site=ehost-live>
- Department of Health and Human Services (D.H.H.S.). *Toxicology and Carcinogenesis Studies of Dimethyl Methylphosphonate in F334/N Rats and B6C3F₁ Mice*. National Toxicology Program Technical Report Series No. 323. NIH Publication No. 88-2579. Research Triangle Park (NC): November 1987.
- Di Lorenzo, M., Curtis, T. P., Head, I. M., & Scott, K. (2009). A single-chamber microbial fuel cell as a biosensor for wastewaters. *Water Research*, 43(13), 3145-3154. doi:10.1016/j.watres.2009.01.005
- Fan, Yanzhen, Sharbrough, E., & Hong, L. I. U. (2008). Quantification of the internal resistance distribution of microbial fuel cells. *Environmental Science & Technology*, 42(21), 8101-8107. Retrieved from <http://search.ebscohost.com/login.aspx?direct=true&db=a9h&AN=35406010&site=ehost-live>
- Fan, Y., Hu, H., & Liu, H. (2007). Sustainable power generation in microbial fuel cells using bicarbonate buffer and proton transfer mechanisms. *Environmental Science & Technology*, 41(23), 8154-8158. doi:10.1021/es071739c CCC: \$37.00
- Feng, Y., Barr, W., & Harper Jr., W. F. (2013a). Neural network processing of microbial fuel cell signals for the identification of chemicals present in water. *Journal of Environmental Management*, 120(0), 84-92. doi:<http://dx.doi.org/10.1016/j.jenvman.2013.01.018>
- Feng, Y., Kayode, O., & Harper Jr., W. F. (2013b). Using microbial fuel cell output metrics and nonlinear modeling techniques for smart biosensing. *Science of the Total Environment*, 449(0), 223-228. doi:<http://dx.doi.org/10.1016/j.scitotenv.2013.01.004>
- Feng, Y., Yang, Q., Wang, X., & Logan, B. E. (2010). Treatment of carbon fiber brush anodes for improving power generation in air-cathode microbial fuel cells. *Journal of Power Sources*, 195(7), 1841-1844. doi:10.1016/j.jpowsour.2009.10.030
- Gazzaz, N. M., Yusoff, M. K., Aris, A. Z., Juahir, H., & Ramli, M. F. (2012). Artificial neural network modeling of the water quality index for kinta river (malaysia) using water quality variables as predictors. *Marine Pollution Bulletin*, 64(11), 2409-2420. doi:<http://dx.doi.org/10.1016/j.marpolbul.2012.08.005>

- Given, C.J. and F.E. Dierberg (1985). "Effect of pH on the rate of aldicarb hydrolysis," *Bull. Environ. Contam. Toxicol.* 34: 627-633.
- Gorby, Y.A. and Beveridge, T.J. (2005). Composition, reactivity, and regulation of extracellular metal-reducing structures (nanowires) produced by dissimilatory metal reducing bacteria. *Warrenton, VA*,
- Gregory, K.B., Bond, D.R. and Lovley, D.R. (2004). Graphite electrodes as electron donors for anaerobic respiration. *Environ. Microbiol.*, 6, 596-604.
- Gregory, K. B., & Lovley, D. R. (2005). Remediation and recovery of uranium from contaminated subsurface environments with electrodes. *Environmental Science & Technology*, 39(22), 8943-8947. doi:10.1021/es050457e
- Hatch, J. L., & Finneran, K. T. (2008). Influence of reduced electron shuttling compounds on biological H₂ production in the fermentative pure culture *Clostridium beijerinckii*. *Current Microbiology*, 56(3), 268-273. doi:10.1007/s00284-007-9073-9
- Hauschild, V. D., & Bratt, G. M. (2005). Prioritizing industrial chemical hazards. *Journal of Toxicology & Environmental Health: Part A*, 68(11), 857-876. doi:10.1080/15287390590912162
- Hazardous Substances Data Bank (H.S.D.B.) [Internet] (2013a). *Aldicarb*. National Library of Medicine (US), Division of Specialized Information Services. n. pag. Bethesda (MD): (n.d.). 16 November 2013. <http://toxnet.nlm.nih.gov/cgi-bin/sis/search/a?dbs+hsdb:@term+@DOCNO+1510>
- (2013b). *Bisphenol A*. National Library of Medicine (US), Division of Specialized Information Services. n. pag. Bethesda (MD): (n.d.). 16 November 2013. <http://toxnet.nlm.nih.gov/cgi-bin/sis/search/a?dbs+hsdb:@term+@DOCNO+513>
- (2013c). *Dimethyl Methylphosphonate*. National Library of Medicine (US), Division of Specialized Information Services. n. pag. Bethesda (MD): (n.d.). 16 November 2013. <http://toxnet.nlm.nih.gov/cgi-bin/sis/search/a?dbs+hsdb:@term+@DOCNO+2590>
- Holmes, D. E., Chaudhuri, S. K., Nevin, K. P., Mehta, T., Methé, B. A., Liu, A., . . . Lovley, D. R. (2006). Microarray and genetic analysis of electron transfer to electrodes in *Geobacter sulfurreducens*. *Environmental Microbiology*, 8(10), 1805-1815. doi:10.1111/j.1462-2920.2006.01065.x
- Holmes, D. E., Mester, T., O'Neil, R. A., Perpetua, L. A., Larrahondo, M. J., Glaven, R., . . . Lovley, D. R. (2008). Genes for two multicopper proteins required for Fe(III) oxide reduction in *Geobacter sulfurreducens* have different expression patterns

- both in the subsurface and on energy-harvesting electrodes. *Microbiology* (13500872), 154(5), 1422-1435. doi:10.1099/mic.0.2007/014365-0
- Jung, R. K., Min, B., & Logan, B. (2005). Evaluation of procedures to acclimate a microbial fuel cell for electricity production. *Applied Microbiology & Biotechnology*, 68(1), 23-30. doi:10.1007/s00253-004-1845-6
- Kang, J., & Kondo, F. (2005). Bisphenol A degradation in seawater is different from that in river water. *Chemosphere*, 60(9), 1288-1292. doi:10.1016/j.chemosphere.2005.01.058
- Kim, B.-H., Ikeda, T., Park, H.-S., Kim, H.-J., Hyun, M.-S., Kano, K., Takagi, K. and Tatsumi, H. (1999a). Electrochemical activity of an Fe(III)-reducing bacterium, *shewanella putrefaciens* IR-1, in the presence of alternative electron acceptors. *Biotechnol. Techniques*, 13(7), 475-478.
- Kim, B.H., Kim, H.-J., Hyun, M.-S. and Park, D.-H. (1999b). Direct electrode reaction of Fe(III)-reducing bacterium, *shewanella putrefaciens*. *J. Microbiol. Biotechnol.*, 9(2), 127-131.
- Kim, B.H., Park, D.H., Shin, P.K., Chang, I.S. and Kim, H.J. (1999c). Mediator-less biofuel cell. *U.S. Patent 5976719*,
- Kim, B., Postier, B. L., DiDonato, R. J., Chaudhuri, S. K., Nevin, K. P., & Lovley, D. R. (2008). Insights into genes involved in electricity generation in *Geobacter sulfurreducens* via whole genome microarray analysis of the OmcF-deficient mutant. *Bioelectrochemistry*, 73(1), 70-75. doi:<http://dx.doi.org/10.1016/j.bioelechem.2008.04.023>
- Kim, I. S., Hwang, M. H., Jang, N. J., Hyun, S. H., & Lee, S. T. (2004). Effect of low pH on the activity of hydrogen utilizing methanogen in bio-hydrogen process. *International Journal of Hydrogen Energy*, 29(11), 1133-1140. doi:10.1016/j.ijhydene.2003.08.017
- Kök, F. N., Arıca, M. Y., Halıcıgil, C., Alaeddinoğlu, G., & Hasırcı, V. (1999). Biodegradation of aldicarb in a packed-bed reactor by immobilized *Methylosinus*. *Enzyme and Microbial Technology*, 24(5-6), 291-296. doi:[http://dx.doi.org/10.1016/S0141-0229\(98\)00124-0](http://dx.doi.org/10.1016/S0141-0229(98)00124-0)
- Krogh, Anders (2008). "What are artificial neural networks?" *Nature Biotechnology*, 26(2), 195-197 (February 2008).
- Kumlanghan, A., Liu, J., Thavarungkul, P., Kanatharana, P., & Mattiasson, B. (2007). Microbial fuel cell-based biosensor for fast analysis of biodegradable organic

- matter. *Biosensors and Bioelectronics*, 22(12), 2939-2944.
doi:<http://dx.doi.org/10.1016/j.bios.2006.12.014>
- Li, C., & Fang, H. H. P. (2007). Fermentative hydrogen production from wastewater and solid wastes by mixed cultures. *Critical Reviews in Environmental Science & Technology*, 37(1), 1-39. doi:10.1080/10643380600729071
- Liu, H., Ramnarayanan, R. and Logan, B.E. (2004). Production of electricity during wastewater treatment using a single chamber microbial fuel cell. *Environ. Sci. Technol.*, 38(7), 2281-2285.
- Liu, H., Cheng, S., Huang, L., & Logan, B. E. (2008). Scale-up of membrane-free single-chamber microbial fuel cells. *Journal of Power Sources*, 179(1), 274-279.
doi:10.1016/j.jpowsour.2007.12.120
- Liu, H., Cheng, S., & Logan, B. B. (2005). Production of electricity from acetate or butyrate using a single-chamber microbial fuel cell. *Environmental Science & Technology*, 39(2), 658-662. Retrieved from
<http://search.ebscohost.com/login.aspx?direct=true&db=a9h&AN=15998115&site=ehost-live>
- Liu, H., & Logan, B. E. (2004). Electricity generation using an air-cathode single chamber microbial fuel cell in the presence and absence of a proton exchange membrane. *Environmental Science & Technology*, 38(14), 4040-4046. Retrieved from
<http://search.ebscohost.com/login.aspx?direct=true&db=a9h&AN=13997121&site=ehost-live>
- Logan, B. E. (2008). *Microbial fuel cells*. Hoboken, NJ: John Wiley & Sons, Inc.
- Logan, B. E. (2004). Extracting hydrogen and electricity from RENEWABLE resources. *Environmental Science & Technology*, 38(9), 160A-167A. Retrieved from
<http://search.ebscohost.com/login.aspx?direct=true&db=a9h&AN=13111153&site=ehost-live>
- Lovley, D. R. (2008). The microbe electric: Conversion of organic matter to electricity. *Current Opinion in Biotechnology*, 19(6), 564-571.
doi:<http://dx.doi.org/10.1016/j.copbio.2008.10.005>
- Lovley, D. R., Ueki, T., Zhang, T., Malvankar, N. S., Shrestha, P. M., Flanagan, K. A., . . . Nevin, K. P. (2011). Geobacter: The microbe electric's physiology, ecology, and practical applications. *Advances in microbial physiology* (pp. 1-100) Academic Press. doi:<http://dx.doi.org/10.1016/B978-0-12-387661-4.00004-5>

- Mahle, John, Mancinho, D., Buettner, L., and Wayne G. (2003). *Chemical filtration performance of a pressure and temperature swing absorber (PTSA) system Phase I:chloroethane, cyanogen chloride, ammonia, and 2-Chloroethyl ethyl sulfide pulse testing*,Edgewood Chemical and Biological Center, Aberdeen Proving Ground, Document ECBC-TR-306, July 2003.
- Maier, H. R., Morgan, N., & Chow, C. W. K. (2004). Use of artificial neural networks for predicting optimal alum doses and treated water quality parameters. *Environmental Modelling & Software*, 19(5), 485-494.
doi:[http://dx.doi.org/10.1016/S1364-8152\(03\)00163-4](http://dx.doi.org/10.1016/S1364-8152(03)00163-4)
- Maran, E., Fernández, M., Barbieri, P., Font, G., & Ruiz, M. J. (2009). Effects of four carbamate compounds on antioxidant parameters. *Ecotoxicology and Environmental Safety*, 72(3), 922-930.
doi:<http://dx.doi.org/10.1016/j.ecoenv.2008.01.018>
- Marsili, E., Baron, D. B., Shikhare, I. D., Coursolle, D., Gralnick, J. A., & Bond, D. R. (2008). Shewanella secretes flavins that mediate extracellular electron transfer. *Proceedings of the National Academy of Sciences of the United States of America*, 105(10), 3968-3973. doi:10.1073/pnas.0710525105
- McCulloch, W. S., & Pitts, W. (1990). A logical calculus of the ideas immanent in nervous activity. *Bulletin of Mathematical Biology*, 52(1-2), 99-115.
doi:[http://dx.doi.org/10.1016/S0092-8240\(05\)80006-0](http://dx.doi.org/10.1016/S0092-8240(05)80006-0)
- Min, B., & Logan, B. E. (2004). Continuous electricity generation from domestic wastewater and organic substrates in a flat plate microbial fuel cell. *Environmental Science & Technology*, 38(21), 5809-5814. Retrieved from <http://search.ebscohost.com/login.aspx?direct=true&db=a9h&AN=15121916&site=ehost-live>
- National Oceanic and Atmospheric Administration (N.O.A.A.). *Dimethyl Methylphosphonate*. CAMEO Chemicals entry. n. pag. (n.d.). 16 November 2013. <http://cameochemicals.noaa.gov/chemical/20244>
- Park, D. H., & Laivenieks, M. (1999). Microbial utilization of electrically reduced neutral reagents as the sole electron donor for growth.. *Applied & Environmental Microbiology*, 65(7), 2912. Retrieved from <http://search.ebscohost.com/login.aspx?direct=true&db=a9h&AN=2148404&site=ehost-live>
- Perez, P. (2012). Combined model for PM10 forecasting in a large city. *Atmospheric Environment*, 60(0), 271-276.
doi:<http://dx.doi.org/10.1016/j.atmosenv.2012.06.024>

- Potter, M. C. (1911). Electrical effects accompanying the decomposition of organic compounds. *Proc. Roy. Soc. London Ser. B* 84, , 260-276.
- Rabaey, K., Lissens, G., Siciliano, S.D. and Verstraete, W. (2003). A microbial fuel cell capable of converting glucos to electricity at high rate and efficiency. *Biotechnol. Lett.*, 25(18), 1531-1535.
- Rabaey, K., Boon, N., Höfte, M., & Verstraete, W. (2005). Microbial phenazine production enhances electron transfer in biofuel cells. *Environmental Science & Technology*, 39(9), 3401-3408. Retrieved from <http://search.ebscohost.com/login.aspx?direct=true&db=a9h&AN=17105608&site=ehost-live>
- Rabaey, K., & Verstraete, W. (2005). Microbial fuel cells: Novel biotechnology for energy generation. *Trends in Biotechnology*, 23(6), 291-298. doi:10.1016/j.tibtech.2005.04.008
- Reguera, G., McCarthy, K. D., Mehta, T., Nicoll, J. S., Tuominen, M. T., & Lovley, D. R. (2005). Extracellular electron transfer via microbial nanowires. *Nature*, 435(7045), 1098-1101. doi:10.1038/nature03661
- Reguera, G., Nevin, K. P., Nicoll, J. S., Covalla, S. F., Woodard, T. L., & Lovley, D. R. (2006). Biofilm and nanowire production leads to increased current in geobacter sulfurreducens fuel cells. *Applied & Environmental Microbiology*, 72(11), 7345-7348. doi:10.1128/AEM.01444-06
- Reimers, C. E., & Tender, L. M. (2001). Harvesting energy from the marine sediment-water interface. *Environmental Science & Technology*, 35(1), 192. Retrieved from <http://search.ebscohost.com/login.aspx?direct=true&db=a9h&AN=4072130&site=ehost-live>
- Rismani-Yazdi, H., Carver, S. M., Christy, A. D., Yu, Z., Bibby, K., Peccia, J., & Tuovinen, O. H. (2013). Suppression of methanogenesis in cellulose-fed microbial fuel cells in relation to performance, metabolite formation, and microbial population. *Bioresour. Technol.*, 129(0), 281-288. doi:<http://dx.doi.org/10.1016/j.biortech.2012.10.137>
- Robinson, B. J., & Hellou, J. (2009). Biodegradation of endocrine disrupting compounds in harbour seawater and sediments. *Science of the Total Environment*, 407(21), 5713-5718. doi:<http://dx.doi.org/10.1016/j.scitotenv.2009.07.003>
- Sang-Eun Oh, & Logan, B. E. (2006). Proton exchange membrane and electrode surface areas as factors that affect power generation in microbial fuel cells. *Applied Microbiology & Biotechnology*, 70(2), 162-169. doi:10.1007/s00253-005-0066-y

- Stein, N. E., Hamelers, H. M. V., van Straten, G., & Keesman, K. J. (2012). On-line detection of toxic components using a microbial fuel cell-based biosensor. *Journal of Process Control*, 22(9), 1755-1761. doi:10.1016/j.jprocont.2012.07.009
- Steinbusch, K. J. J., Hamelers, H. V. M., Schaap, J. D., Kampman, C., & Buisman, C. J. N. (2010). Bioelectrochemical ethanol production through mediated acetate reduction by mixed cultures. *Environmental Science & Technology*, 44(1), 513-517. Retrieved from <http://search.ebscohost.com/login.aspx?direct=true&db=a9h&AN=48143476&site=ehost-live>
- Sun, M., Zhang, F., Tong, Z., Sheng, G., Chen, Y., Zhao, Y., . . . Yu, H. (2010). A gold-sputtered carbon paper as an anode for improved electricity generation from a microbial fuel cell inoculated with shewanella oneidensis MR-1. *Biosensors and Bioelectronics*, 26(2), 338-343. doi:<http://dx.doi.org/10.1016/j.bios.2010.08.010>
- Tront, J. M., Fortner, J. D., Plötze, M., Hughes, J. B., & Puzrin, A. M. (2008). Microbial fuel cell biosensor for in situ assessment of microbial activity. *Biosensors and Bioelectronics*, 24(4), 586-590.
- USEPA. (2007). *Reregistration Eligibility Decision for Aldicarb*. Office of Prevention, Pesticides and Toxic Substances. Case Number 0140. September 2007.
- (2010). *Agreement to Terminate All Uses of Aldicarb*. Summary of E.P.A. regulatory action. n. pag. (October 2010). 16 November 2013. http://www.epa.gov/oppsrrd1/REDS/factsheets/aldicarb_fs.html#action
- (2013). *Bisphenol A Action Plan Summary*. Summary of E.P.A. regulatory action. n. pag. (n.d.). 16 November 2013. <http://www.epa.gov/oppt/existingchemicals/pubs/actionplans/bpa.html>
- Ying, G., Kookana, R. S., & Dillon, P. (2003). Sorption and degradation of selected five endocrine disrupting chemicals in aquifer material. *Water Research*, 37(15), 3785-3791. doi:[http://dx.doi.org/10.1016/S0043-1354\(03\)00261-6](http://dx.doi.org/10.1016/S0043-1354(03)00261-6)
- Zhang, F., K.S. Jacobson, P. Torres, and Z. He. (2010). Effects of anolyte recirculation rates and catholytes on electricity generation in a litre-scale upflow microbial fuel cell. *Energy Environ. Sci.*, 3, 1347-1352.
- Zhang, X.Y., S.A. Cheng, X. Huang, and B.E. Logan. (2010). The use of nylon and glass fiber filter separators with different pore sizes in air-cathode single-chamber microbial fuel cells. *Energy Environ. Sci.*, 3, 659-664.

Zhang, X., Cheng, S., Liang, P., Huang, X., & Logan, B. E. (2011). Scalable air cathode microbial fuel cells using glass fiber separators, plastic mesh supporters, and graphite fiber brush anodes. *Bioresource Technology*, *102*(1), 372-375. doi:10.1016/j.biortech.2010.05.090

Zuo, Y., & Logan, B. E. (2011). Power generation in MFCs with architectures based on tubular cathodes or fully tubular reactors. *Water Science & Technology*, *64*(11), 2253-2258. doi:10.2166/wst.2011.429

REPORT DOCUMENTATION PAGE				<i>Form Approved</i> <i>OMB No. 074-0188</i>	
The public reporting burden for this collection of information is estimated to average 1 hour per response, including the time for reviewing instructions, searching existing data sources, gathering and maintaining the data needed, and completing and reviewing the collection of information. Send comments regarding this burden estimate or any other aspect of the collection of information, including suggestions for reducing this burden to Department of Defense, Washington Headquarters Services, Directorate for Information Operations and Reports (0704-0188), 1215 Jefferson Davis Highway, Suite 1204, Arlington, VA 22202-4302. Respondents should be aware that notwithstanding any other provision of law, no person shall be subject to a penalty for failing to comply with a collection of information if it does not display a currently valid OMB control number. PLEASE DO NOT RETURN YOUR FORM TO THE ABOVE ADDRESS.					
1. REPORT DATE (DD-MM-YYYY) 27-03-2014		2. REPORT TYPE Master's Thesis		3. DATES COVERED (From – To) Sept 2012 – 27 March 2014	
TITLE AND SUBTITLE Detecting Industrial Chemicals In Water With Microbial Fuel Cells And Artificial Neural Networks				5a. CONTRACT NUMBER	
				5b. GRANT NUMBER	
				5c. PROGRAM ELEMENT NUMBER	
6. AUTHOR(S) King, Scott T., Maj, USAF				5d. PROJECT NUMBER 13V210B	
				5e. TASK NUMBER	
				5f. WORK UNIT NUMBER	
7. PERFORMING ORGANIZATION NAMES(S) AND ADDRESS(S) Air Force Institute of Technology Graduate School of Engineering and Management (AFIT/EN) 2950 Hobson Way WPAFB OH 45433-7765				8. PERFORMING ORGANIZATION REPORT NUMBER AFIT-ENV-14-M-33	
9. SPONSORING/MONITORING AGENCY NAME(S) AND ADDRESS(ES) Air Force Medical Support Agency POC: Nereyda Sevilla, AFMSA/SG9 7700 Arlington Blvd, Ste 5164 Falls Church, VA 22042-5164 Nereyda.Sevilla@pentagon.af.mil				10. SPONSOR/MONITOR'S ACRONYM(S) AFMSA/SG9	
				11. SPONSOR/MONITOR'S REPORT NUMBER(S)	
12. DISTRIBUTION/AVAILABILITY STATEMENT Distribution Statement A: Approved for Public Release; Distribution Unlimited.					
13. SUPPLEMENTARY NOTES This material is declared a work of the U.S. Government and is not subject to copyright protection in the United States.					
14. ABSTRACT Water quality monitoring is critically important in efforts to both limit human exposure to toxic chemicals and to protect ecosystems. This study integrates artificial neural network (ANN) processing with MFC-based biosensing in the detection of three organic pollutants that have relevance to DoD operations: aldicarb, dimethyl-methylphosphonate (DMMP), and bisphenol-A (BPA). Overall, the use of the ANN proved to be more reliable than direct correlations with raw data in the prediction of both chemical concentration and type. The ANN made no errors in the identification and quantification of all chemicals in three concentration ranges. Additionally, chemical mixtures and chemicals dissolved in the standard feed medium were accurately identified by the ANN. Finally, the newly-tested metrics of 10-hour Subsidence Rate (10SR) and First Moment (FrM) proved to be useful in ANN development. This study is the first to incorporate ANN modeling with MFC-based biosensing for the detection and quantification of organic pollutants that are not readily biodegradable. It is also the first to evaluate the utility of 10-hr SR and FM as metrics. Furthermore, this work provides insight into MFC-based biosensing as it pertains to limits of detection and its applicability to scenarios where mixtures of pollutants and unique solvents are involved.					
15. SUBJECT TERMS microbial fuel cells, artificial neural networks, water quality, biosensors, signal processing					
16. SECURITY CLASSIFICATION OF:			17. LIMITATION OF ABSTRACT	18. NUMBER OF PAGES	19a. NAME OF RESPONSIBLE PERSON
a. REPORT	b. ABSTRACT	c. THIS PAGE			Willie F. Harper, Jr., Ph.D., P.E. (AFIT/ENV)
U	U	U	UU	135	19b. TELEPHONE NUMBER (937) 255-3636, ext 4528 (Willie.Harper@afit.edu)

Standard Form 298 (Rev. 8/98)
Prescribed by ANSI Std. Z39-18